3S'18

SYMPOSIUM ON SURFACE SCIENCE 2018

St. Christoph am Arlberg, Austria
February 25 – March 3, 2018

CONTRIBUTIONS

EDITORS
Friedrich Aumayr, Ulrike Diebold, Christoph Lemell and Peter Varga
TU Wien

scientaomicron

Three new SPM Systems

Fermi DryCool™ SPM

Infinite Measurement Time & Convenient Cooling below T = 10K

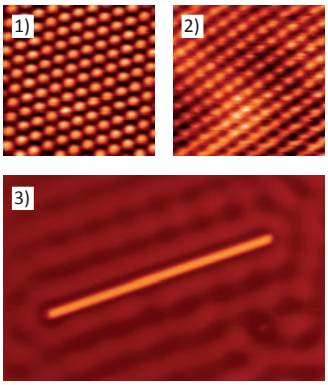

1): STM measurement on Ag(111) at T = 9.8 K with running CC-cooler (5 x 5 nm)
2): nc-AFM QPlus measurement on NaCl(100) (3 x 3 nm)
3): Ag nanowire on Ag(111) surface (40 x 30 nm)

- Cryogen-free cooling for unlimited operation at low & variable temperatures
- Independent tip & sample temperature control from LT to above RT
- Ultra-low noise level below 1 pm with active cooling
- Superior drift performance
- Scienta Omicron's leading QPlus AFM technology

Tesla JT SPM

STM & QPlus AFM in High Magnetic Fields down to 1 K

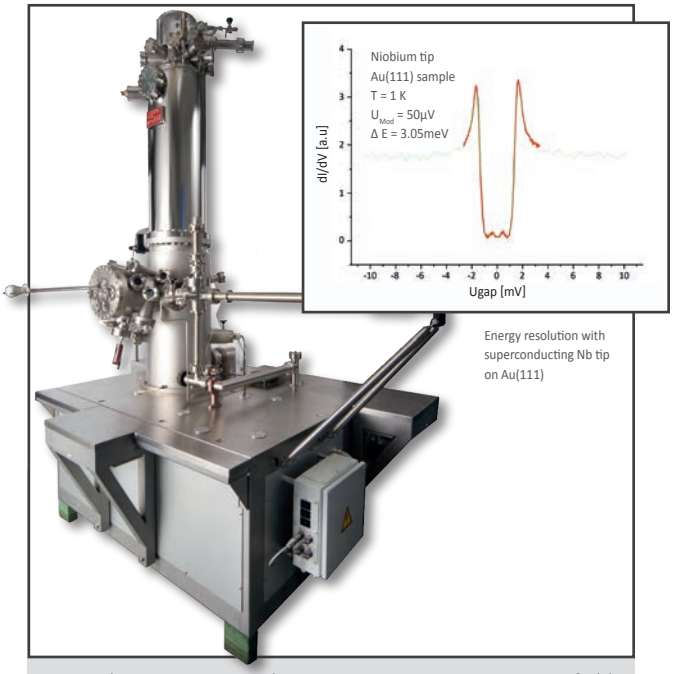

Energy resolution with superconducting Nb tip on Au(111)

- > 5 days uninterrupted measurement time in magnetic fields
- Base temperature down to 1 K with 4He
- Dry UHV magnet B_z > 3 T
- Optical access & ease of use
- STM and advanced spectroscopy and leading QPlus AFM

LT STM III

The Third Generation of the LT STM

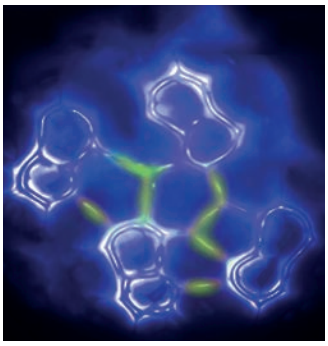

QPlus AFM:
8-hydroxyquiline molecular assemblies on Cu(111).
Xiaohui Qiu et al. (China)

- Extended hold times to > 65 hours
- STS with ΔE < 1 meV
- New cabling for GHz signals for improved time resolution
- Scienta Omicron's leading QPlus AFM technology

HIDEN ANALYTICAL

Mass Spectrometers for Surface Science

Residual Gas Analysis

- Vacuum diagnostics, leak detection and trend analysis
- Ultra-fast data acquisition
- Mass range options: 50, 100, 200, 300 510 amu
- Pulse ion counting detector option for fast event studies including UHV TPD

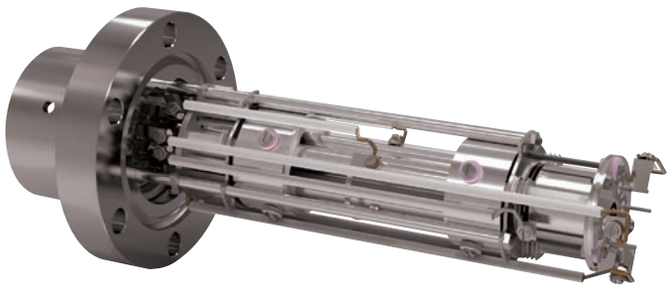

SIMS Systems

- Detect elements, molecules and isotopes
- Static SIMS & dynamic SIMS
- Depth profiling
- Nanometre depth resolution
- Chemical imaging
- Measurement depth from top monolayer to over 30 microns

Mass Spectrometers for Gas Analysis & Catalysis

- Atmospheric pressure gas and vapour analysis
- Fast data acquisition
- 150 ms response time
- Detection from PPB to 100%
- TPD/TPR/TPO and reaction studies

W www.HidenAnalytical.com E info@hiden.co.uk

3S'18

SYMPOSIUM ON SURFACE SCIENCE 2018

St. Christoph am Arlberg, Austria
February 25 – March 3, 2018

CONTRIBUTIONS

EDITORS
Friedrich Aumayr, Ulrike Diebold, Christoph Lemell and Peter Varga
TU Wien

This symposium is organized by

Friedrich Aumayr, Ulrike Diebold and Peter Varga
TU Wien, Institute of Applied Physics (IAP)
Wiedner Hauptstr. 8-10/E134
1040 Vienna, Austria
http://www.iap.tuwien.ac.at/www/3s18/

Venue
Ski Austria Academy, St. Christoph 10,
6580 St. Anton a. Arlberg, Austria
www.skiakademie.at

Medieninhaber: F. Aumayr, U. Diebold und P. Varga, Institut für Angewandte Physik, Technische Universität Wien, Adresse: Wiedner Hauptstr. 8-10/E134, A-1040 Wien
Druck: R. & W. Smutny OEG, A-1110 Wien

PREFACE

We welcome all participants and accompanying persons to the 31st Symposium on Surface Science (3S). The 3S was founded as a winter school by members of the Institute of Applied Physics of the Vienna University of Technology (TU Wien) in 1983. The conference seeks to promote the growth of scientific knowledge and its effective exchange among scientists in the field of surface physics and chemistry and related areas, including applied topics. Its format is similar to that of Gordon Conferences, with ample time for discussions and joint outdoor activities. The number of participants is kept below 100 in order to guarantee active communication between all attendees.

Initially the 3S was held exclusively in Austria and took place every other year. It became an annual event in 1990, and the site started to alternate between locations in France and Austria. In 1998 the 3S evolved into a truly global conference, with venues in the US, Canada, Bulgaria, Japan, Switzerland, Spain, France and Sweden, always returning to Austria in alternate years. This year we are again happy to host the 3S in Austria; for the 9th time in the Arlberg area.

We hope that all participants will experience a lively and successful meeting while enjoying the surroundings in this beautiful mountain region.

Fritz Aumayr Ulrike Diebold Peter Varga

Dates and locations of 3S conferences:

1983	(31.01.-04.02.)	Obertraun	AT
1985	(27.01.-02.02.)	Obertraun	AT
1988	(22.05.-28.05.)	Kaprun	AT
1990	(11.03.-17.03.)	La Plagne	FR
1991	(10.02.-16.02.)	Obertraun	AT
1992	(15.03.-21.03.)	La Plagne	FR
1993	(09.05.-15.05.)	Kaprun	AT
1994	(06.03.-12.03.)	Les Arcs	FR
1995	(23.04.-29.04.)	Kaprun	AT
1997	(26.01.-31.01.)	Aussois	FR
1998	(29.03.-04.04.)	Park City	US
1999	(21.02.-27.02)	Pamporova	BG
2000	(15.02.-18.02.)	Kananaskis	CA
2001	(07.01.-13.01.)	Furano	JP
2002	(03.03.-09.03.)	St.Christoph/Arlberg	AT
2003	(30.03.-05.04.)	La Plagne	FR
2004	(29.02.-06.03.)	St.Christoph/Arlberg	AT
2005	(13.03.-19.03.)	Les Arcs 1800	FR
2006	(05.03.-11.03.)	St. Christoph/Arlberg	AT
2007	(11.03.-17.03.)	Les Arcs 2000	FR
2008	(02.03.-08.03.)	St. Christoph/Arlberg	AT
2009	(08.03.-14.03.)	St. Moritz	CH
2010	(07.03.-13.03.)	St. Christoph/Arlberg	AT
2011	(06.03.-12.03.)	Baqueira Beret	ES
2012	(11.03.-17.03.)	St. Christoph/Arlberg	AT
2013	(03.03.-09.03.)	Åre	SE
2014	(09.03.-15.03.)	St. Christoph/Arlberg	AT
2015	(22.03.-28.03.)	Les Arcs 1800	FR
2016	(21.02.-27.02.)	St. Christoph/Arlberg	AT
2017	(05.03.-10.03.)	St. Moritz	CH
2018	(25.02.-03.03.)	St. Christoph/Arlberg	AT

3S'18

SYMPOSIUM ON SURFACE SCIENCE 2018

St. Christoph am Arlberg, Austria
February 25 – March 3, 2018

Time Schedule

Sunday, 25 February 2018

16:00 – 18:30	**Registration**
20:00 – 20:20	**Opening**
	Chair: P. Varga
20:25 – 20:45	**J. Libuda** *Electrifying model catalysis: Electrochemisty with atomically defined model interfaces*
20:45 – 21:05	**K. Reuter** *On the Active Site Model in Computational Catalyst Screening*
21:05 – 21:25	**R. Fasel** *Topological electronic phases in graphene nanoribbons*

Monday, 26 February 2018

Chair: E. Taglauer

08:00 – 08:20 **J. I. Pascual**
Elementary phenomena in hybrid graphene nanoribbons on surfaces

08:20 – 08:40 **M. Setvin**
Polarity compensation mechanisms on the perovskite surface $KTaO_3(001)$

Chair: U. Diebold

16:40 – 17:00 **Ch. Wöll**
Oxide thin films on metal substrates: The Chameleon character of ZnO

17:00 – 17:20 **M. S. Altman**
Fe Oxide Thin Film Growth on Pt(111) for Applications in Catalysis

17:20 – 17:40 **M. A. Schneider**
Adsorbate Phases and Structural Evolution Upon Reduction of CoO_2 Chains on Ir(100)

17:40 – 18:00 **W.-D. Schneider**
From adatoms to superlattices: Sensing the spin of individual Ce-atoms

18:00 – 18:20 **F. P. Netzer**
From gas-phase oxide clusters to 2-D oxide layers: Tungsten oxide on Ag(100)

Chair: A. Enders

19:30 – 19:50 **U. Starke**
Inforcing strong correlation effects into Graphene

19:50 – 20:10 **A. Curcella**
Structure of Si layers on Ag(111) and mechanism for the stabilization of epitaxial silicene

20:10 – 20:30 **B. Schuler**
Exploring optoelectronic properties of point defects in monolayer WS_2 with atomic resolution

20:30 – 20:50 **K. N. Eltsov**
Mechanism of gold intercalation under monocrystalline graphene synthesized on Ni(111) by TPG

Tuesday, 27 February 2018

Chair: T. Koshikawa

08:00 – 08:20 **A. Gölzhäuser**
Carbon Nanomembranes with sub-nanometer channels: Two-dimensional materials for water purification with high selectivity and highest permeance

08:20 – 08:40 **J. Gustafson**
On the role of steps in catalysis

Chair: G. Renaud

16:40 – 17:00 **G. Rupprechter**
Operando sum frequency generation (SFG) spectroscopy at atmospheric pressure: Cu clusters and Pt/ZrO_2

17:00 – 17:20 **G. Thornton**
Gold nanoparticle interactions with rutile TiO_2(110)

17:20 – 17:40 **G. Feldbauer**
Shape-controlled Synthesis of Anatase TiO_2 Nanoparticles - Insights from DFT calculations

17:40 – 18:00 **D. Sánchez-Portal**
Effect of Structural Fluctuations on Elastic Lifetimes of Adsorbate States: Isonicotinic Acid on Rutile(110)

18:00 – 18:20 **H. Brune**
CO-Oxidation on Size-Selected Surface-Adsorbed Platinum Clusters

Chair: F. Aumayr

19:30 – 19:50 **M. Buck**
Solution Based Assembly of Non-Planar Molecules: Tetraphenylmethane Carboxylic Acids on A

19:50 – 20:10 **J. V. Barth**
Convergent multistep on-surface reaction yielding complex supramolecular tiling

20:10 – 20:30 **H. Marbach**
Surface-Anchored Metal-Organic Frameworks as Versatile Resists for E-Beam Lithography: Fabrication of sub-10 nm Structures

20:30 – 20:50 **P. Kocan**
PTCDA on Ge(001) surface - adsorption and surprising self-assembly

Wednesday, 28 February 2018

Chair: C. Lemell

08:00 – 08:20 **P. M. Echenique**
Surface attophysics

08:20 – 08:40 **W. Eberhardt**
Attosecond lifetimes of excited electronic states in solids - determined without an attosecond laser

Chair: R. Kalousek

16:40 – 17:00 **T. Stempel**
Advanced ARPES Analyzer and Electron Detection Concepts - KREIOS energy analyzer with CMOS detector

17:00 – 17:20 **M. Maier**
The TESLA JT SPM

Chair: H. J. Hug

17:25 – 18:20 **Posterintroduction**

A. Arnau
Exploring the Relation Between Intramolecular Conjugation and Band Dispersion in One-Dimensional Polymers

A. Bettac
Development and Integration of a Universal SPM head for Low Temperature SPM measurements

R. Bliem
Modifying the surface stability of perovskite oxide cathode materials: Polarization and metal adsorption

U. Diebold
Surface chemistry of ruthenates

G. Franceschi
In-situ investigations of pulsed-laser-deposited Sr-doped lanthanum manganite thin films

J. Hulva
Reactivity of Pt and Rh adatoms, dimers, and small clusters on $Fe_3O_4(001)$

R. Kalousek
Babinet principle and localized surface plasmon resonances: HR STEM - EELS studies

T. Koshikawa
Application of SPLEEM and highly performed strain-compensated super lattice photocathode

Ch. Linsmeier
Investigation of hydrogen isotope retention mechanisms in beryllium: High resolution TDS measurements

M. Müllner
Electrochemical Surface Science of Magnetite Fe_3O_4 under Oxygen Evolution Conditions

J. Oelmann
Surface composition analysis of volatile species using Laser-Induced Ablation- Quadrupole Mass Spectroscopy (LIA-QMS) and Laser-Induced Breakdown Spectroscopy (LIBS)

M. Rebarz
Femtosecond spectroscopic ellipsometry on optoelectronic materials and photonic structures

G. Renaud
X-ray investigation of Van der Waals Epitaxy of 2D diselenides and ditellurides

M. Riva
Effects of surface structure on oxygen exchange on $SrTiO_3(110)$

W.-D. Schneider
The atomic structure of a metal-supported two-dimensional Germania film

J. Schwestka
Interaction of highly charged ions with 2D materials

S. Silkin
Surface and quantum-well electronic states in ultra-thin Ir and Pt films on the Au(111) surface

R. Stadlmayr
Sputtering of Fusion Relevant Materials and Comparison to SDTrimSP-2D and TRI3DYN

19:30 – 21:30 **Postersession**

Thursday, 1 March 2018

Chair: A. Bettac

08:00 – 08:20 **P. Jelínek**
SPM discrimination of the spin-state in organometallic complex and its control by positioning on N-doped graphene

08:20 – 08:40 **G. Michelitsch**
Surface-adsorbed magnetic materials: A challenge for first-principles theory

Chair: Ch. Linsmeier

16:40 – 17:00 **E. Lundgren**
The misfit structure between the Pd(100) and PdO(101) under reaction conditions

17:00 – 17:20 **J. E. Ortega**
Vicinal Ag(111) surfaces with fully-kinked steps

17:20 – 17:40 **L. Hammer**
Structure Determination Considering Surface Dynamics: The O/Rh(100) System revisited

17:40 – 18:00 **T. Šikola**
LEEM and STM - a valuable combination for the study of organic-inorganic interface heterostructures

18:00 – 18:20 **Y. Suchorski**
Dome-shaped μm-sized curved Rh crystals as a playground for H_2 oxidation

Chair: P. Muller

19:30 – 19:50 **D. G. de Oteyza**
Shifting from reactant to substrate engineering in the selective synthesis of graphene nanoribbons

19:50 – 20:10 **S. Godlewski**
Long acenes generated by on-surface dehydrogenation

20:10 – 20:30 **H. Dil**
Wannier Stark localisation and Rashba splitting in ferroelectrics and multiferroics

20:30 – 20:50 **S. Espinoza**
VUV Magneto-Optical Transient Ellipsometer: ELIps

Friday, 2 March 2018

Chair: T. Berghaus

08:00 – 08:20 **M. Kolmer**
Two-probe STM/STS experiments performed on atomic wires and single molecules supported on Ge(001) surface

08:20 – 08:40 **F. J. Giessibl**
Coulomb's law at the nanoscale: imaging CaF_2(111) with atomically engineered tips

Chair: M. Riva

16:30 – 16:50 **J. Kunze-Liebhäuser**
Surface science and DEMS studies of electrochemical CO and ethanol oxidation on TiOC supported Pt catalysts

16:50 – 17:10 **W. Linpe**
In-situ X-ray observations of Sn electrodeposition into two-step anodized alumina

17:10 – 17:30 **V. Vonk**
Unusual and stable Ga bonding at its solid-liquid interface with GaN

17:30 – 17:50 **S. Curiotto**
Dynamics of Si surface nanostructures under electromigration

17:50 – 18:10 **M. E. Messing**
Iron-based magnetic nanoparticles with tuned composition and crystal structure

Chair: A. Arnau

18:30 – 18:50 **K. Morgenstern**
Hydrophilicity and microsolvation of organic molecules resolved on the sub- molecular level by scanning tunneling microscopy

18:50 – 19:10 **K.-H. Ernst**
Molecular machines driven with electrons on surfaces: walkers and nanocars

19:10 – 19:40 **Giant Slalom Race Award Ceremony**

20:00 **Conference Dinner**

CONTRIBUTIONS

Content

PFEIFFER VACUUM

VACUUM SOLUTIONS

A one stop source for the highest standard in vacuums

No two vacuum processes are alike since individual requirements are what matters. Together with our customers, we obtain a vacuum solution based on their specific needs. This process includes all steps in creating a perfect vacuum condition. Besides best-in-class products for vacuum generation, measurement and analysis, we also offer accessories, application training programs and worldwide service.

See for yourself what Pfeiffer Vacuum solutions are about at:

www.pfeiffer-vacuum.com

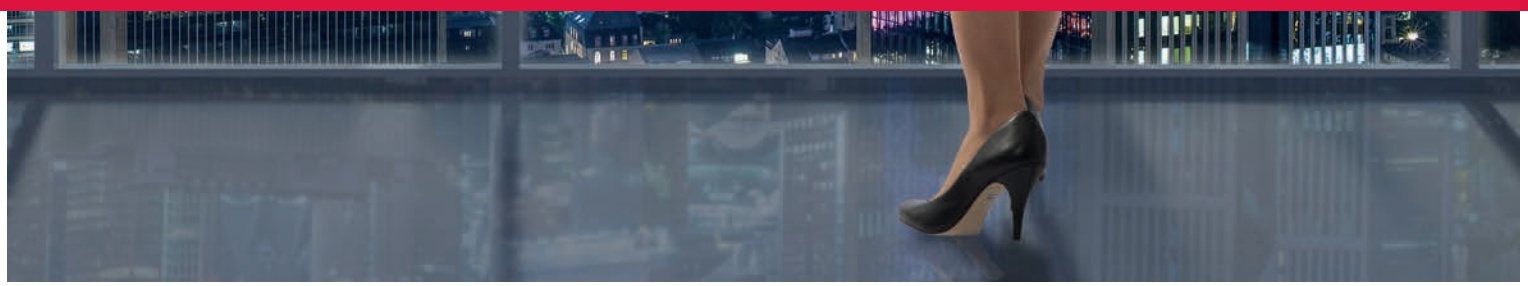

Sunday

Electrifying model catalysis: Electrochemisty with atomically defined model interfaces

F. Faisal[1], C. Stumm[1], M. Bertram[1], F. Waidhas[1], Y. Lykhach[1], S. Cherevko[2,3], F. Xiang[4], M. Vorokhta[5], B. Šmíd[5], T. Skála[5], N. Tsud[5], A. Neitzel[1], K. Beranová[6], K. C. Prince[6], S. Geiger[2], O. Kasian[2], T. Wähler[1], R. Schuster[1], M. A. Schneider[4], V. Matolín[5], Karl J.J. Mayrhofer[2,3], O. Brummel[1], J. Libuda[1]

Physikalische Chemie II, Universität Erlangen-Nürnberg, D-91058 Erlangen, Germany
(corresponding author: J. Libuda, e-mail: joerg.libuda@fau.de)
[1] *Max-Planck-Institut für Eisenforschung GmbH, 40237, Düsseldorf, Germany*
[2] *Helmholtz-Institute Erlangen-Nürnberg, FZ Jülich GmbH, Erlangen, 91058, Germany*
[3] *Lehrstuhl für Festkörperphysik, Universität Erlangen-Nürnberg, D-91058 Erlangen, Germany*
[4] *Dept. of Surface and Plasma Science, Charles University, CZ-18000 Prague, Czech Republic*
[5] *Elettra-Sincrotrone Trieste SCpA, I-34149 Basovizza-Trieste, Italy*

Electrocatalytic processes are the key to our future transition to a renewable energy system. Yet, our fundamental understanding of electrocatalysis lags behind classical heterogeneous catalysis which has been dominating chemical technology for a long time. Here, we describe a new strategy to advance fundamental studies on electrocatalytic materials. We propose to "electrify" complex model catalysts made by surface science methods to explore electrocatalytic reactions in liquid environments.

We demonstrate the feasibility of this concept focusing on oxide-based electrocatalysts, which play an essential role in energy-related applications. In the first step, we study the interaction of a well-characterized and atomically-defined Co_3O_4(111) film on Ir(100) with H_2O under UHV conditions. Combining *infrared reflection absorption spectroscopy* (IRAS) and *synchrotron radiation photoelectron spectroscopy* (SR-PES), we show that H_2O forms strongly bound OH^- groups followed by the formation of partially dissociated $OH^-(H_2O)_n$ clusters.

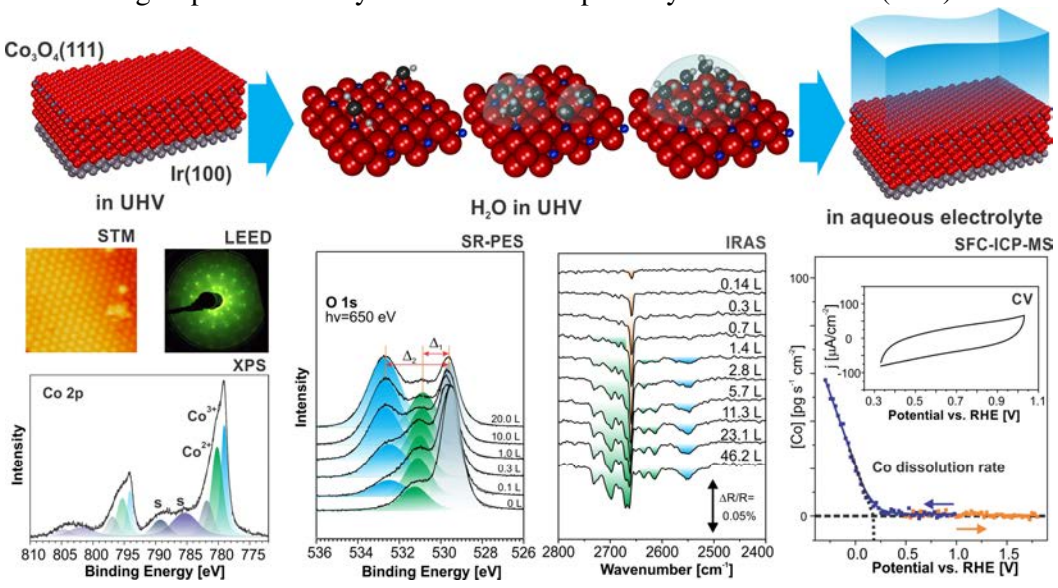

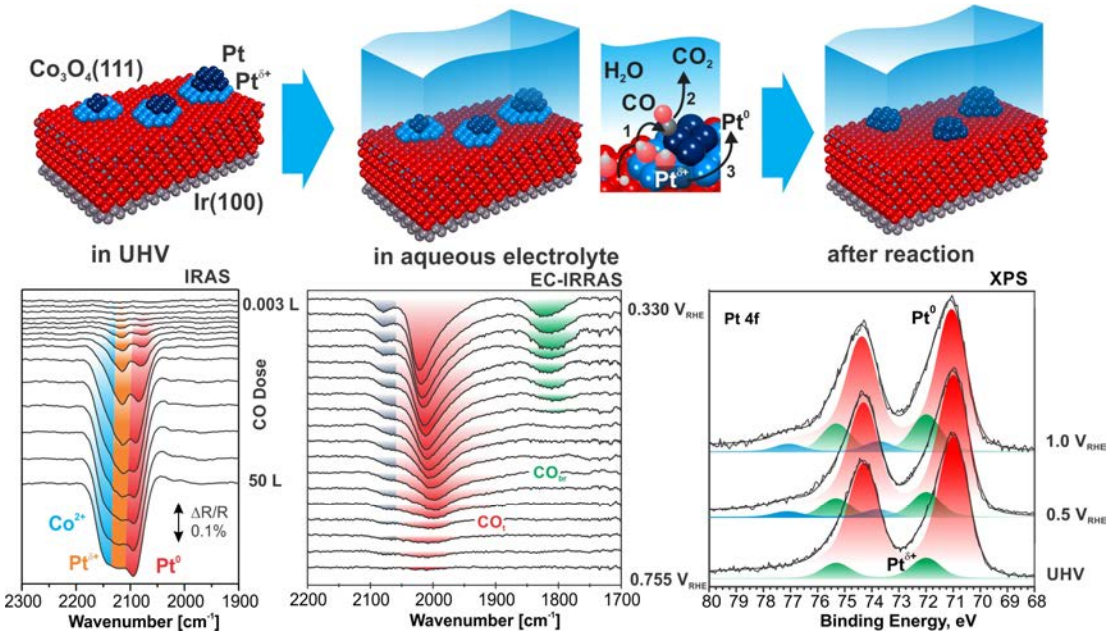

In the next step, we transfer the Co_3O_4(111) films from UHV into the electrochemical environment. By means of *cyclic voltammetry* (CV), *scanning flow cell inductively coupled plasma mass spectrometry* (SCF-ICP-MS), and *electrochemical infrared reflection absorption spectroscopy* (EC-IRRAS) we identify a pH and potential window in which the films are perfectly stable in phosphate buffered aqueous solution. As shown by *low-energy electron diffraction* (LEED) and *near ambient pressure X-ray photoelectron spectroscopy* (NAP-XPS) both the long-range order and the composition of the films are preserved under electrochemical conditions.

In the last step, we deposit Pt nanoparticles (NPs) on the Co_3O_4 film by *physical vapor deposition* (PVD) and characterize the model electrocatalysts by *scanning tunneling microscopy* (STM), SR-PES, *temperature programmed desorption* (TPD) and IRAS with CO as a probe molecule. We show that *electronic metal–support interactions* (EMSI) stabilize oxidized platinum at the NP interface, thereby opening a new synergistic reaction pathway that involves both metallic and oxidized platinum. After transferring the same model catalysts into the EC cell, we show by EC-IRRAS, CV and *EC-coupled* NAPXPS that the same phenomena can be observed at the electrified interface: Electronic metal support interactions at the NP interface lead to partial oxidation of Pt and the activation of lattice oxygen, which is thereby activated and becomes involved in the electrocatalytic reaction.

Our results illustrate the potential of the proposed concept, which offers a systematic approach to build atomically-defined model electrodes for fundamental electrocatalytic studies.

The authors acknowledge financial support by the Deutsche Forschungsgemeinschaft (DFG) within the Cluster of Excellence “Engineering of Advanced Materials” (project EXC 315) (Bridge Funding) and support by the DFG within the Research Unit FOR 1878 “Functional Molecular Structures on Complex Oxide Surfaces”.

[1] F. Faisal, C. Stumm, M. Bertram, F. Waidhas, Y. Lykhach, S. Cherevko, F. Xiang, M. Vorokhta, B. Šmíd, T. Skála, N. Tsud, A. Neitzel, K. Beranová, K. C. Prince, S. Geiger, O. Kasian, T. Wähler, R. Schuster, M. A. Schneider, V. Matolín, Karl J.J. Mayrhofer, O. Brummel, J. Libuda, submitted.

On the Active Site Model in Computational Catalyst Screening

K. Reuter

Chair for Theoretical Chemistry and Catalysis Research Institute
Technische Universität München, Lichtenbergstr. 4, D-85747 Garching, Germany
(corresponding author: K. Reuter, e-mail: karsten.reuter@ch.tum.de)

Over the last decade, a new theme has made a staggering appearance in theoretical surface catalysis research: computational screening as a means of catalyst discovery [1-3]. The basis for such screening approaches is the realization that there are many dependencies in the adsorbate and transition state (TS) energetics, so-called scaling relations, that largely govern the microkinetics of a given catalyst material. Brønsted-Evans-Polanyi relationships link activation barriers to thermochemical reaction energies, while thermochemical scaling relations correlate the underlying adsorption strengths of reaction intermediates to those of their constituting base elements. Together with (sometimes drastic) assumptions on the reaction mechanism, these dependencies often allow for the description of the catalytic activity in terms of only a few simple parameters. Common examples of such parameters, generally called descriptors, are the adsorption energies of one or more reaction intermediates or constituting base elements like C, N, or O. Since these adsorption energies also follow simple trends (at least over the transition metal series), one can either deduce clear guiding principles for catalyst design or screen a large number of catalyst materials on the basis of only a limited number of first-principles calculations.

One can hardly overstate the impact that this type of work has made in recent years. Computational screening is now a widely accepted (sometimes already considered essential) strategy to guide experimental catalyst synthesis. Reports on the corresponding identification of improved catalyst materials are already piling up. Maybe even more important though is the conceptual framework that has come with this approach. Thinking in terms of volcano plots and understanding the underlying trends that give rise to them; all this has become natural to us and thereby encompasses much, if not most, of the knowledge that had been obtained in a century of empirical catalyst research. An understanding of these trends has furthermore clarified the fundamental limitations to the maximal catalytic activity achievable for a given class of catalysts. It has provided leads on how to overcome such limitations employing, e.g., promotion, multidimensional or multifunctional binding sites, and support effects [4,5].

That said, it is however also clear that the approach necessarily has limitations – even though this is less emphasized in the wake of its current of success [6]. In this talk I will argue that our still limited understanding of the structure of active sites is actually one of the major

bottlenecks towards an ever extended and reliable use of such computational screening for catalyst discovery [7]. For low-index transition metal surfaces, the prevalently chosen high-symmetry (terrace and step) sites offered by the nominal bulk-truncated crystal lattice might be justified. For more complex surfaces and composite catalyst materials, computational screening studies will need to actively embrace a considerable uncertainty with respect to what truly are the active sites. Systematically extending the screening over many candidate sites, an intriguing perspective is to establish "material - site type - activity" maps. Just as much as the present "material - activity" volcanos help to identify promising materials, such extended maps will identify geometric motifs that would further optimize the performance of a given material – and thereby guide synthesis endeavors aiming to stabilize such motifs. In light of this, an interesting direction for methodological work would be to employ global geometry optimization approaches to generate (diverse) pools of candidate sites. Accounting for a simultaneous presence of different active site types within extended microkinetic models would in turn even allow one to capture (and engineer) a possible synergistic interplay. In this respect, the evident uncertainty in the choice of active site today offers exciting prospects for new research directions in the future. Eventually, actively embracing the space of active site models in screening studies may thus even provide leads towards the targeted design of optimized sites in future catalysts.

Funding through the Deutsche Forschungsgemeinschaft is acknowledged within project RE1509/27-1.

[1] J. K. Nørskov, T. Bligaard, J. Rossmeisl, and C. H. Christensen, Nat. Chem. 1, 37 (2009)
[2] J. K. Nørskov and A. Vojvodic, Nat. Sci. Rev. 2, 140 (2015)
[3] J. Greeley, Annu. Rev. Chem. Biomol. Eng. 7, 605 (2016)
[4] M. Andersen, A. J. Medford, J. K. Nørskov, and K. Reuter, Angew. Chem. Int. Ed. 55, 5210 (2016)
[5] M. Andersen, A. J. Medford, J. K. Nørskov, and K. Reuter, ACS Catal. 7, 3960 (2017)
[6] M. Andersen, C. P. Plaisance, and K. Reuter, J. Chem. Phys. 147, 152705 (2017)
[7] K. Reuter, C. P. Plaisance, H. Oberhofer, and M. Andersen, J. Chem. Phys. 146, 040901 (2017)

Topological electronic phases in graphene nanoribbons

O. Gröning, S. Wang, C. Pignedoli, G. Borin Barin, V. Meunier[1],
A. Narita[2], K. Müllen[2], P. Ruffieux, and R. Fasel

Empa, Swiss Federal Laboratories for Materials Science and Technology, nanotech@surfaces Laboratory, Überlandstrasse 129, 8600 Dübendorf, Switzerland
(corresponding author: R. Fasel, e-mail: roman.fasel@empa.ch)

[1] *Dep. of Physics, Appl. Physics and Astronomy, Rensselaer Polytechnic Institute, Troy, USA*

[2] *Max Planck Institute for Polymer Research, 55124 Mainz, Germany*

Among graphene related materials, graphene nanoribbons (GNRs) – narrow stripes of graphene – have emerged as promising building blocks for nanoelectronic devices. The lateral confinement in GNRs opens a bandgap that sensitively depends on the ribbon width, allowing in principle for the design of GNR-based structures with tunable properties. However, structuring with atomic precision is required to avoid detrimental effects induced by edge irregularities. A recently developed bottom-up fabrication route [1] allows for the required atomically precise synthesis of GNRs with different shapes and edge structures [2] as well as heterojunctions between dissimilar ribbon segments (e.g. doped/undoped [3], different widths [4]). In this presentation, the emergence of junction states at such hetero-interfaces will be discussed from a conceptual as well as experimental point of view.

Based on a topological classification of GNRs, S. Louie and coworkers have recently predicted that topological junction states develop whenever two joining GNR segments belong to different topological classes [5]. I will discuss a first experimental realization of such situation, at the example of GNR quantum dot (GQD) heterostructures formed by cross-dehydrogenative coupling of armchair GNRs of width N=7 (7-AGNRs) [4]. The so-formed intraribbon quantum dots reveal deterministically defined, atomically sharp interfaces between wide and narrow AGNR segments and host a pair of low-lying interface states. Scanning tunneling microscopy/spectroscopy measurements complemented by extensive simulations reveal that their energy splitting depends exponentially on the length of the central narrow bandgap segment. This allows tuning of the fundamental gap of the GQDs over one order of magnitude within a few nanometers length range.

Even more intriguing topological properties are predicted for a family of zigzag edge-extended AGNRs, of which we have synthesized and characterized two first members in some detail (for one of them, see Fig. 1). I will show that variations of the AGNR backbone width and the zigzag edge segment spacing drive this family of GNR structures into trivial, metallic and topological insulating phases [6]. Their respective topological class is experimentally determined by exploiting the bulk-boundary correspondence [7] and measuring the absence or

presence of localized end states by scanning tunneling spectroscopy. With graphene nanoribbons hosting robust topological quantum phases, the band width of the the topological bands may be tuned close to the energy scale of proximity induced spin-orbit coupling [8] or superconductivity [9], which may allow the realization of Kitaev like Hamiltonians [10] and Majorana type end states [11].

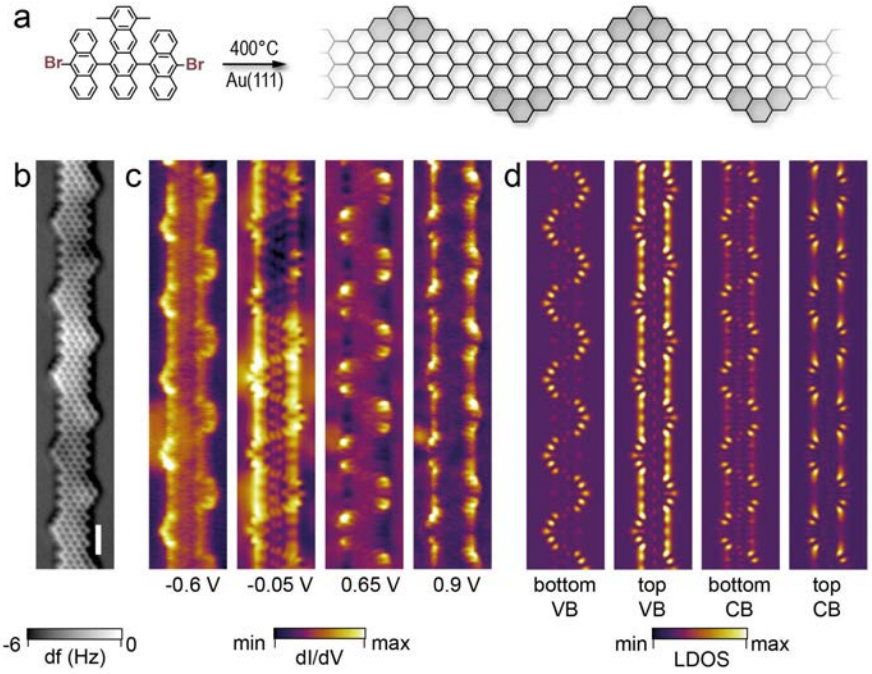

Figure 1: (a) Synthesis of edge-extended 7-AGNR. (b) Constant height nc-AFM image (with CO functionalized tip) of the ribbon structure on Au(111). (c) Series of constant height dI/dV maps of the GNR shown in b) at selected energies close to E_f. (d) Sequence of TB derived constant height charge density maps at the VB and CB extrema (at -1 eV, -0.2 eV, +0.2 and +1.0 eV from bottom VB to top CB). The 1 nm scale bar in b) applies to all maps.

(1) Cai, J.; Ruffieux, P.; Jaafar, R.; Bieri, M.; Braun, T.; Blankenburg, S.; Muoth, M.; Seitsonen, A. P.; Saleh, M.; Feng, X.; *et al.* Atomically Precise Bottom-up Fabrication of Graphene Nanoribbons. *Nature* **2010**, *466*, 470–473.

(2) Talirz, L.; Ruffieux, P.; Fasel, R. On-Surface Synthesis of Atomically Precise Graphene Nanoribbons. *Adv. Mater.* **2016**, *28*, 6222–6231.

(3) Cai, J.; Pignedoli, C. A.; Talirz, L.; Ruffieux, P.; Söde, H.; Liang, L.; Meunier, V.; Berger, R.; Li, R.; Feng, X.; *et al.* Graphene Nanoribbon Heterojunctions. *Nat. Nanotechnol.* **2014**, *9*, 896–900.

(4) Wang, S.; Kharche, N.; Costa Girão, E.; Feng, X.; Müllen, K.; Meunier, V.; Fasel, R.; Ruffieux, P. Quantum Dots in Graphene Nanoribbons. *Nano Lett.* **2017**, *17*, 4277–4283.

(5) Cao, T.; Zhao, F.; Louie, S. G. Topological Phases in Graphene Nanoribbons: Junction States, Spin Centers, and Quantum Spin Chains. *Phys. Rev. Lett.* **2017**, *119*, 076401.

(6) Gröning, O.; Wang, S.; *et al.* Engineering of Robust Topological Quantum Phases in Graphene Nanoribbons. *Submitted* **2018**.

(7) Meier, E. J.; An, F. A.; Gadway, B. Observation of the Topological Soliton State in the Su–Schrieffer–Heeger Model. *Nat. Commun.* **2016**, *7*, 13986.

(8) Wang, Z.; Ki, D.; Chen, H.; Berger, H.; MacDonald, A. H.; Morpurgo, A. F. Strong Interface-Induced Spin–orbit Interaction in Graphene on WS2. *Nat. Commun.* **2015**, *6*, 8339.

(9) Feigel'man, M. V.; Skvortsov, M. A.; Tikhonov, K. S. Theory of Proximity-Induced Superconductivity in Graphene. *Solid State Commun.* **2009**, *149*, 1101–1105.

(10) Kitaev, A. Y. Unpaired Majorana Fermions in Quantum Wires. *Phys.-Uspekhi* **2001**, *44*, 131.

(11) Nadj-Perge, S.; Drozdov, I. K.; Li, J.; Chen, H.; Jeon, S.; Seo, J.; MacDonald, A. H.; Bernevig, B. A.; Yazdani, A. Observation of Majorana Fermions in Ferromagnetic Atomic Chains on a Superconductor. *Science* **2014**, *346*, 602–607.

VIDEKO

our vision. your success.

ELEKTRONEN-MIKROSKOPIE.

VAKUUM-TECHNIK.

Mit über 20 Jahren Erfahrung im Bereich Vakuumtechnik und Elektronenmikroskopie sind wir Ihr lokaler und flexibler Ansprechpartner in Österreich mit dem Produkt KnowHow internationaler Marktführer.

Wir stehen für:

- **Kundennähe**
- **Flexibilität**
- **Individuelle Kundenlösungen**
- **direkte und unkomplizierte Beratung**
- **hohe Qualitätsstandards**

contact us.

VIDEKO GmbH

Handelsstraße 14
A-2512 Tribuswinkel

Tel.: +43 2252 93 1800
Fax: +43 1 2533033

EMail: office@videko.at
www.videko.at

EDWARDS

THYRACONT
Vacuum Instruments

HITACHI
Inspire the Next

novotek
VAKUUMTECHNIK

PRECISION Plus
VACUUM PARTS

Monday

Elementary phenomena in hybrid graphene nanoribbons on surfaces

E. Carbonell[1], Jingchen Li[1], Nestor Merino[1,2], Martina Corso[3], Diego Peña[4], Dimas G. De Oteyza[2] and J.I. Pascual[1]

[1]*CIC nanoGUNE, Donostia San Sebatián, Spain*
[2]*Donostia International Physics Center- DIPC, Donostia San Sebatián, Spain*
[3]*Centro de F'isica de Materiales CFM-CSIC/UPV-EHU*
[4]*CIQUS, Universidad de Santiago de Compostela, Spain*

Large aromatic carbon nanostructures are cornerstone materials due to their increasingly role in functional devices, but their synthesis in solution encounters size and shape limitations. Recently, it has been shown that the production of large graphenoid nanostructures with atomic precision can be realized on a metal surface using strategies of on-surface chemistry [1]. Chemical routes have been established allowing us to steer synthesis by properly selecting the shape of organic precursors and produce large molecular platforms with tunable intrinsic properties such as the electronic band-gap, its magnetic behavior, or its reactivity.

In this presentation, I will summarize results regarding the production of graphene nanoribbons and other carbon nanostructures with interesting electronic phenomenology. We combine high resolution STM imaging (Fig. 1) with local spectroscopy to unveil the success of a reaction pathway and to explore the effect of precursor shape and composition in electronic functionality of the ribbon.

I will show that these ribbons behave as one-dimensional semiconductors and their band structure can be tuned by modifying their width [2]. Doping can be introduced by incorporating additional species [3] (see image of a high resolution GNR doped with CN groups). Furthermore, we developed a method to create quantum dots embedded in hybrid graphene nanoribbon. We found that ribbon bands are confined in them selectively, according to their symmetry [4]. Quantum states can also be localized in extended flat platforms with cavities holding confined states.

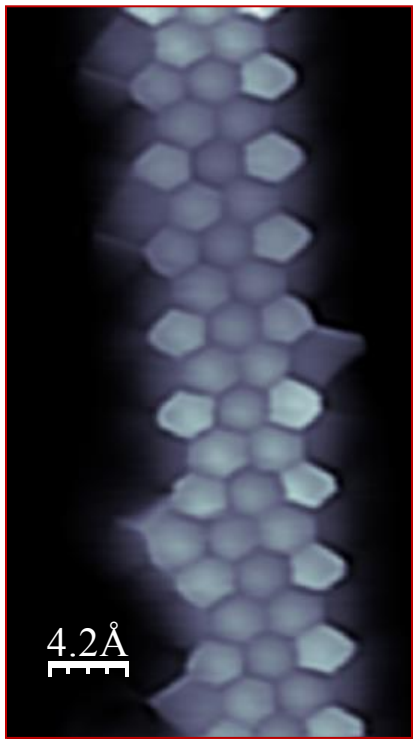

Finally, I will show that it is possible to incorporate magnetic molecular species bound to a ribbon [5]. We show that the molecular spin survives in the ribbon by using spin-excitation inelastic spectroscopy.

[1] J. Cai et al, Nature 466, 470 (2010).
[2] N. Merino et al. ACS Nano 11, 11661 (2017)

[3] E.Carbonell et al. ACS Nano 11, 7355 (2017)
[4] E. Carbonell, et al. Nano Letters 17, 50 (2017)
[5] J. Li, et al, Science Adv. In Press (2018)

Polarity compensation mechanisms on the perovskite surface $KTaO_3$ (001)

M. Setvin[1], M. Retticioli[2], F. Poelzleitner[1], I. Sokolovic,[1] J. Hulva[1], M. Schmid[1], L. A. Boatner[3], C. Franchini[2], U. Diebold[1]

[1] Institut of Applied Physics, TU Wien, A-1040 Wien, Austria
(corresponding author: M. Setvin, e-mail: setvin@iap.tuwien.ac.at)

2 University of Vienna, Faculty of Physics and Center for Computational Materials Science, Vienna, Austria

3 Materials Science and Technology Division, Oak Ridge National Laboratory, Oak Ridge, Tennessee 37831, USA

All ionic crystals bear polar surfaces along specific orientations. The stacking of alternatingly charged lattice planes causes a diverging electrostatic energy, which can be compensated in various ways [*1, 2*] charge transfer, structural reconstructions, changes in the surface morphology, and chemical doping. Such compensation mechanisms often create novel physical and chemical materials properties. Tantalates and niobates are prototypical examples of polar perovskites. Many exhibit (incipient) ferroelectricity providing attractive options for electronics and sensors. The built-in field can also enhance electron-hole separation in light-harvesting schemes; indeed these materials are highly efficient photocatalysts with a record quantum efficiency for photochemical water splitting exceeding 50% [*3*]. Since the surface plays a major role in all these applications, it is important to understand which response the system "selects" to relieve the electrostatic instability.

This study of $KTaO_3$ (001) directly shows how a whole series of polarity compensations evolves: The as-cleaved surface consists of a mixture of KO and TaO_2 terraces with the bulk (1×1) termination (see Figure 1a,b). After cleaving in vacuum, the surface atoms are frozen in place and cannot rearrange; instead the material responds with an insulator-to-metal transition and ferroelectric lattice distortions. Upon annealing, isolated oxygen vacancies first form on KO terraces, and then the surface rearranges into a periodic pattern of 5-atom wide, alternating KO and TaO_2 stripes. While this is the lowest-energy configuration in vacuum, exposure to water vapour disperses the KO across the surface, creating a hydroxylated overlayer with (2×1) symmetry (Figure 1c). All these polarity-compensation mechanism are known from different systems, but here we could observe them on one material, and use a proper control of the surrounding environment to tailor which one is at work.

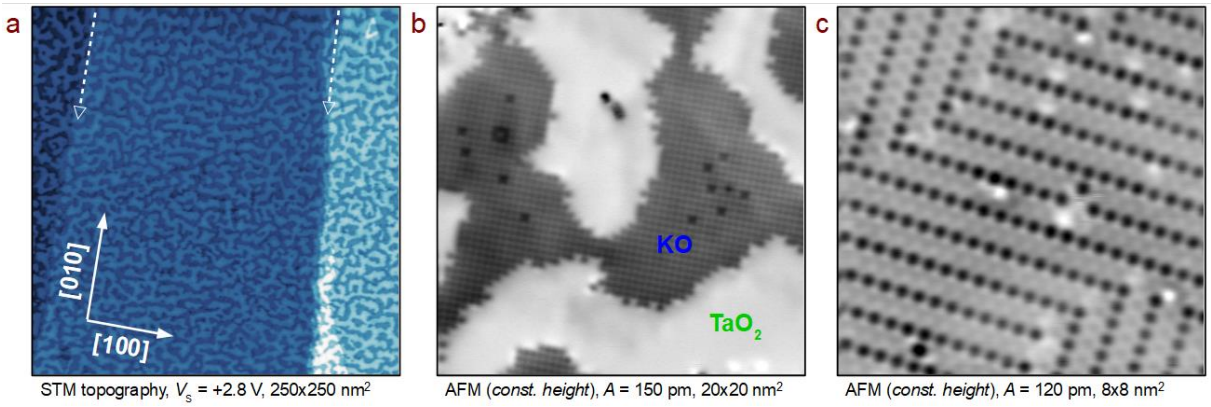

Figure 1: Cleaved $KTaO_3$ (001). (a) Overview STM image of an as-cleaved surface. (b) Atomically resolved AFM image with KO and TaO_2 terminations. (c) AFM image of water-induced (2×1) reconstruction.

The work was supported by European Research Council (ERC) advanced grant "Oxide Surfaces" (ERC-2011-ADG-20110209), Austrian Science Fund (FWF) Project Wittgenstein Prize (Z 250), Project F45 (FOXSI) and the FWF-SFB project VICOM (Grant no. F41). Research at the Oak Ridge National Laboratory for one author (LAB) was supported by the U.S. Department of Energy, Office of Science, Basic Energy Sciences, Materials Sciences and Engineering Division

[1] C. Noguera. *J. Phys. Cond. Mat.* **12**, R367-R410 (2000).
[2] J. Goniakowski, F. Finocchi, C. Noguera. *Rep. Prog. Phys.* **71**, 016501 (2008).
[3] H. Kato, K. Asakura, A. Kudo. *J. Am. Chem. Soc.* **125**, 3082-3089 (2003).

Oxide thin films on metal substrates: The Chameleon character of ZnO

Christof Wöll
Institute of Functional Interfaces (IFG), Karlsruhe Institute of Technology (KIT), FRG
christof.woell@kit.edu, www.ifg.kit.edu

The modification of metal particle properties occurring when depositing them on oxides, often referred to as strong metal-support interaction (SMSI), as well as the opposite case, the influence of metals on thin oxide layers covering them, are topics of considerable importance in heterogeneous catalysis and in nanotechnology. ZnO is a particular interesting case, since the properties of this oxide differ strongly depending on the geometry of the sample and the substrate they are deposited on. While for bulk ZnO the most stable modification is wurtzite, for which some of the surfaces show an electrostatic instability (so-called polar surfaces), 2D slabs with a thickness of below 10 layers have been predicted theoretically to crystallize in a graphite-like BN structure, where the electrostatic instability of e.g. the (000-1) and the (0001) surface is absent. If thin layers of ZnO are deposited on a metal, further polymorphs are observed, with the properties of the ZnO thin layers depending strongly on the type of supporting metal. A novel, rumpled structure of such thin ZnO layers has been predicted [1] for the case of Cu(111) substrates. In a recent theoretical study strong changes of the properties of such ZnO adlayers were reported when changing the metal support from Cu to Ag and Au [2].

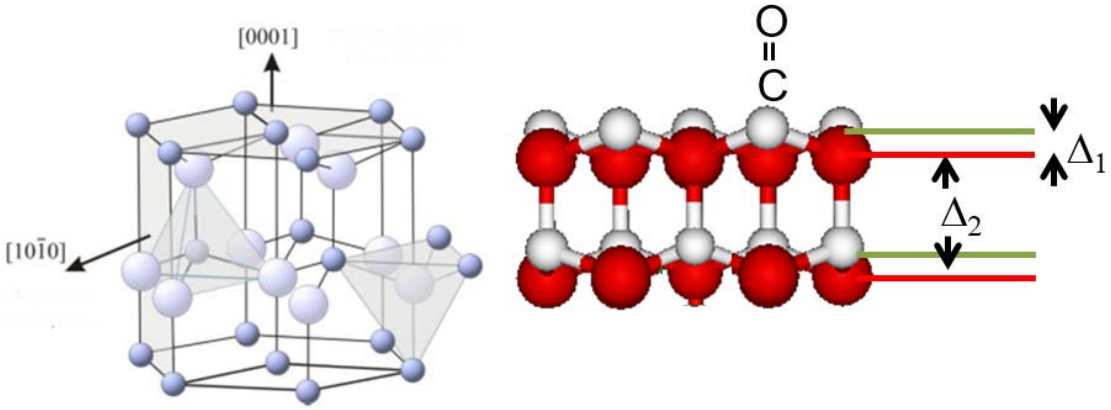

Fig. 1 While bulk ZnO crystallizes in the Wurtzite structure (left), in thin films a different arrangement of metal and oxygen ions is observed. By reducing the distance Δ_1 between Zn and O layers to zero, a graphite-like structure is realized. When such layers are deposited on a metal, a charge transfer into the oxide layers may result in a pronounced structural relaxation. The resulting changes in chemical properties can conveniently be detected by investigating the binding energy and the stretch frequency of adsorbed CO molecules.

The most direct way to experimentally investigate the corresponding changes in chemical properties has been the investigation of the binding of carbon monoxide (CO) to such substrates. Binding energies and the frequencies of the CO stretch vibration are important observables, which are ideally suited to validate theoretical approaches. In addition, IR spectroscopy makes it possible to directly connect experiments on model systems with real catalysts [3]. Using this approach, recently it could be demonstrated that a new modification of ZnO stabilized on Cu(111) substrates is also present in the technological relevant form of ZnO-supported Cu particles used in industrial methanol synthesis [4]. Interestingly, for these systems the graphitic-like structure of ZnO coating on Cu substrates observed for the model systems [1] could be imaged for catalytically active powder particles using high-resolution TEM [5].

Here, we report on a study using vibrational spectroscopy and grazing-incidence x-ray photoelectron spectroscopy on thin ZnO layers grown by oxidizing a single-crystal Ag/Zn alloy. Again, CO was used as a probe molecule to determine the chemical activity of ZnO thin layers supported on Ag(111) substrates [6]. Interestingly, the corresponding stretch frequencies of adsorbed CO show pronounced differences to the case of Cu(111) and are in good agreement with the results of theoretical work [2]. These results demonstrate that the properties of ZnO thin layers depend crucially on the charge transfer from the metal into this oxide, opening the possibility to tune the catalytic properties of this material by varying the supporting metal.

References:

[1] V. Schott, H. Oberhofer, A. Birkner, M. Xu, Y. Wang, M. Muhler, K. Reuter, Ch. Wöll, Angew. Chemie Int. Ed., **52**, 11925–11929 (2013)
[2] S. Tosoni, C. Li, P. Schlexer, G. Pacchioni, J. Phys. Chem C, DOI: 10.1021/acs.jpcc.7b08781, (2018)
[3] Y. Wang, Ch. Wöll, Chem. Soc. Rev., 46, 1875-1932, (2017)
[4] J. Schumann, J. Kröhnert, E. Frei, R. Schlögl, A. Trunschke, Topics in Catalysis (2017) DOI: 10.1007/s11244-017-0850-9
[5] T. Lunkenbein, J. Schumann, M. Behrens, R. Schlögl, M.G. Willinger, Angew. Chemie. Int. Ed. 54, 4544, (2015)
[6] M. Andersen, X. Yu, M. Kick, Y. Wang, C. Wöll, K Reuter, submitted for publication (2018)

Fe Oxide Thin Film Growth on Pt(111) for Applications in Catalysis

Zichun Miao, Ka Man Yu, M.S. Altman

[1]*Department of Physics, Hong Kong University of Science and Technology, Hong Kong SAR, China (corresponding author: M.S. Altman, e-mail: phaltman@ust.hk)*

The discovery by Haruta et al. that Au nanoparticles dispersed on α-Fe_2O_3 and other transition metal oxides exhibit exceptionally high catalytic activity for CO and H_2 oxidation at low temperature [1,2] triggered wide interest in catalysis by Au. However, it has become clear from many studies using different industrial or wet-chemical catalyst preparations that impurities can produce extrinsic effects that obscure an understanding of these phenomena. The shortcoming of these approaches to identifying the intrinsic fundamental principles of Au nanoparticle catalysis may be addressed by investigating α-Fe_2O_3 model thin film substrates prepared under ultrahigh-vacuum (UHV) conditions and characterized using surface sensitive techniques. In order to implement this approach, an FeO monolayer is commonly used as a buffer layer to prevent interfacial alloying during the growth of thick iron oxides with higher oxidation states, Fe_3O_4 and α-Fe_2O_3, on metal surfaces. The FeO layer on Pt(111) also attracts interest in its own right because it has been shown to exhibit greatly enhanced catalytic activity under high pressure reaction conditions [3]. It has been proposed that the FeO monolayer restructures from an Fe-O bilayer to a highly reactive O-Fe-O trilayer structure that is responsible for the reactivity under reaction conditions [4].

Iron oxides that can be formed by the oxidation of Fe films using molecular oxygen at pressure that is compatible with UHV are limited to FeO or Fe_3O_4. The growth of α-Fe_2O_3 must be carried out under oxidizing conditions closer to atmospheric pressure that α-Fe_2O_3 is the most stable form. The supposed reactive form of FeO is likewise inaccessible by oxidation of Fe with molecular oxygen in the UHV-compatible range. In order to overcome these limitations, we have explored the preparation of iron oxide thin films on the Pt(111) surface at low pressure using atomic oxygen that is generated by a thermal cracker. Using low energy electron microscopy (LEEM) and low energy electron diffraction (LEED), we performed a comparative study of the growth and structure of FeO and α-Fe_2O_3 on Pt(111) using atomic and molecular oxygen. Although the observed growth modes of the FeO formed using atomic and molecular oxygen are similar, the coincidence lattices between FeO and the underlying Pt substrate produced by the two oxidizing species appear to differ in periodicity, orientation and mosaicity (Fig. 1). Oxidation using atomic oxygen also drives the formation of a higher order coincidence (HOC) lattice (Fig. 1) with a significantly reduced work function compared to the FeO layer. Thus, the identification of this new iron oxide structure may shed light on the restructuring of FeO under reaction conditions to a highly reactive form that has been proposed previously [4]. The significant differences observed here between the FeO produced

using the two species raise prospects for preparing α-Fe_2O_3 films using atomic oxygen under similar conditions. Progress in this direction will also be presented. This will advance further explorations using LEEM/LEED and other powerful surface science techniques using this model Fe oxide thin film aimed at understanding Au nanoparticle catalysis.

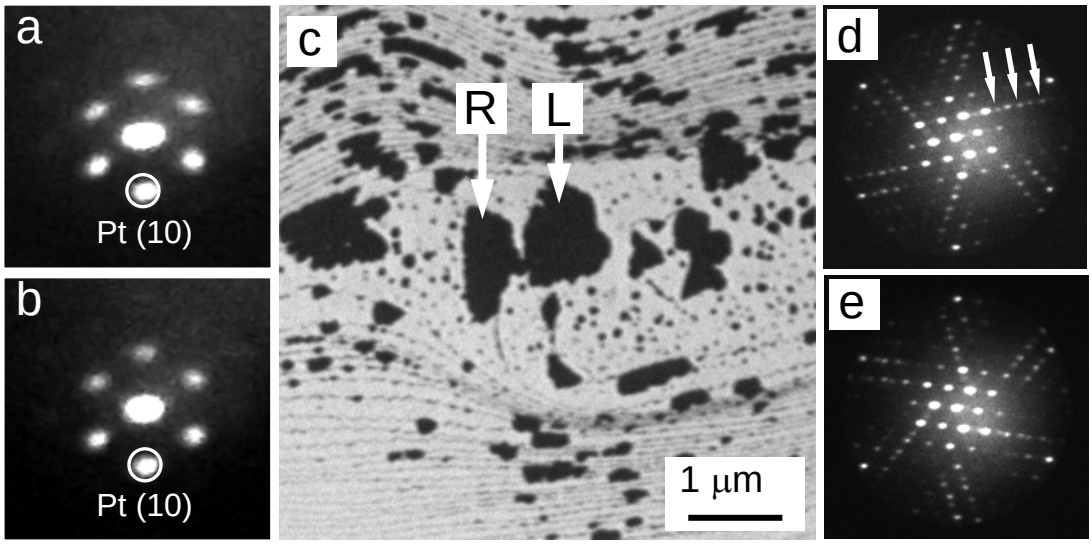

Figure 1: LEED patterns for FeO grown using (a) molecular, (b) atomic oxygen exhibit differences between superstructure spot positions and widths that correspond to differences in coincidence lattices, orientation and mosaicity. (c) LEEM image of domains with higher order coincidence (HOC) structure formed during FeO growth on Pt(111) using atomic oxygen. (d), (e) Selected area LEED patterns obtained from the HOC domains with right (R) and left (L) handed rotation identified in (c). Arrows in (d) highlight additional diffraction spots that articulate the higher order coincidence.

Support from the Hong Kong Research Grants Council (Grant No. 16300014) is gratefully acknowledged.

References

[1] M. Haruta, T. Kobayashi, H. Sano, N. Yamada, Chem. Lett. **16**, 405 (1987)

[2] M. Haruta, N. Yamada, T. Kobayashi and S. Iijima, J. Catal. **115**, 301 (1989);

[3] Y.N. Sun, Z.-H. Qin, M. Lewandowski, E. Carrasco, M. Sterrer, S. Shaikhutdinov, H.J. Freund, *J. Catal.* **266**, 359 (2009).

[4] Y.N. Sun, L. Giordano, J. Goniakowski, M. Lewandowski, Z.-H. Qin, C. Noguera, S. Shaikhutdinov, G. Pacchioni, H.J. Freund, *Angew. Chem.* **122**, 4520 (2010).

Adsorbate Phases and Structural Evolution Upon Reduction of CoO_2 Chains on Ir(100)

M. A. Schneider, P. Ferstl, M. Ammon, T. Kißlinger, M. A. Arman[1], J. Knudsen[1], E. Lundgren[1], J. Redinger[2], and L. Hammer

Lehrstuhl für Festkörperphysik, Universität Erlangen-Nürnberg, Germany
(corresponding author: M.A Schneider, e-mail: alexander.schneider@fau.de)

[1] *Division of Synchrotron Radiation Research, Department of Physics, Lund University, Sweden*

[2] *Institut für Angewandte Physik and Center for Computational Materials Science, Technische Universität Wien, A-1060 Wien, Austria*

On the Ir(100) surface one can prepare highly ordered, quasi one-dimensional, transition metal oxide chains in a (3×1) superstructure [1]. These oxide chains have an unusual MO_2 stoichiometry in which the metal atom (M = Mn, Fe, Co, Ni) is decoupled from the iridium substrate (Figure 1a).

Using the example of CoO_2 chains we analyze structural changes and phases upon adsorption and reaction with reducing species like H_2 [2] and CO in an UHV environment. Due to the long-range order of the system before and after the reactions it is possible to quantify these structural changes by means of high-precision, full-dynamical LEED analyses. Combining the detailed structural information with data obtained by HR-XPS, STM, TDS, and supporting DFT calculations we are able to follow the processes during the reactions on the atomic scale. The reduction of the CoO_2 chains by H_2 or CO is observed near room temperature and leads eventually to a well-ordered (3×1) Ir_2Co surface alloy.

When CO is adsorbed on the (3x1)-CoO_2 phase a maximum coverage of 0.37 ML (with respect to the Ir(100)-1x1 cell) is obtained below 100 K. This adsorbate phase contains CO in two different adsorption states of which the weaker bound species desorbs unreacted below 200 K. The remaining CO forms an ordered c(6×2)-(CoO_2+CO) adsorbate phase, in which CO occupies an Ir bridge site (Figure 1b). This adsorbate phase is revealed by LEED-IV analyses (R_P = 0.13) and corroborated by DFT calculations. The reduction of the oxide chains by CO proceeds from this phase whereby CO_2 desorbs immediately from the surfaces. However, increasing the temperature beyond 320 K, the initially high CO oxidation rate is reduced because the CO molecules assemble on the freshly formed Ir_2Co alloy and hence are spatially separated from the remaining intact or partially reduced cobalt oxide chains.

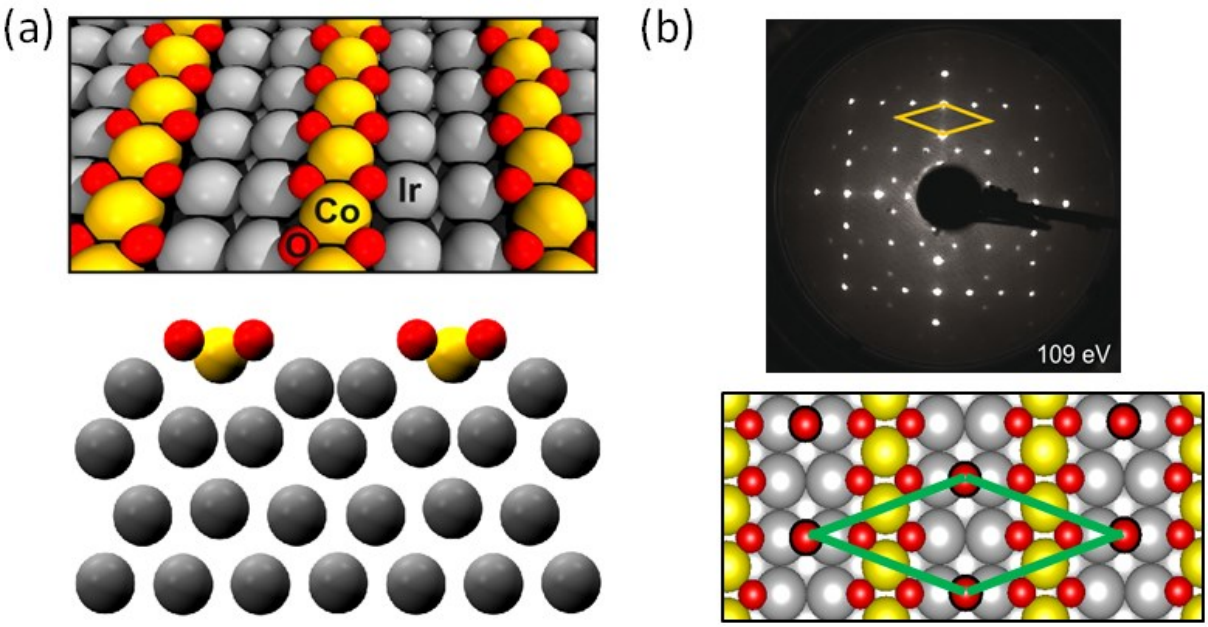

Figure 1: (a) (3×1)-CoO_2 chain structure on Ir(100) and (b) c(6x2)-(CoO_2+CO) adsorbate phase (CO: red circled in black). Shown are the best-fit models as determined by LEED structural analyses. Pendry R-factors (a) $R_p = 0.10$, (b) $R_p = 0.13$.

When the CoO_2 chains are reduced by molecular hydrogen, an intermediate, weakly ordered (6x1) phase is observed. STM results indicate that this structure consists of alternating rows of (hydrogen covered) intact CoO_2 and fully reduced Co chains. Additionally, as evidenced by HR-XPS spectra, the reaction with H_2 proceeds via the formation of an intermediate OH-species on the surface. These experimental findings will be discussed in conjunction with corresponding DFT calculations.

Support by the Deutsche Forschungsgemeinschaft (DFG) (projects COMCAT and FOR 1878“funCOS”), by the Vienna Scientific Cluster (VSC), and the MAX IV Laboratory is gratefully acknowledged.

[1] P. Ferstl, et al., Phys. Rev. Lett. **117**, 046101 (2016)

[2] P. Ferstl, F. Mittendorfer, J. Redinger, M. A. Schneider, and L. Hammer, Phys. Rev. B **96**, 085407 (2017)

From adatoms to superlattices: Sensing the spin of individual Ce-atoms

Markus Ternes[1], Christopher P. Lutz[2], Andreas J. Heinrich[3,4], and Wolf-Dieter Schneider[5,6]

[1]Max Planck Institute for Solid State Research, Heisenbergstr.1, D-70569 Stuttgart, Germany
[2]IBM Almaden Research Center, San Jose, California 95120, USA
[3]Center for Quantum Nanoscience, Institute for Basic Science (IBS), Seoul 03760, Republic of Korea
[4]Physics Department, Ewha Womans University,Seoul, Republic of Korea
[5]Ecole Polytechnique Fédérale de Lausanne (EPFL), Institut de Physique,CH-1015 Lausanne, Switzerland
[6]Fritz-Haber-Institut der Max-Planck-Gesellschaft, Faradayweg 4-6, 14195 Berlin, Germany
(e-mail: wolf-dieter.schneider@epfl.ch)

Recently, correlation-driven transport asymmetries, reminiscent of spin-polarized transport in a magnetic field, have been observed in the tunneling spectra between two magnetic impurities, one at the tip of a scanning tunneling microscope, the other one on the sample surface[1]. Here we apply this technique in zero magnetic field and at a temperature of 0.5 K, to reveal the spin of an individual Ce adatom on the surface of a Cu_2N ultrathin film. The presence of the Ce 4f spin manifests itself in the differential conductance spectra recorded in a tunneling junction between a PtIr tip, functionalized with a Ce-cluster at its apex, and a single Ce adatom on the sample surface. By identifying this cluster as a Ce-trimer at the tip apex via its Kondo and spin excitation spectrum a fundamental understanding of the manifestations of the 4f spin in Ce adatoms is obtained. The three Ce-atoms forming the trimer are shown to couple ferromagnetically to a total spin of 3/2 with a degenerate Kondo ground state of spin 1/2 [2]. The degeneracy of the ground state of the Ce-trimer at the tip is gradually lifted by decreasing the tunneling resistance (decreasing the tip surface distance) and thereby increasing the interaction with the 4f spin of a single Ce-adatom at the sample surface. The induced splitting of this spin ½ system of about 2 meV corresponds to an effective magnetic field of 5 Tesla. Thus, employing the vertical atom manipulation capabilities of the STM, the functionalized tip is used as a spin detector for single magnetic Ce-adatoms in the absence of an external magnetic field. This achievement indicates an alternative route to the study of magnetic nanostructures circumventing the application of spin-polarized STM tips.

When Ce-atoms assemble to create a superlattice on Ag(111) with an interatomic lattice spacing of 3.2 nm [3], a Kondo lattice is formed. The differential conductance spectra obtained on single Ce-adatoms within the superlattice reveal a considerably broadened Kondo resonance of about 70 meV as compared to the one of 1 meV found for isolated Ce-trimers, indicating the presence of antiferromagnetic indirect exchange interactions (RKKY) in the superlattice. In the light of these experimental results, the present study opens new insights into the interplay between Kondo physics, localized spin-flip excitations, and the magnetic exchange interaction.

[1] M. Muenks, P. Jakobson, M. Ternes, and K. Kern, Nature Comm. **8**, 14119 (2017).

[2] A. F. Otte, M. Ternes, K. von Bergmann, S. Loth, H. Brune, C. P. Lutz, C. F. Hirjibehedin, and A. J. Heinrich, Nature Physics **4**, 847 (2008).

[3] F. Silly, M. Pivetta, M. Ternes, F. Patthey, J. P. Pelz, and W.-D. Schneider, Phys. Rev. Lett. 92, 016101 (2004)

From gas-phase oxide clusters to 2-D oxide layers: Tungsten oxide on Ag(100)

Falko P. Netzer,* Thomas Obermüller, Svetlozar Surnev

Surface and Interface Physics, Institute of Physics, Karl-Franzens University Graz, A-8010 Graz, Austria

*falko.netzer@uni-graz.at

Two-dimensional (2-D) transition metal oxide layers have attracted significant interest during the past decade due to their novel emergent properties and high potential for nanotechnology applications [1,2]. For practical reasons 2-D oxide layers are usually supported on metal surfaces. This leads to a coupling of the oxide overlayer to the metal substrate, often strong coupling, which creates a metal-oxide hybrid system with properties that are largely determined by the oxide-metal interface. Here, we report the formation of a 2-D W-oxide layer on a Ag(100) surface, where the oxide appears to be only weakly coupled to the substrate. The 2-D W-oxide layer has been prepared by a vapor phase deposition methodology, involving adsorption of gas phase $(WO_3)_3$ molecular clusters onto Ag(100) and subsequent condensation of the clusters into a 2-D oxide layer at elevated temperature [3]. The WO_x grows in the form of a well-ordered incommensurate 2-D wetting layer, with mesoscopically large domains in a variety of azimuth orientations with respect to the substrate. The different azimuth orientations of the oxide domains can easily be recognized in LEED and in the STM by their different Moiré patterns. The overlayer lattice can be imaged with atomic resolution in the STM and analyzed using the Moiré formula, from which the square overlayer lattice constant can be accurately evaluated to a = 3.72 Å; this is close to the respective WO_3 bulk lattice constant. AES and XPS spectra indicate an overlayer stoichiometry close to WO_3, although the W 4f peaks occur at a lower binding energy than characteristic for W^{6+}. Structure models in terms of 2-D WO_x sheets are proposed. The oxide lattice is elastically flexible as demonstrated by the easy distortion in the vicinity of defects. It is suggested that this incommensurate, rotationally disordered WO_x sheet on Ag(100) behaves essentially like a decoupled 2-D oxide layer. Interestingly, despite this weak overlayer-substrate interaction, an unusual anisotropic behavior is observed for the growth of WO_3 beyond the monolayer, where unidirectional needle formation suggests a symmetry break of the square lattices. A second-order interfacial strain interaction effect is conjectured.

[1] G. Pacchioni, *Two-dimensional oxides: multifunctional materials for advanced technologies.* Chem. Eur. J. 18(2012) 10144

[2] *Oxide materials at the two-dimensional limit.* F.P. Netzer, A. Fortunelli, Eds. (Springer Series in Materials Science, Vol. 234, Springer 2016)

[3] T. Obermüller, N. Doudin, D. Kuhness, S. Surnev, F.P. Netzer, *Ultrathin oxide films: epitaxy at the two-dimensional limit,* J. Mater. Res. 32 (2017) 3924

Inforcing strong correlation effects into Graphene

U. Starke, S. Link, S. Forti, A. Stöhr, M. Roesner[1], D. Hirschmeier[2], C. Chen[3], J. Avila[3], M.C. Asensio[3], A.A. Zakharov[4], T.O. Wehling[1], A.I. Lichtenstein[2], M.I. Katsnelson[5]

Max-Planck-Institut für Festkörperforschung, Heisenbergstr. 1, D-70569 Stuttgart, Germany
(corresponding author: U.Starke, e-mail: u.starke@fkf.mpg.de)

[1]*Univ. Bremen, Inst. Theoret. Phys., POB 330 440, D-28334 Bremen, Germany*

[2]*Univ. Hamburg, Inst. Theoret. Phys., D-20355 Hamburg, Germany*

[3]*Synchrotron SOLEIL & Université Paris-Saclay, Orme des Merisiers, Saint-Aubin-BP 48, 91192 Gif sur Yvette, France*

[4]*MAX IV laboratory, Lund University, Ole Römers väg 1, 22363 Lund, Sweden*

[5]*Radboud Univ. Nijmegen, Inst. Mol. & Mat.,Heijendaalseweg 135, 6525 AJ Nijmegen, Netherlands.*

Wafer scale epitaxial graphene grown on Silicon Carbide (SiC) is regarded as a suitable candidate for carbon based electronics. Yet, the peculiar physical properties of graphene are also promising for complementary applications such as sensing, quantum metrology and even superconductivity seems possible. The electronic and structural properties of the graphene layer can be manipulated by functionalizing the graphene/SiC interface on an atomic scale. Intercalation under the first carbon layer can relieve the covalent bonds of its atoms to the SiC(0001) substrate and manipulate the π-band structure in a large range of aspects.

By intercalation various materials, the carrier concentration in the epitaxial graphene layer can be tailored in a wide range by design. At extreme doping levels, the electronic spectrum of a graphene monolayer is influenced by severe renormalization effects. When approaching the Van Hove singularity (VHs) at the Fermi level, which corresponds to the saddle point at the $\overline{\mathrm{M}}$-point in the π-band dispersion, a flat band develops near the Fermi level over a range of about 1 A^{-1}, connecting the $\overline{\mathrm{K}}$- and $\overline{\mathrm{K}}'$-points. We show, that this then called extended VHs (eVHs) state can be induced by the intercalation of Gd in the so-called zero-layer graphene on SiC(0001). The energetic shift of the electronic bands is accompanied by a strong bending of the bands in the vicinity of the Fermi energy. This strong alteration of the π-band shape can be explained by electron-electron interaction. Additionally, strong electron-phonon coupling is observed. On the flat band section near the Fermi level (along the Brillouin zone boundary, i.e. $\overline{\mathrm{K}}$-$\overline{\mathrm{M}}$-$\overline{\mathrm{K}}'$), correlation effects with the optical phonon branch of graphene result in the formation of a polaron. In the steeper sections of the π-band (between the $\overline{\Gamma}$- and the $\overline{\mathrm{K}}$-point),

the electron-phonon interaction leads to strong renormalization effects. By Fermi surface nesting also lower energy phonons are involved. This combination leads to an unprecedented electron-phonon coupling strength.

The Gd intercalated epitaxial graphene systems was investigated using various surface science techniques. The atomic structure and chemical bond configuration were studied using low-energy electron diffraction (LEED) and X-ray photoelectron spectroscopy (XPS), respectively. The electronic structure is analyzed using angle-resolved photoemission spectroscopy (ARPES). The spatial homogeneity of the graphene layers is controlled *in situ* by low energy electron microscopy (LEEM), μ-LEED, photoelectron microscopy (PEEM) and μ-XPS. In addition, the electronic structure can be resolved on the nanoscale using μ-ARPES in the LEEM and a nano-ARPES beamline.

This work was supported by the Deutsche Forschungsgemeinschaft within the framework of the Priority Programme 1459 Graphene (Sta315/8-1,2) and within the Flag-ERA project TAILSPIN (Sta315/8-1). This research was partially funded by the European Community's Seventh Framework Programme: Research Infrastructures (FP7/2007-2013) under grant agreement no 226716. We are indebted to the staff at MAX-Lab (Lund, Sweden), BESSY II (Berlin, Germany) and SOLEIL (Gif-sur-Yvette, France) for their advice and support.

Structure of Si layers on Ag(111) and mechanism for the stabilization of epitaxial silicene

A. Curcella,[1] R. Bernard,[1] Y. Borensztein,[1] H.Cruguel,[1] M. Lazzeri[2], Y. Garreau,[3] A. Resta,[3] and G. Prévot[1]

[1]*Sorbonne Universités, UPMC Univ Paris 06, CNRS-UMR 7588, Institut des NanoSciences de Paris, F-75005, Paris, France*
(corresponding author: A. Curcella, e-mail: alberto.curcella@gmail.com)
[2]*Sorbonne Universités, UPMC Univ Paris 06, CNRS-UMR 7590, MNHN, IRD UMR 206, Institut de Minéralogie, de Physique des Matériaux et de Cosmochimie, F-75005, Paris, France*
[3]*Synchrotron SOLEIL, L'Orme des Merisiers Saint-Aubin - BP 48 91192 Gif-sur-Yvette CEDEX*

In the last decade, the advent of graphene has stimulated the research 2D materials. An outstanding example is silicene, the bidimensional allotrope of silicon, for which a metastable configuration, consisting in a low-buckled hexagonal structure, has been predicted.[1] The great interest in such a material resides in the exciting properties that its free-standing form should possess: Dirac cones, quantum spin Hall effect, giant magneto-resistance and many others. Experimentally, silicene cannot be obtained by exfoliation of the bulk material, as in the case of graphene, phosphorene and chalcogenides. The successful growth of epitaxial silicene monolayers (MLs) has been reported on several substrates; the most thoroughly studied is Ag(111). On this surface, various ordered structures coexist which display a buckled hexagonal organization,[2] but the strong interaction with the Ag(111) substrate modifies the electronic properties which are far from the one expected for a free-standing silicene layer.[3]

By analogy with graphene multilayers, attempts have been made to synthesize silicene multilayers that would be decoupled from the Ag(111) substrate. It has been reported that, below 540 K, a pseudo layer-by-layer growth is observed, leading to the growth of a thin Si film terminated by a $(\sqrt{3}\times\sqrt{3})R30°$ reconstruction. On the basis of *ex-situ* X-ray diffraction[4] and Raman spectroscopy, such films have been described as multi-layer silicene or silicite, i.e. the silicon counterpart of graphite. Accordingly, several models have been put forward, based on density functional theory (DFT) simulations. Yet, spectroscopic and microscopic studies have shown the presence of Ag atoms segregating at the surface of the Si films, revealing similarities between the observed $(\sqrt{3}\times\sqrt{3})R30°$ and the well-known Ag/Si(111) reconstructions, in agreement with independent low-energy electron (LEED) and optical studies[5]. In order to discern between the two proposed interpretations, we have performed real-time in-situ experiments.

Concerning the determination of the atomic structure of the Si film and of the (√3×√3)R30°, we have first performed, in the temperature regime where multi-layer silicene has been claimed to form, grazing incident X-ray diffraction (GIXD), Auger electron spectroscopy (AES) and surface differential reflectance spectroscopy (SDRS). GIXD and SDRS results demonstrate that the Si film shows a diamond-like structure, unambiguously rejecting the hypothesis of a new layered allotrope of Si. Moreover, AES confirms the Ag segregation at the surface, even for large Si coverages (> 10 MLs) whereas the GIXD intensities of the (√3×√3)R30° reconstruction are well reproduced by the Ag/Si(111) model, while all the Ag-free models proposed in the literature fail to reproduce our data[6].

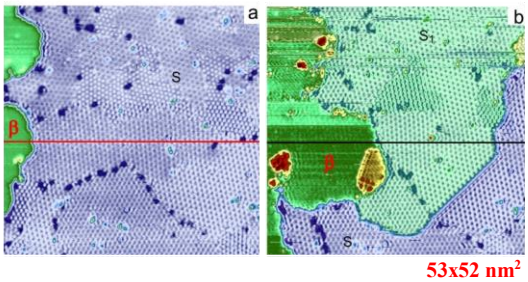

Light blue and light green: silicene
Forest green: (√3×√3)R30°

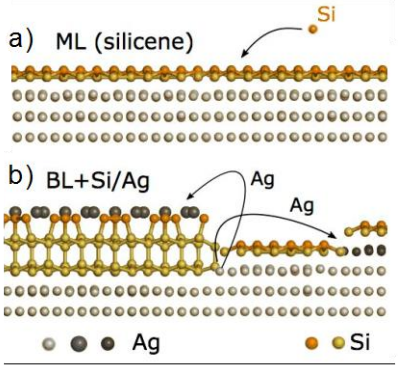

Figure 1
Left: real-time STM images of the same area. (√3×√3)R30° grows and Ag atoms insert below silicene. *Right*: schematics of the associated process.

However, few open questions still remain unanswered after these evidences. In particular, how does the surface evolve from a single silicene layer to a thick bulk Si film terminated by Ag? Moreover, silicene is commonly obtained in standard growth conditions, despite being energetically unfavored with respect to diamond bulk. What mechanism ensures its stability? We have addressed these questions by performing a combined STM and DFT study. Experimentally, we have followed in real-time the first stages of growth beyond the Si ML. We have observed that the formation of the second layer, terminated by the (√3×√3)R30° reconstruction, is concomitant with the insertion of Ag atoms below the remaining silicene layer (Fig. 1 left). The only possible explanation, confirmed by ab-initio thermodynamics based on DFT calculations, is that there is a direct transition from the silicene layer to a Si bilayer structure, which grows digging in the Ag substrate and expulsing Ag atoms, which can reinsert below the first Si sheet (Fig. 1 right). The high kinematic barrier of the process is the key behind the stability of the metastable silicene layer.[7] Such model is further used simulate the evolution of AES intensities during growth. A very good agreement is found between experimental and simulated intensities, which cannot be reproduce in the framework of "multilayer silicene".[8]

Fundings: Cluster of Excellence MATISSE led by Sorbonne Universités

[1] S. Cahangirov et al., *Phys. Rev. Lett.*, 2009, **102**, 236804.
[2] P. Vogt et al., *Phys. Rev. Lett.*, 2012, **108**, 155501.
[3] S.K. Mahathaet et al., *Journal of Electron Spectroscopy and Related Phenomena*, 2016, **219**, 0368-2048
[4] P. De Padova et al., *2D Mater.,* 2016, **3**, 031011
[5] Y. Borensztein et al., Phys. Rev. B, 2015, **92,** 155407
[6] A. Curcella, et al., *2D Mater.*, 2017, **4**, 025067.
[7] A. Curcella et al., Nanoscale 2018
[8] A. Curcella et al., Beilstein J. Nano. 2018

Exploring optoelectronic properties of point defects in monolayer WS_2 with atomic resolution

B. Schuler, C. Kastl, C. Chen, S. Refaely-Abramson, S. Yuan[1], R. Roldan[2], N. Borys, T. Kuykendall, R. Koch[3], F. Ogletree, J. Neaton, S. Aloni, A. Schwartzberg, and A. Weber-Bargioni

Molecular Foundry, Lawrence Berkeley National Laboratory, Berkeley, USA
(corresponding author: B. Schuler, e-mail: bschuler@lbl.gov)

[1] *Department of Physics, Wuhan University, Wuan, China*

[2] *Instituto de Ciencia de Materiales de Madrid, Madrid, Spain*

[3] *Advanced Light Source, Lawrence Berkeley National Laboratory, Berkeley, USA*

The advent of transition metal dichalcogenides (TMDs) and other two-dimensional (2D) materials has attracted considerable attention due to unique material properties emerging from their reduced dimensionality. Because of this strong confinement, structural defects greatly modify such properties and have therfore become of increasing interest to the 2D materials community. Particularly the creation of in-gap defect states is decisive for their optoelectronic properties and catalytic activity.

Using low-temperature scanning probe microscopy with CO functionalized tips we identified and characterized common point defects in monolayer WS_2: sulfur vacancies in the top and bottom chalcogen layer, sulfur antisite defects, molybdenum impurities and a composite defect involving a top or bottom sulfur vacancy (see Fig. 1).

We could show that out of these defects only the S antisite (S_W) and the composite defect creates defect states within the band gap of WS_2. Interestingly, both of these point defects exhibit spin-orbit split defect states with a splitting on the order of 100 meV. For the composite defect that features narrow defect resonances of 9 meV, phonon satelite peaks and a charging peak were identified as well.

The same sample was also characterized with nano-ARPES and photoluminescence specroscopy, which shows that thermally grown graphene on SiC consitutes a suitable platform for cross-correlation microscopy of TMD materials (and potentially other van der Waals materials) in both, UHV and ambient conditions.

The atomic-scale characterization allows an unprecedentedly detailed picture on the structure and functionality of point defects in 2D-TMDs.

B.S. gratefully acknowledges support by the Swiss National Science Foundation.

Fig. 1: (a-f) STM topography of different point defects of CVD-grown monolayer WS_2 on multilayer graphene on SiC. (g-l) CO-tip AFM images of the same defects with the unit cell of WS_2 indicated. (m-r) Strain map derived from the AFM measurements.

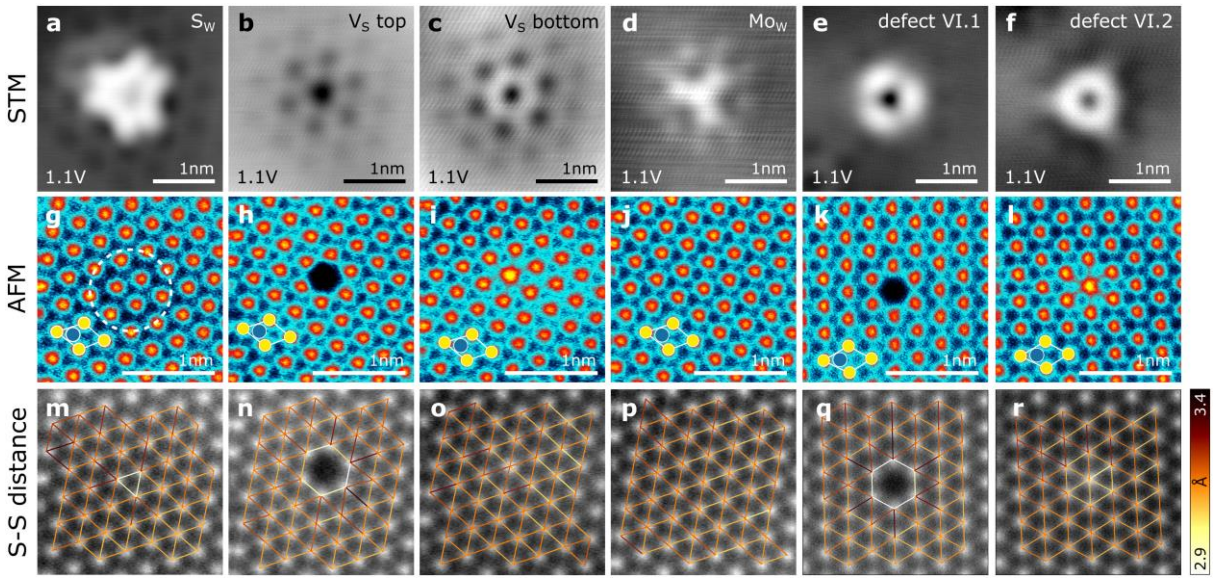

Mechanism of gold intercalation under monocrystalline graphene synthesized on Ni(111) by TPG

T. V. Pavlova, S. L. Kovalenko, K. N. Eltsov

A.M. Prokhorov General Physics Institute, RAS, Moscow, Russia
(corresponding author: K.N. Eltsov, e-mail: eltsov@kapella.gpi.ru)

Understanding the mechanism of the intercalation of foreign atoms into the interlayer "graphene/ substrate" is key point to creating a quasi-freestanding graphene in CVD (Chemical Vapor Deposition) or TPG (temperature programmed growth) processes on the surface of active (catalytically active) metals such as Ni , Co, Ru, Ir, etc. Due to interaction with the bulk states of the substrate (usually d-states), the resulting graphene layer does not have a linear dispersion of electrons. Atoms of noble metals (usually gold) are intercalated to separate graphene from such a substrate. As a result, the carbon monolayer acquires all the features inherent in graphene, the atomic structure and linear dispersion of electrons (the Dirac cone), since it becomes weakly bound to the substrate.

Until now, the intelligible answer to the question of how the atoms of gold (or other foreign atoms) penetrate graphene does not exist for a number of reasons. First, few people succeed in obtaining monocrystalline monolayer graphene, and for polycrystalline graphene it is considered that intercalation can be carried out through grain (domain) boundaries, although this issue has not been essentially studied. Secondly, there are practically no works in which mechanisms of intercalation of foreign atoms would be studied at the atomic level *in situ*.

Recently [1], monocrystalline graphene monolayer of size 6x6 mm has been synthesized on Ni(111) by TPG: propene adsorption at 25° C and annealing at 500°C. The method allowed us to grow epitaxial graphene without rotated domains, and the only defects are point defects, which we attribute to Ni atom in C vacancy (or divacancy). We experimentally, step by step at the atomic level, studied the intercalation of gold for such graphene. As a result of gold intercalation at 450° C, graphene monolayer is detached from nickel without any damage and point defects are disappeared. After intercalation by gold atoms, angle resolved photoemission spectroscopy (ARPES) measurements show perfect Dirac cone in electron dispersion corresponding to quasi free-standing graphene.

The density functional theory (DFT) calculations were performed to understand the mechanism of gold intercalation at the graphene/Ni(111) interface. All calculations have been done using VASP code [2] with PAW potentials [3] (400 eV cut-off) and GGA PBE exchange-correlation functional [4] as the basis for the DFT-D2 (Grimme) correction [5]. The reaction barriers were evaluated using the nudged elastic band (NEB) method [6] implemented into VASP.

Different scenarios of intercalation process have been tested. The pathway for gold atoms penetration underneath a perfect graphene monolayer on Ni(111) has very high activation energy due to strong C-C bonds in graphene, in agreement with other calculations for Pd intercalation at the interface graphene/Ru(0001) [7]. According to our calculations, C-C bond breaking in graphene near C vacancy is easier than that in the absence of defect. It means that collective mechanism of Au atoms penetration can be through C atoms dissolution in nickel and re-grown of graphene after all Au atoms reach Ni surface. Also, we discuss intercalation process when one metal atom penetrates through single atom vacancy (or bivacancy) in graphene on Ni(111). Theoretically investigated mechanisms of gold atoms penetration through graphene via vacancies are consistent with our STM experiments. According to STM images, most of intercalated islands are located close to chains of point defects (see fig.1).

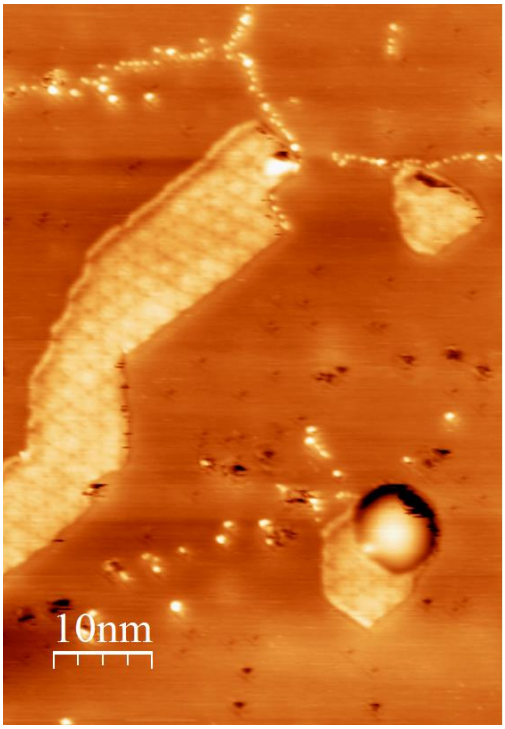

Thus the mechanisms of gold penetration into graphene on the surface of nickel (111) are proposed and justified.

Figure 1. STM image of the graphene on Ni (111) after deposition of gold (substrate temperature 450 °C) of 0.14 ML. The presence of islands with the superstructure 9.5x9.5 means the formation of dislocation loops Ni(111)-9.5x9.5-Au in upper layer of Ni substrate, which confirms the gold intercalation in the graphene/Ni (111) interface. It can be seen that all islands of intercalate are formed near atomic defect chains

This work was supported in part by grant of the Russian Science Foundation (Grant 16-12-00050). We are grateful to the Joint Supercomputer Center of RAS for the possibility of using their computational resources for our calculations.

[1] S. L. Kovalenko, T. V. Pavlova, B. V. Andryushechkin, O.I. Kanishcheva, K. N. Eltsov. JETP. Lett. 105, 170 (2017).

[2] G. Kresse and J. Hafner, Phys. Rev. B **47**, 558 (1993).

[3] G. Kresse and D. Joubert, Phys. Rev. B **59**, 1758 (1999).

[4] J. P. Perdew, K. Burke, and M. Ernzerhof, Phys. Rev. Lett. **77**, 3865 (1996).

[5] S. Grimme, J. Comput. Chem. **27**, 1787 (2006).

[6] H. Jonsson, G. Mills, K. W. Jacobsen, *Classical and Quantum Dynamics in Condensed Phase Simulations*; World Scientific: Singapore (1998).

[7] Li Huang, Yi Pan, Lida Pan, Min Gao, Wenyan Xu, Yande Que, Haitao Zhou, Yeliang Wang, Shixuan Du, and H.-J. Gao, Appl. Phys. Lett. **99**, 163107 (2011).

Innovative SPM and XPS Solutions for Surface Analysis

POLAR Bath Cryostat UHV SPM

qPlus® and STM
Bath Cryostat
3D Coarse Motor
5K-300K
Optical Access to Tip & Sample
Hold Time: > 200h
Peerless Helium Consumption
B_z = ±5T (option)

INFINITY Closed Cycle UHV SPM

qPlus® and STM
Pulse Tube Cryostat
3D Coarse Motor
10K-300K
No Helium Consumption
Interruption Free: No Cryostat Refill
Acoustic Noise Cancellation

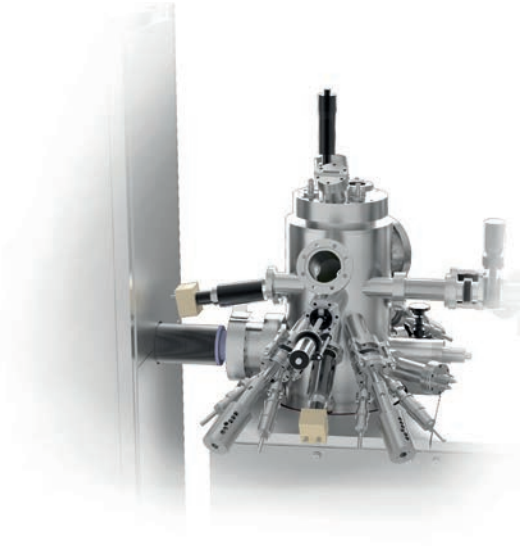

STREAM Flow Cryostat UHV SPM

qPlus® and STM
Flow Cryostat for LN_2 and LHe
3D Coarse Motor
9K-300K

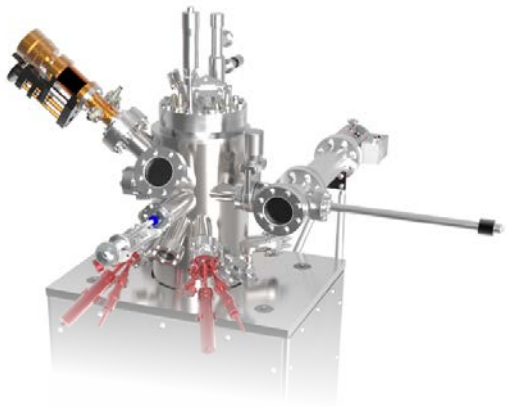

NEW
upgradeable
1.5K option
for POLAR!

PULSE for Dynamic XPS

Real-time Observation of Surface Transformations
Fast Data Acquisition
High Transmission Aspect Analyser and Sophisticated Neo Control Suite
High Power Monochromated and Dual-anode X-ray Source
Flexible and Fully Accessible System Layout

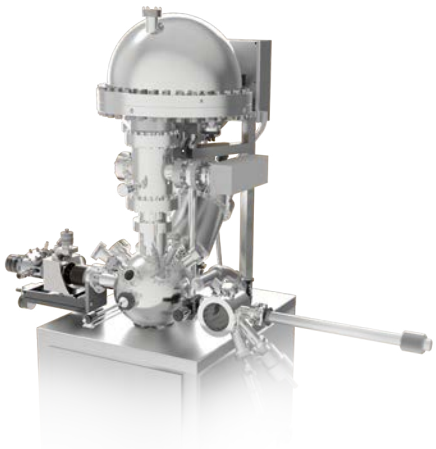

ASPECT Analyser

Highest Transmission
Snapshot Capability with Multichannel Detector
Energy Range up to 3.5 keV
Dynamic XPS with Multi Peak Monitoring
Fast XPS with Survey Spectrum Acquisition in 2 Seconds
Neo Control Suite for Advanced Data Acquisition

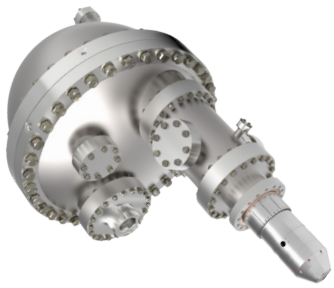

Discover more about our new low-temperature SPMs and XPS Instruments.

Contact Us:
sales@mantis-sigma.com
www.sigma-surface-science.com

SIGMA Surface Science
Partnered with MANTIS Deposition

Tuesday

Carbon Nanomembranes with sub-nanometer channels: Two-dimensional materials for water purification with high selectivity and highest permeance

Yang Yang, Petr Dementyev, Niklas Biere, Daniel Emmrich, Patrick Stohmann, Riko Korzetz, Xianghui Zhang, André Beyer, Sascha Koch, Dario Anselmetti and Armin Gölzhäuser

Faculty of Physics, Bielefeld University, 33615 Bielefeld, Germany
e-mail: ag@uni-bielefeld.de

Clean water is a global challenge, and membrane filtration is a key technology to achieve it. We report on the fabrication, characterization and application of terphenylthiol carbon nanomembrane (TPT-CNM), a 2D-material perforated by sub-nanometer channels. We show that free-standing TPT-CNMs are excellent water filters, combining a high selectivity with a record-breaking water permeance.

TPT-CNMs are fabricated from terphenylthiol molecules by a well-established procedure [1] of (i) self-assembled monolayer formation on a gold surface, (ii) electron radiation induced cross-linking, and (iii) a lift-off of the 2D network of cross-linked molecules, cf. Fig. 1. This results in the creation of a ~1.2 nm thick carbon nanomembrane that is perforated by a network of sub-nanometer channels. The channels can be clearly seen by tapping mode atomic force microscopy, cf. Fig. 2. Analysis of the AFM images yields average channel diameters below ~0.7 nm and areal channel densities of $\sim 10^{18}$ m^{-2}.

We tested TPT-CNMs as molecular filter membranes and found that they efficiently block the passage of most gases and liquids. However, water passes through, and it does this with a record-breaking permeance of $\sim 1.1 \times 10^{-4}$ $mol \cdot m^{-2} \cdot s^{-1} \cdot Pa^{-1}$, cf. Fig. 3. This suggests that water molecules translocate fast and cooperatively through the sub-nanometer channels. Assuming all channels in a TPT-CNMs are active in mass transport, we find a single-channel permeation of ~66 water molecules$\cdot s^{-1} \cdot Pa^{-1}$. We will compare this with molecular transport through other carbon nanoconduits, such as carbon nanotubes or membrane proteins (aquaporins) [3,4,5]. As the fabrication of TPT-CNMs is scalable, their utilization opens a path towards the application of 2D-materials in energy-efficient water purification.

[1] A. Turchanin and A. Gölzhäuser: Carbon Nanomembranes, *Adv. Mater*. **2016,** 28, 6075.
[2] Y. Yang, P. Dementyev, N. Biere, D. Emmrich, P. Stohmann, R. Korzetz, X. Zhang, A. Beyer, S. Koch, D. Anselmetti, A. Gölzhäuser, submitted **2017**.
[3] B. Corry, *J. Phys. Chem. B* **2008**, *112*, 1427.
[4] T. Walz, B. L. Smith, M. L. Zeidel, A. Engel, P. Agre, *J. Biol. Chem.* **1994**, *269*, 1583.
[5] M.J. Borgnia, D. Kozono, G. Calamita, P.C. Maloney, P. Agre, *J. Mol. Biol.* **1999**, *291*, 1169.

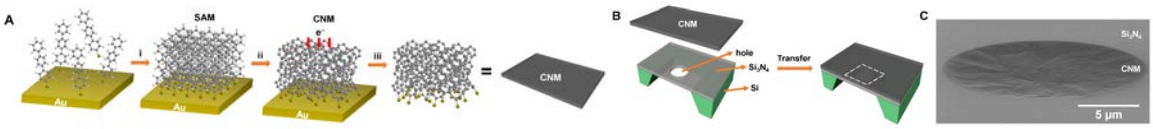

Figure 1. Fabrication and transfer of TPT-CNMs. A) Fabrication of CNMs: i) TPT self-assembles on a gold substrate; ii) Exposure to electrons forms intermolecular crosslinks and the SAM is converted into an CNM; iii) CNM detaches from the substrate. B) Schematic of transferring the CNM onto a Si_3N_4/Si chip with a 18 µm hole. Area with dashed lines indicates the image area shown in C). C) HIM image of a CNM suspended over the hole.

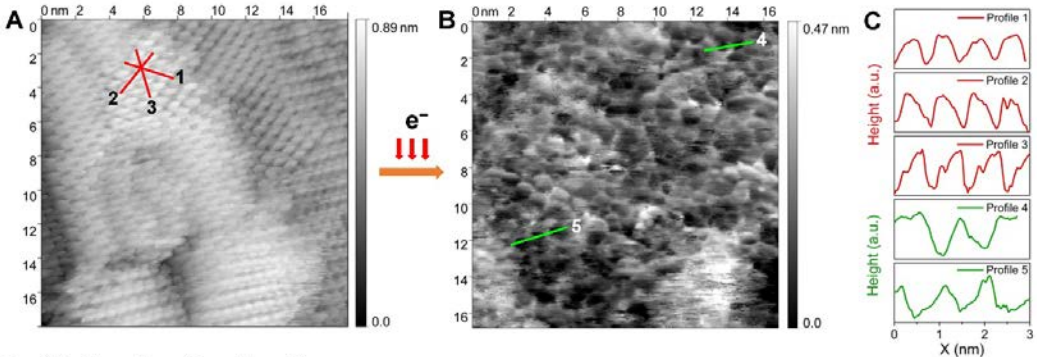

Figure 2. Morphology of TPT SAM and TPT-CNM. A) STM image of TPT SAM at room temperature in ultra-high vacuum (U_{Bias} = 500 mV, I_T = 70 pA). B) AFM image of TPT-CNM measured at 93 K in UHV in tapping mode. C) Line profiles in A) (red lines) and B) (green lines). Profiles 1–3 of TPT SAM show an intermolecular distance of ~0.8 nm. Profiles 4 and 5 of TPT-CNM indicate a pore diameter of ~0.6 nm.

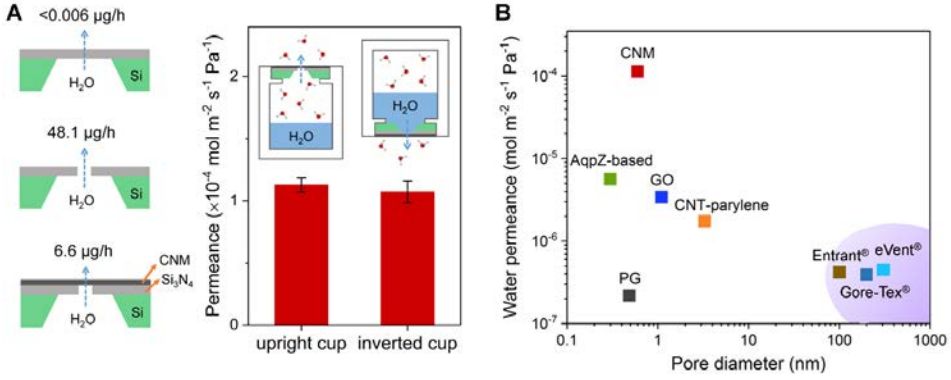

Figure 3. Comparative permeances of freestanding TPT-CNMs. **A**) Mass loss measurements; the left panel shows mass loss rates measured for Si_3N_4/Si chip (top), an 18-µm-sized hole open (middle) and covered with TPT-CNMs (bottom). The right panel shows water permeance of TPT-CNMs — upright cup (liquid water not in contact with CNMs) inverted cup (liquid water in contact with CNMs). B) Water permeance of TPT-CNMs and other membranes: commercial polymers, CNT-parylene composite films, membrane proteins (AqpZ aquaporin), perforated graphene (PG) with pore diameter of ~0.5 nm and porosity of 0.6% and graphene oxide (GO) as a function of pore diameter.

On the role of steps in catalysis

Benjamin Hagman, Andreas Schaefer[1], Chu Zhang, Mikhail Shipilin, Lindsay Merte[1], Baochang Wang[1], Sara Blomberg, Xueting Wang[1], Per-Anders Carlsson[1], Anders Hellman[1] Edvin Lundgren, Alvaro P. Borbon[1], Henrik Grönbeck[1] and Johan Gustafson

Synchrotron Radiation Research, Lund University, Box 118, 22100 Lund, Sweden
(corresponding author: J. Gustafson, e-mail: johan.gustafson@sljus.lu.se)

[1]*Chalmers University of Technology, SE-412 96, Gothenburg, Sweden*

Due to their higher reactivity, undercoordinated surface sites, such as steps and kinks, are generally believed to play a crucial role in many catalytic reactions. A closer look at the kinetics, however, suggests that the effect of such sites should, in many cases, result in a lower catalytic activity, since the higher reactivity results in a tighter binding of the reactants to the surface. We have studied the effect of steps on dissociative adsorption of CO_2 on Cu as well as CO oxidation on Rh, using *in-situ* X-ray photoelectron spectroscopy (XPS) and density functional theory. In both cases, we find a positive effect of the steps on the catalytic activity, but the mechanisms behind the effect are very different.

A promising way to reduce the greenhouse effect and slow down global warming is to recycle CO_2 instead of releasing it into the atmosphere. In order to develop this kind of catalysis further, it is crucial to understand the interaction between CO_2 and relevant surfaces in detail. Last year, we presented a high-pressure (HP) XPS study of the CO_2 adsorption on Cu(100). We found that the CO_2 adsorbs dissociatively followed by CO desorption, leaving O on the surface in structures similar to those found from O_2 exposure. The corresponding uptake is shown in Figure 1, where the most surprising detail is the linear increase of the oxygen coverage up to 0.25 ML and then further up to 0.5 ML.

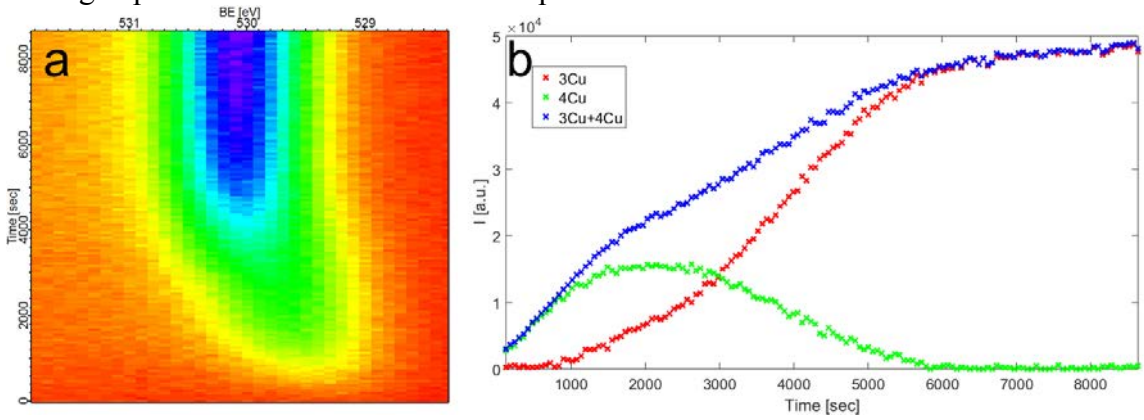

Figure 2: Uptake of CO_2 on Cu(100). a) 2D plot clearly showing a shift towards higher binding energy as the O coverages increases. b) The peak areas as a function of exposure time. After about 1500 seconds, the adsorption speed drops as the component corresponding to 4-fold coordinated O atoms (4Cu) stops increasing and the 3Cu peak becomes significant, at a coverage of about 0.25 ML.

Since last year we have complemented this study with further DFT calculations. The results show that the dissociation occurs at the steps and the resulting surface oxygen diffuses out on the terraces. In this way, the active sites are always kept free and that dissociation rate is constant during building up of the O structures. This may also resolve some of the disambiguates in previous studies, for instance by Eren *et al.* [1].

In the second study, we have followed the reaction between gas-phase CO and preadsorbed O on Rh(553). The reaction rate on this surface at room temperature is approximately as high as on Rh(111) at 100°C, showing that the steps have a positive effect on the catalytic reaction. The reaction slows down after removal of 50% of the oxygen, however, and the O atoms that are left are adsorbed to the steps. Hence, the reaction rate is not high on the steps. Instead, our DFT calculations show that the reaction occurs on a site on the terrace but close to the step, where the reaction barrier is lowered due to relaxation enabled by the step, as has previously been found for Pd [2]. When the O atoms in these active sites are removed, the reaction proceeds by diffusion of O to these sites.

Support by the Knut and Alice Wallenberg Foundation, the Swedish Research Council and the Röntgen-Ångström Cluster is gratefully acknowledged.

[1] B. Eren, R. S. Weatherup, N. Liakakos, G. A. Somorjai and M. Salmeron, J. Am. Chem. Soc. **138**, 8207−8211 (2016).

[2] S. Blomberg *et al.*, ACS Catalysis **7**, 110-114 (2016).

Operando sum frequency generation (SFG) spectroscopy at atmospheric pressure: Cu clusters and Pt/ZrO_2

Matteo Roiaz, Verena Pramhaas, Xia Li, Christoph Rameshan, and Günther Rupprechter*

Institut für Materialchemie, Technische Universität Wien, 1060 Vienna, Austria
(corresponding author: G. Rupprechter, e-mail: guenther.rupprechter@tuwien.ac.at)

We have recently designed a new "high pressure cell" for *operando* IR-vis sum frequency generation (SFG) spectroscopy during atmospheric pressure catalytic reactions [1,2]. The new SFG cell is coupled to an ultra-high vacuum (UHV) chamber (Figure 1) for surface preparation and characterization (low energy electron diffraction LEED, Auger electron spectroscopy AES). A transfer mechanism moves the sample under UHV to the SFG cell, where spectroscopy and catalytic tests (reactant/product analysis by mass spectrometry and gas chromatography) are performed *simultaneously*.

For post-reaction analysis, the SFG cell is rapidly evacuated and samples are transferred back to the UHV chamber. The new setup allows to perform surface science, SFG spectroscopy, catalysis, and electrochemical investigations on model systems, including single crystals, thin films, and deposited metal nanoparticles, under well-controlled conditions of gas composition, pressure, temperature, and potential.

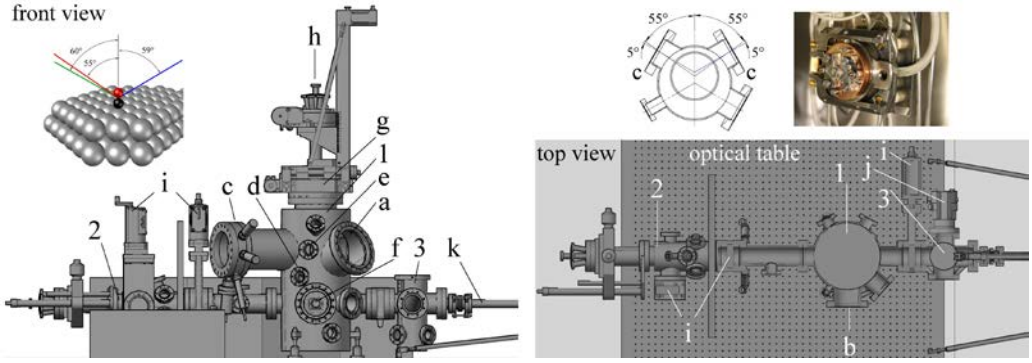

Figure 1: Overview: UHV chamber (1), SFG spectroscopic cell (2), and load lock (3). The insets show the SFG geometry and the sample car receiver on the UHV manipulator.

SFG spectroscopy is an exceptional tool for studing vibrational properties of surface adsorbates under UHV but also under *operando* conditions [3]. The capabilities of the new setup are demonstrated by benchmark results of CO-induced surface roughening of Cu(100) and CO adsorption/oxidation on ZrO_2 supported Pt nanoparticle model catalyst.

1. CO-induced Cu cluster formation on Cu(100)

The interaction of CO with Cu(100), from UHV to mbar gas pressure, was studied *in situ* by SFG and polarization-modulation infrared reflection absorption spectroscopy PM-IRAS (in

another setup [2]), and *ex situ* by LEED, X-ray photoelectron spectroscopy (XPS), temperature programmed desorption (TPD), and density functional theory (DFT). Upon UHV dosing, the well-known ordered c(2×2) on-top CO overlayer on Cu terraces was identified (2082 cm^{-1}, 44 kJ mol^{-1}).

As reported earlier [4,5], mbar CO exposure of Pt or Cu may lead to surface morphology changes (roughening). At elevated gas pressure (up to 5 mbar; 200-300 K) the shifted vibrational bands (2093 and 2112 cm^{-1}) indicated CO adsorbed on Cu adatoms (detached from step edges and forming Cu_1CO complexes on terraces), as well as CO adsorbed on coalesced Cu_5 clusters. Assignments are based on comparison with ion-bombarded Cu(100) and DFT.

2. CO adsorption and oxidation on Pt/ZrO_2 ALD model catalysts

CO adsorption and oxidation (up to 30 mbar) were examined on Pt/ZrO_2 model catalysts prepared by atomic layer deposition (ALD), another approach to bridge the "materials gap". On the 40 nm thick ZrO_2 ALD film, Pt surfaces were prepared with various roughess, ranging from smooth Pt films to oxide supported Pt nanoparticles (Figure 2). Polarization-dependent *in situ* SFG spectra revealed the effect of surface rougness on CO adsorption and the reaction onset temperature (catalytic ignition [6]).

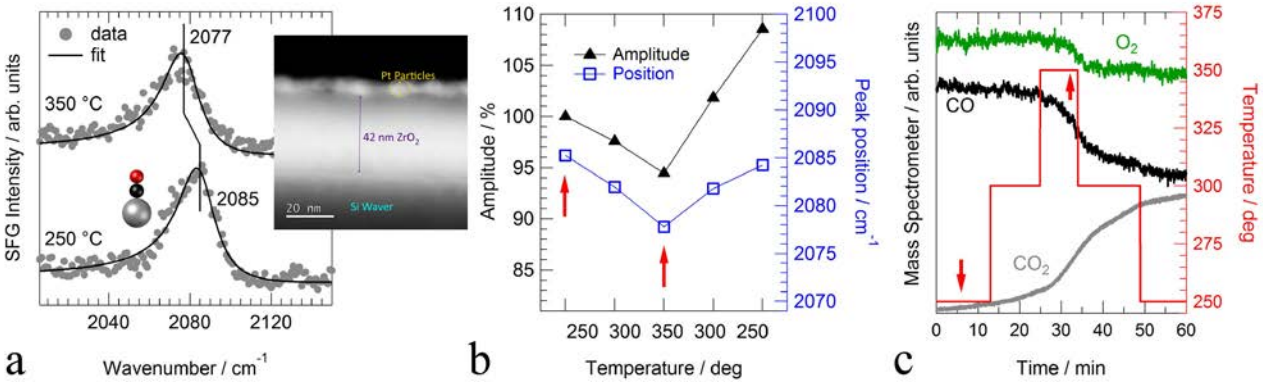

Figure 2: Operando SFG/MS measurements of CO oxidation (15 mbar CO, 15 mbar O_2) on Pt/ZrO_2. The inset shows an HAADF-STEM cross section of the ALD model catalyst.

This work was supported by the Austrian Science Fund FWF via projects DryRef (I 942-N17), ComCat (I 1041-N28), SFB FOXSI (F4502-N16) and DK Solids4Fun (W1243). We acknowledge Laura Falivene, Sergey M. Kozlov and Luigi Cavallo (KAUST Catalysis Center, Saudi Arabia) for DFT calculations, and Olle Bethge (Center for Micro and Nano Structures ZNMS of TU Wien) for preparing ALD films.

[1] G. Rupprechter, T. Dellwig, H. Unterhalt, H.-J. Freund, Topics in Catalysis, 15 (2001) 19-26.

[2] G. Rupprechter, Advances in Catalysis, 51 (2007) 133-263.

[3] G. Rupprechter, C. Weilach, J. Phys.: Condens. Matter 20 (2008) 184020 (17p).

[4] A. Haghofer, P. Sonström, D. Fenske, K. Föttinger, S. Schwarz, J. Bernardi, K. Al-Shamery, M. Bäumer, G. Rupprechter, Langmuir, 26 (2010) 16330–16338.

[5] B. Eren, D. Zherebetskyy, L.L. Patera, C.H. Wu, H. Bluhm, C. Africh, L.W. Wang, G.A. Somorjai, M. Salmeron, Science 351 (2016) 475-478.

[6] D. Vogel, C. Spiel, Y. Suchorski, A. Trinchero, R. Schlögl, H. Grönbeck, G. Rupprechter, Angew. Chem. Intern. Ed. 51 (2012) 10041-10044.

Gold nanoparticle interactions with rutile TiO_2(110)

A. Mellor, A. Wilson, D. Humphrey, H. Idriss, C.M. Yim, C.L. Pang, F. Machetti[1], S. Dhesi[1] and G. Thornton

London Centre for Nanotechnology, University College London, 17-19 Gordon Street, London WC1H 0AJ, United Kingdom
(corresponding author: G. Thornton, e-mail: g.thornton@ucl.ac.uk)

[1] *Diamond Light Source, Harwell Science and Innovation Campus, Didcot, Oxfordshire, OX11 0DE, United Kingdom*

The geometric, electronic and chemical properties of Au nanoparticles supported by TiO_2 have been the subject of much work since the discovery by Haruta that Au is a low temperature oxidation catalyst [1]. Despite this earlier work there is no definitive evidence for the binding site or the direction of charge transfer associated with gold atoms and nanoparticles on the model substrate TiO_2(110). In this work we have used STM to examine the nucleation properties of Au nanoparticles dispersed over a reduced rutile TiO_2(110) surface. From comparisons of the surface before and after Au deposition, and using atomic manipulation, the nucleation site of single Au atoms was directly observed to be at oxygen vacancies on the substrate (Ob-vacs). Statistical analysis of the atomic manipulation method applied provides some insight into the nature of the bonding between Au and Ob-vac sites. In an attempt to gauge the degree of Au/TiO_2 charge transfer, synchrotron based X-ray photoelectron emission microscopy (XPEEM) was used in conjunction with STM and low energy electron microscopy (LEEM) to probe the electronic character of Au nanoparticles as a function of particle size and coverage. Core-level binding energy measurements reveal a two stage shift in Au 4f binding energy as the nanoparticle size increased in line with electron transfer from bridging oxygen vacancies to Au for small nanoparticles (<4 nm) on TiO_2(110). To reduce experimental error, a method was developed to precisely pattern the substrate with discrete regions of varying Au coverage on the nanometer scale.

Support by a European Research Grant *EnergySurf*, Royal Society (London), and EPSRC (UK) is gratefully acknowledged.

[1] M. Haruta, S. Tsubota, T. Kobayashi, H. Kageyama, M.J. Genet, B. Delman, J. Catal. 144, 175 (1993)

Shape-controlled Synthesis of Anatase TiO2 Nanoparticles - Insights from DFT calculations

Kai Sellschopp[1], Wolfgang Heckel[1], Andreas Hensel[2], Clemens Schröter[2], Tobias Vossmeyer[2], Horst Weller[2], Stefan Müller[1], and Gregor Feldbauer[1]

[1] *Institute of Advanced Ceramics, Hamburg University of Technology*
Denickestr. 15, D-21075 Hamburg, Germany
(corresponding author: G. Feldbauer, e-mail: gregor.feldbauer@tuhh.de)

[2] *Institute of Physical Chemistry, University of Hamburg*
Grindelallee 117, 20146 Hamburg, Germany

Titania (TiO_2) nanoparticles (NP) are used for many applications ranging from photocatalysis to hybrid materials [1, 2]. A more detailed understanding of hybrid materials combining inorganic and organic constituents is the main motivation for this work. Within the approach we focus on, hierarchical hybrid materials are prepared by connecting oxide NPs via organic molecules such as carboxylic acids on a first level of hierarchy. The faceting and accordingly the shape of the NPs determine the performance in their applications. Particularly, the properties of hybrid materials depend heavily on the shape of the employed building blocks. Therefore, shape control during synthesis is essential.

Figure 1: Hybrid material linking NPs via organic molecules on 2 hierarchy levels.

Various chemical compounds including e.g. hydrohalic acids, carboxylic acids and amines are involved in the synthesis and assembly of titania NPs. A detailed analysis of their influence is crucial to achieve well-defined hybrid materials. Here, the focus is put on the anatase structure of TiO_2, because for small NPs this is the prevailing structure and the corresponding surfaces exhibit good reactivities. In thermodynamic equilibrium anatase TiO_2 particles are dominated by (101) surfaces causing a bi-pyramidal shape. It is known that fluoric acid stabilizes the anatase (001) surface through a substitution of surface oxygen atoms [3, 4]. This leads to platelet shaped particles with a large percentage of reactive (001) facets. The influence of other hydrohalic and organic acids on the particle shape, however, is less studied. In this work, our latest results on the adsorption and surface energies of all hydrohalic acids and some carboxylic acids at the major anatase TiO_2 surfaces are presented.
The relevant adsorption and surface energies are calculated within the framework of density functional theory (DFT). The Vienna Ab Initio Simulation Package (VASP) is used to perform these calculations. Van der Waals corrected exchange-correlation (XC) functionals [5] are employed to account for interactions between adsorbed molecules [6]. The equilibrium shape of pristine NPs are determined from the DFT results via the Wulff construction neglecting the effects from corners and edges. The effect of adsorbates is

then rationalized by parameter studies for variations of the surface energies. Finally, the predicted shapes are compared to experimental TEM results.
At first, the known impact of fluoric acid was reproduced here. However, no similar effect is found for the acids of other halides (Cl, Br, I). Although dissociative adsorption of these acids is favourable on the relevant surfaces, no changes in the energetical hierarchy of the surfaces occurs upon adsorption. Unlike for HF, substitution processes are not favourable for the other hydrohalic acids. This can be rationalized by the increasing size of the involved atoms hindering the substitution of oxygen.
Very good agreement has been found between the experimental and computational analyses for most of the investigated systems. However, not all of the experimentally observed shapes can be explained by the effect of hydrohalic acids. For example, rod-like structures are observed indicating a stabilization of the (100) surface. These structures are produced during some syntheses including amines. Thus, currently, such compounds are computationally screened for clarification. Furthermore, organic acids like carboxylic ones are investigated since they promise the potential to influence the shapes and they are often used as linkers between NPs.

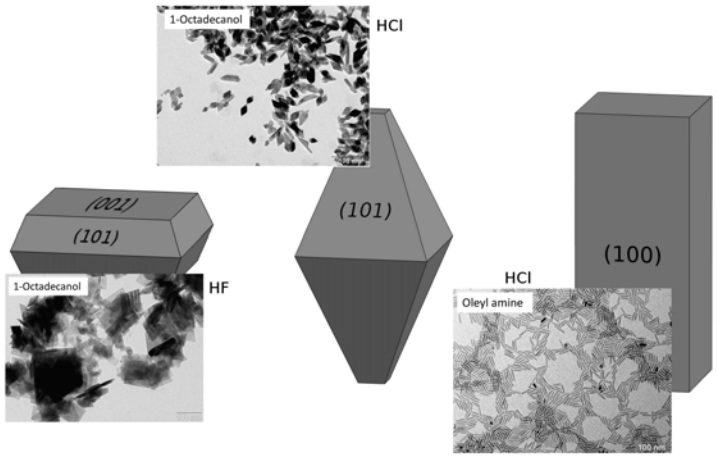

Figure 2: Influence of various additives on the shape of anatase TiO_2 NPs. Theoretical shapes versus TEM images.

Supported by the Deutsche Forschungsgemeinschaft (DFG),
via SFB 986 "M^3", projects A1 and A4.

References

[1] S. U. Khan *et al.*, Science **297** 2243 (2002).

[2] K. Brandt *et al.*, Scientific Reports **3** 2322 (2013).

[3] H. G. Yang *et al.*, Nature **453**, 638 (2008).

[4] Y. Wang *et al.*, Chemical Communications **47**, 2829 (2011).

[5] J. Klimeš *et al.*, J. Phys.: Condens. Matter **22** 022201 (2010).

[6] W. Heckel *et al.*, J. Phys. Chem. C **121** 17207 (2017).

Effect of Structural Fluctuations on Elastic Lifetimes of Adsorbate States: Isonicotinic Acid on Rutile(110)

M. Müller[1,2,3], D. Sánchez-Portal[2,3], H. Lin[4], G.-P. Brivio[4], A. Selloni[5], and G. Fratesi[6]

[1] *CIC nanoGUNE, Tolosa Hiribidea 76, San Sebastián, 20018, Spain*
[2] *Centro de Física de Materiales CSIC-UPV/EHU, Paseo Manuel de Lardizabal 5, San Sebastián, 20018, Spain*
[3] *Donostia International Physics Center, Paseo Manuel de Lardizabal 4, San Sebastián, 20018, Spain*
[4] *Materials Science Department, University of Milano-Bicocca, Piazza dell'Ateneo Nuovo, 1, Milan, 20126, Italy*
[5] *Department of Chemistry, Princeton University, Princeton, New Jersey, 08544, USA*
[6] *Dipartimento di Fisica, Università degli Studi di Milano, Via Celoria 16, Milano, 20133, Italy*
(corresponding author: D. Sánchez-Portal, e-mail: daniel.sanchez@ehu.eus)

We sample *ab initio* molecular dynamics trajectories to address the impact of structural fluctuations on elastic lifetimes of adsorbate states at room temperature focusing on heterogeneous charge injection from isonicotinic acid as a key anchoring unit in dye-sensitized energy devices. Complementing related theoretical studies, we employ a Green's function technique based on density functional theory to account for a fully semi-infinite substrate of rutile TiO_2(110). [1, 2, 3] We explicitly address the effect of a core-excitation, thus enabling the comparison with soft X-ray experiments.

We find that taking into account room temperature fluctuations drastically improves the agreement with the experimental lifetime measurements. The presence of a core-hole plays an important role shifting down in energy the spectra and reducing the electron-vibrational coupling of the adsorbate states. This last observation is probably related to the larger localization of the molecular resonance under the presence of a core-hole.

The cumulative resonance spectra (see Figure 1) can be described by Voigt-type profiles obtained by convoluting a Lorentzian peak describing the electronic resonance with a Gaussian distribution modeling the temperature broadening. However, we found that in order to get an optimal description it is crucial to account for the energy dependence of the statistically averaged electronic widths. This energy dependence is dominated by the variation of the density of acceptor states in the substrate.

We acknowledge financial support from EU FP7 under the grant agreement No. 607232 (THINFACE), the Spanish MINECO (Grant No. MAT2016-78293-C6-4-R), the Basque Dep. de Educación and the UPV/EHU (Grant No. IT-756-13). MM work was performed within the PCAM European doctorate.

[1] D. Sánchez-Portal, Prog. Surf. Sci. **82**, 313-335 (2007).
[2] D. Sánchez-Portal, D. Menzel and P. Echenique, Phys. Rev. B **72**, 235406 (2007).
[3] G. Fratesi, C. Motta, M. I. Trioni, G.-P. Brivio and D. Sánchez-Portal **118**, 8775-8782 (2014).

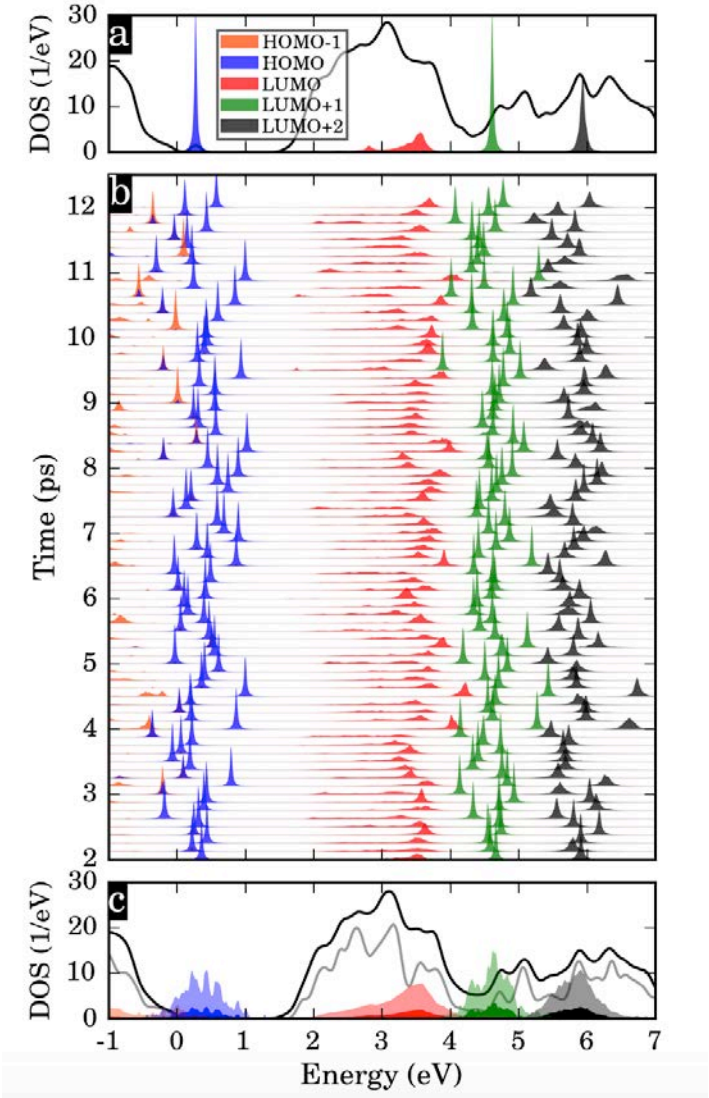

Figure 1. Density of states projected onto the frontier orbitals (HOMO-1 up to LUMO+2) of isonicotinic acid: (a) Spectrum for the equilibrium structure; (b) 81 snapshots during 10 ps of the CPMD at 300 K (every second snapshot of the full sampling shown); (c) Cumulative spectra after averaging all 161 snapshots (colored areas), additionally repeated after rescaling (x4) to facilitate visualization (light shaded areas). Black lines in (a) and (c) show the density of states (DOS) (x0.14) from finite slab calculation. The gray line in (c) shows the bulk TiO_2 DOS (x0.6). The origin of all the spectra was shifted to the VBM of the bulk DOS as a common energy reference.

CO-Oxidation on Size-Selected Surface-Adsorbed Platinum Clusters

Hamed Achour, Simon Bonanni, Kamel Aït-Mansour, Wolfgang Harbich, and Harald Brune,

Institute of Physics, École Polytechnique Fédérale de Lausanne, Station 3, CH-1015 Lausanne
(corresponding author: Harald Brune, harald.brune@epfl.ch)

Fundamental questions in heterogeneous catalysis are often addressed in model systems. We create such systems by depositing size-selected clusters of the catalytically active metal onto single-crystal support surfaces. The size-selection is done with mass spectrometers, requiring a minimum kinetic energy of the clusters with which they hit the surface. Its dissipation upon adsorption may lead to cluster or surface damage. This can be avoided by soft-landing, either reducing the energy per atom below a threshold of typically 1 eV, or by pre-adsorbing inert gas buffer layers that take up the energy and are subsequently evaporated from the surface [1, 2]. This creates surfaces with well-defined starting conditions for catalytic reactions, *i.e.*, monodisperse metal clusters adsorbed on a single crystal support. We investigate the cluster morphology and mean size, as well as the substrate morphology and chemical composition before and after the reaction by means of low-temperature STM. The reaction itself is studied in front of a custom designed mass spectrometer that allows to dose the reactants and detect the products from the sample surface [3].

For the CO oxidation on size-selected Pt clusters on rutile TiO_2(110) we demonstrate that the substrate reduction state plays an important role in the chemical reactivity of the clusters [4]. When titania has only very few oxygen vacancies (and Ti^{3+} interstitials) the substrate is transparent and CO oxidation takes place on Pt_7. Samples with a high reduction state have more oxygen vacancies at that surface and the Ti^{3+} interstitials surface segregate under reaction conditions. Their oxidation competes with the CO oxidation for the atomic oxygen produced on the Pt clusters. In extreme cases, no CO_2 at all is produced, not because the clusters are inactive, but because the competing process of TiO_2 production is dominating. For catalytically active samples, we further find that the clusters show significant ripening at the temperature where the reaction takes place and that this ripening is enhanced by the reaction enthalpy [5]. Therefore the reaction does take place on larger clusters than the ones deposited.

Hexagonal (*h*) boron-nitride (BN) grown on Rh(111) forms a (12 *x* 12) moiré pattern [6, 7, 8]. Due to the misfit, the adsorption sites of the B and N atoms change, and since the chemical binding strongly depends on the site, the *h*-BN layer varies between strongly bound and almost detached within the moiré unit cell [9]. The hope was that Pt clusters on that substrate might be immobile and the substrate chemically inert. The experiment shows that Pt_7 clusters are stable and immobile up to 500 K, at 700 K we see Schmolukowski ripening, *i.e.*, ripening caused by entire clusters diffusing and aggregating, and from 900 K on Pt intercalates under

the *h*-BN [10, 11]. This intercalation can be induced at room temperature when clusters are deposited with high kinetic energies. For Pt clusters on the pristine *h*-BN/Rh(111) sample, the CO oxidation sets in at 480 K, very much as for Pt clusters on TiO_2(110). However, when we create samples where Pt clusters are situated on h-BN with intercalated Pt beneath, the CO oxidation sets in already at 380 K [11].

Support by the Swiss Federal Science Foundation is gratefully acknowledged.

[1] K. Bromann, C. Félix, H. Brune, W. Harbich, R. Monot, J. Buttet and K. Kern, Science **274**, 956 (1996).

[2] N. Isomura, X. Wu and Y. Watanabe, J. Chem. Phys. **131**, 164707 (2009).

[3] S. Bonanni, K. Aït-Mansour, M. Hugentobler, H. Brune and W. Harbich, Eur. Phys. J. D **63**, 241-249 (2011).

[4] S. Bonanni, K. Aït-Mansour, W. Harbich and H. Brune, J. Am. Chem. Soc. **134**, 3445 (2012).

[5] 1. S. Bonanni, K. Aït-Mansour, W. Harbich and H. Brune, J. Am. Chem. Soc. **136**, 8702 (2014).

[6] M. Corso, W. Auwärter, M. Muntwiler, A. Tamai, T. Greber and J. Osterwalder, Science **303**, 217-220 (2004).

[7] Y. Ding, M. Iannuzzi and J. Hutter, J. Phys. Chem. C **115**, 13685 (2011).

[8] Q. Dubout, F. Calleja, G. Sclauzero, M. Etzkorn, A. Lehnert, L. Claude, M. Papagno, F. D. Natterer, F. Patthey, S. Rusponi, A. Pasquarello and H. Brune, N. J. Phys. **18**, 103027 (2016).

[9] F. D. Natterer, F. Patthey and H. Brune, *Ring State for Single Transition Metal Atoms on Boron Nitride on Rh(111)*, Phys. Rev. Lett. **109**, 066101 (2012).

[10] H. Achour, *Transition metal clusters on h-BN/Rh(111): surface interaction and catalytic activity*, PhD-Thesis, Swiss Federal Institute of Technology, Lausanne (2016).

[11] H. Achour, W. Harbich, and H. Brune, in preparation (2018).

Solution Based Assembly of Non-Planar Molecules: Tetraphenylmethane Carboxylic Acids on Ag

Rodrigo Ortiz de la Morena[1], Michal Valásek[2], Eric Sauter[3], Hannah Aitchison[1], Stephen Francis[1], Hao Lu[3,4], Michael Zharnikov[3], Marcel Mayor[2,5], Manfred Buck[1]

[1]*EaStCHEM School of Chemistry, Univ. St Andrews, St Andrews, KY16 9ST, UK*
corresponding author: M. Buck, e-mail: mb45@st-andrews.ac.uk
[2]*Institute of Nanotechnology, Karlsruhe Inst. of Technology (KIT), 76021 Karlsruhe,Germany*
[3]*Angewandte Physikalische Chemie, Univ. Heidelberg, 69120 Heidelberg, Germany*
[4]*Max Planck Institute for Polymer Research, 55128 Mainz, Germany*
[5]*Department of Chemistry, Univ. Basel, 4056 Basel, Switzerland*

The large variety of molecular architectures, in combination with the ability of the carboxyl group to adopt different hydrogen and coordination bonding geometries, makes aromatic carboxylic acids (ArCAs) of interest as building blocks for two-dimensional assemblies. Ranging from porous supramolecular networks, where molecules lie flat on the surface, to self-assembled monolayers (SAMs) of densely packed, upright standing molecules, work has mostly focused on the former [1,2] whereas SAM type assemblies have been investigated much less (e.g. refs. [3-5]).

For ArCAs on coordinating metal surfaces such as Cu and Ag it has been established that highly crystalline SAMs can be formed employing a simple solution based preparation protocol [5-8]. The systems studied so far suggest that Ag is particularly suitable substrate as intermolecular interactions dominate over molecule-substrate interactions, thus, greatly facilitating the design of SAM structures. Envisaging SAMs beyond the space filling packing of molecules, a first step in the direction of more complex structures has recently been taken by the assembly of H3BTB (see Fig. 1a for structure) which form an open structure SAM featuring nanotunnels [9].

Extending this approach raises the question of how ArCAs assemble whose molecular architectures are more complex than the essentially linear or planar geometries of molecules such as BPCA [5] (see Fig. 1a) or H3BTB. For tetraphenylmethane as a simple example of a non-planar structure it can be expected that the balance of interactions is significantly altered due to the sterically restricted interactions between the π–systems. Two derivatives of tetraphenylmethane - dicarboxylic acid (H2MDB) and tetracarboxylic acid (H4MTB, see Fig. 1a) - were studied by STM, XPS and NEXAFS. Both molecules form crystalline SAMs as illustrated in Fig. 2b for the case of H2MDB and their structures are analogous with two carboxylic acids groups binding to the Ag surface in a bidentate configuration. Notably, the bipodal anchoring differs from SAMs of other multifunctional ArCAs on Ag studied so far which exhibit a monopodal adsorption geometry. An unexpected behaviour is observed upon coadsorption of a linear molecule (BPCA) and a non-planar one (H2MDB). Contrasting other

binary SAMs where the components are either phase separated or randomly mixed, a regular pattern forms, consisting of alternating rows of the two molecules as shown in Fig. 2c. The formation of well-defined SAM structures also for non-planar tetraphenylmethane based carboxylic acids further consolidates that ArCAs on Ag represent a flexible platform for the design of SAMs.

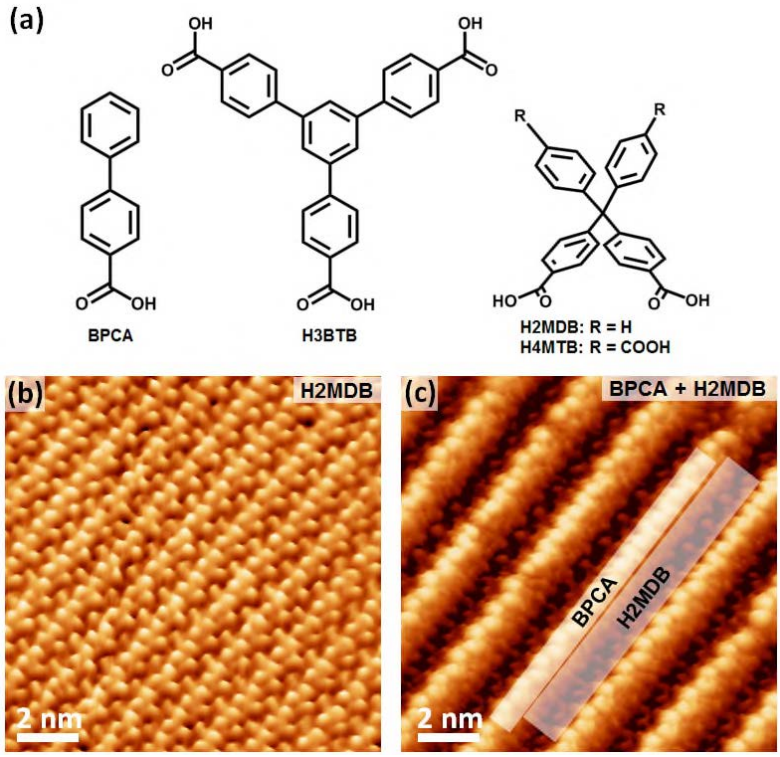

Fig. 1: (a) Selection of aromatic carboxylic acids varying in geometry and number of carboxylic acid moieties. (b,c) STM images of a monolayer of H2MDB (b) and a binary layer of coadsorbed H2MDB and BPCA (c) on Au/mica modified by a bilayer of Ag.

[1] J.V. Barth, Annu. Rev. Phys. Chem. 58 (2007) 375.
[2] A.G. Slater, P.H. Beton, N.R. Champness, Chem. Sci. 2 (2011) 1440.
[3] F. Zasada, W. Piskorz, S. Godlewski, J.S. Prauzner-Bechcicki, A. Tekiel, J. Budzioch, P. Cyganik, M. Szymonski, Z. Sojka, J. Phys. Chem. C 115 (2011) 4134.
[4] T. Bitzer, N.V. Richardson, Surf. Sci. 427-28 (1999) 369.
[5] H. Aitchison, H. Lu, S.W.L. Hogan, H. Früchtl, I. Cebula, M. Zharnikov, M. Buck, Langmuir 32 (2016) 9397.
[6] H. Aitchison, H. Lu, M. Zharnikov, M. Buck, J. Phys. Chem. C 119 (2015) 14114.
[7] I. Cebula, H. Lu, M. Zharnikov, M. Buck, Chem. Sci. 4 (2013) 4455
[8] I. Cebula, C. Shen, M. Buck, Angew. Chem. Int. Ed. 49 (2010) 6220.
[9] H. Aitchison, H. Lu, R. Ortiz de la Morena, I. Cebula, M. Zharnikov, M. Buck, Phys. Chem. Chem. Phys. (accepted, DOI: 10.1039/C7CP06160A).

Convergent multistep on-surface reaction yielding complex supramolecular tiling

Yi-Qi Zhang[1], Mateusz Paszkiewicz[1], Ping Du[2], Liding Zhang[1], Tao Lin[1], Zhi Chen[2], Svetlana Klyatskaya[2], Mario Ruben[2,3], Ari P. Seitsonen[4], Florian Klappenberger[1], Johannes V. Barth[1*]

[1] *Physik-Department E20, Technische Universität München, 85748 Garching, Germany*
**jvb@tum.de*

[2] *Institute of Nanotechnology (INT), Karlsruhe Institute of Technology (KIT), 76344 Eggenstein-Leopoldshafen, Germany*

[3] *IPCMS-CNRS, Université de Strasbourg, 23 rue de Loess, 67034 Strasbourg, France*

[4] *École Normale Supérieure, Département de Chimie, 24 rue Lhomond, F-75005 Paris, France*

Complex two-dimensional molecular tessellations promise unique properties related to their nontrivial structure. Interfacial supramolecular engineering employing well-defined assembly protocols represents a powerful tool for constructing regular and quasicrystalline materials. Nonetheless, architectures representing semiregular Archimedean tilings remain challenging to obtain with established fabrication protocols being largely limited to direct assembling of precursors. Here we employ the *de novo* designed ethynyl-iodophenanthrene (EIP) as the single starting precursor, featuring asymmetry both in geometry and reactivity, and use it to generate a variant of the rare semiregular (3.4.6.4) Archimedean tiling with long-range order on the well-defined Ag(111) substrate via a multistep reaction.

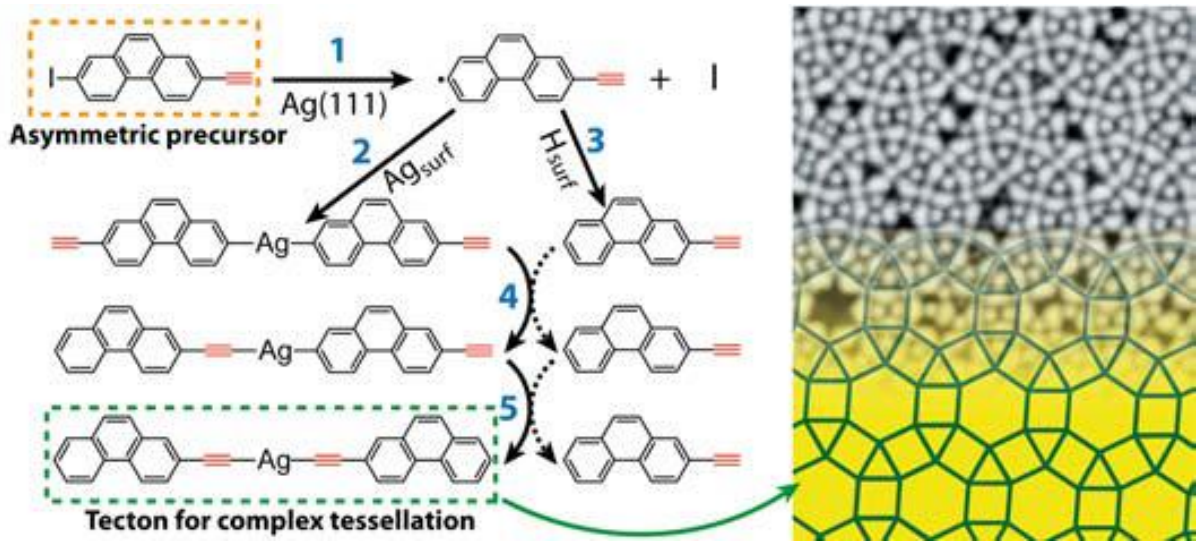

Intriguingly, the individual chemical transformations unite to a convergent pathway and drive an assembly rendering the product with high yield. Using complementary characterization techniques (STM, XPS and NEXAFAS) and computational modeling, we unveil the nature of the tessellation conclusively. A concomitant, detailed analysis of the reaction intermediates disentangles the pertaining tecton conversion pathways, and suggests that they are mediated by in-situ generated catalytic silver complexes, affording alkynyl–Ag–alkynyl complexes as key assembly constituents (cf. scheme above).

Our approach opens up new avenues to construct complex materials via interfacial transformations of adsorbed molecular building blocks. Furthermore, the gained insights can be understood as first steps towards retracing surface-confined covalent engineering protocols in a retrosynthetic way based on the mechanistic understanding obtained by the combination of scanning probe methods and spectroscopic techniques with computational modeling. This introduces novel opportunities to control covalent conversions by designing suitable starting materials, specifically when taking into account the particular laws of surface-confined reactions markedly diverging from solution chemistry. Finally, our findings and methodology contributes to the general understanding of the emergence of complexity and hierarchic systems in chemistry and biology.

Funding by the German Research Foundation (DFG) Excellence Cluster Munich Center for Advanced Photonics, the DFG project KL 2294/3-1, and the ERC Advanced Grant MolArt (No. 247299) is gratefully acknowledged. M.R. would like to thank for the generous support by the DFG-priority programs 1459 and TR88 “3Met” and acknowledge the KNMF facility (KIT, Germany) for the support. We acknowledge the Helmholtz–Zentrum Berlin–Electron storage ring BESSY II for provision of synchrotron radiation at beamline HE-SGM, and thank Professor C. Wöll and A. Nefedov for kindly providing access to the HE-SGM end station. Travelling costs for the BESSY measurements provided by Helmholtz–Zentrum Berlin.

Surface-Anchored Metal-Organic Frameworks as Versatile Resists for E-Beam Lithography: Fabrication of sub-10 nm Structures

Martin Drost[1], Fan Tu[1], Luisa Berger[1], Christian Preischl[1], Wencai Zhou[2], Hartmut Gliemann[2], Christof Wöll[2] and Hubertus Marbach[1]

[1] *Lehrstuhl für Physikalische Chemie II, Universität Erlangen-Nürnberg, Egerlandstr. 3, 91058 Erlangen, Germany,*
(corresponding author: H. Marbach, e-mail: hubertus.marbach@fau.de)

[2] *Institut für Funktionelle Grenzflächen,Karlsruher Institut für Technologie (KIT,) Hermann-von-Helmholtz-Platz 1, D-76344 Eggenstein-Leopoldshafen, Germany*

We demonstrate that Surface-Anchored Metal-Organic Frameworks (SURMOFs)[1] exhibit extraordinary properties, which make them, very well suited as substrates for Focused Electron Beam Induced Processing (FEBIP) techniques. The combination of such powerful lithographic protocols with the huge versatility of MOF materials allows for the fabrication of nanostructures with unique properties. The FEBIP methods applied here (c.f. Fig. 1) rely on the local decomposition of the volatile precursors $Fe(CO)_5$ and $Co(CO)_3NO$, either by the direct impact of the focused electron beam (Electron Beam Induced Deposition, EBID)[2] or through the interaction of the precursor molecules with preirradiated/activated surface areas (Electron Beam Induced Surface Activation, EBISA).[3] We demonstrate the huge potential of the approach for two different types of SURMOFs (HKUST-1 and Zn-DPDCPP). Application of our "surface science" approach, i.e. working in an ultra-high vacuum environment, allows to obtain well-defined deposits with any of the precursor/SURMOF combinations. Local Auger Electron Spectroscopy (AES) reveals that deposits from $Fe(CO)_5$ exclusively consist of iron, whereas deposits from $Co(CO)_3NO$ contain cobalt, nitrogen and oxygen. EBISA experiments were successfully conducted with $Fe(CO)_5$ on both SURMOFs, whereas EBISA with $Co(CO)_3NO$ on both SURMOFs does not result in deposit formation, making the process chemically selective. Most importantly we demonstrate the fabrication of "nested-L test structures" with $Fe(CO)_5$ on HKUST-1 with unusually narrow line width (average FWHM value 9.6 nm, smallest width 7.5 nm, see Fig 2). This resolution can be considered extraordinary high, since the diameter of the electron beam was larger than 6 nm. We attribute this finding to reduced electron proximity effects, i.e. reduced electron scattering and quenching of secondary electrons within the SURMOF material.

[1] Liu, J. X.; Wöll, C., **Chem. Soc. Rev.**, 46 (2017) 5730.

[2] W. van Dorp et al., **J. Appl. Phys.** 104, 081301 (2008); I. Utke et al., **JVST B**, 26, 1197 (2008);

[3] M.Drost et al., **Small Methods**, 1 (2017) 1700095; H. Marbach, **Appl. Phys. A** 117 (2014) 987, F. Vollnhals et al., **J. Phys. Chem. C**, 117, 17674 (2013), M.-M. Walz et al., **Ang. Chem. Int. Ed**., 49, 4669 (2010)

Support by the DFG through grant MA 4246/1-2, MA 4246/2-1/ research Unit funCOS, the Excellence Cluster "Engineering of Advanced Materials" and COST Action CM1301 (CELINA) is gratefully acknowledged.

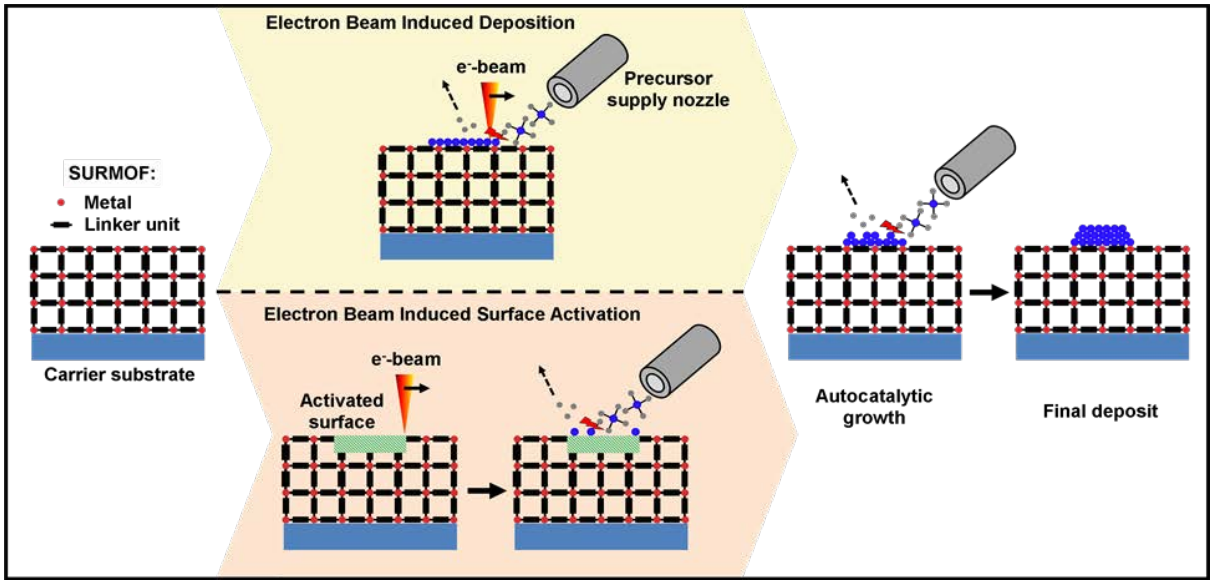

Figure 1: *Schematics of the EBID and EBISA experiments conducted on SURMOFs presented in this work. In EBID (above the dashed line), the electron beam of the scanning electron microscope irradiates the SURMOF in the presence of a precursor gas, leaving behind a deposit. In EBISA (below the dashed line), the SURMOF is irradiated in the absence of a precursor, leading to a chemically modified, activated surface. Subsequently dosed precursor can dissociate at activated sites, also leaving behind a deposit or a seed layer, respectively. In an autocatalytic growth process, the initial deposits fabricated by either method grow in size as long as the precursor is supplied.*

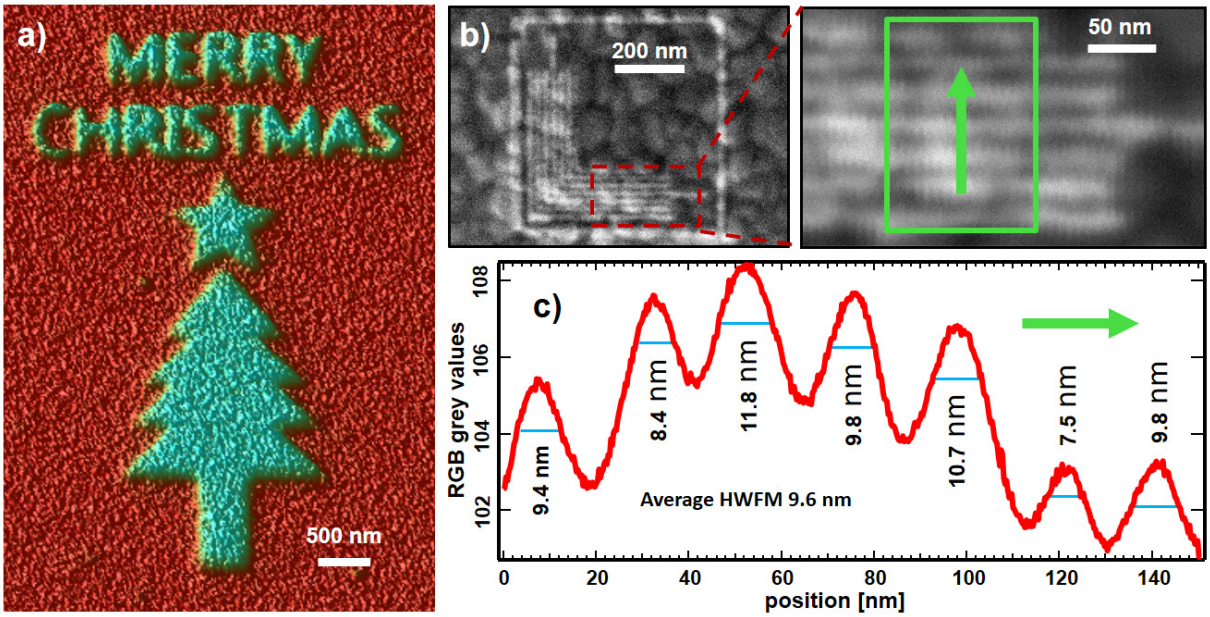

Figure 2: a)-c) *Selected SEM images of FEBIP deposits from $Fe(CO)_5$ on a HKUST-1 SURMOF. a) "Christmas card motif" written with EBID and subsequent AG. The width of the lettering is partially below 100 nm.* ***b)*** *SEM images of "nested L" as prototype test structure for resolution measurements fabricated with 2.3-33.8 µC/cm, 250 sweeps, t_{AG} = 17 min. The red dashed rectange indicates the position of the corresponding blow-up.* **c)** *RGB rofiles extracted from the green rectangle in b). A minimum FWHM of 7.5 nm was measured, with a pitch of 23.6 nm.*

PTCDA on Ge(001) surface - adsorption and surprising self-assembly

P. Kocán, Y. Yoshimoto[1], K. Yagyu[1], H. Tochihara[2], and T. Suzuki[2]

Charles University, Faculty of Mathematics and Physics, Department of Surface and Plasma Science, V Holešovičkách 2, 180 00, Prague, Czech Republic
(corresponding author: P. Kocán, e-mail: pavel.kocan@mff.cuni.cz)

[1] *Department of Computer Science, The University of Tokyo, Tokyo 113-0033, Japan*

[2] *Department of Electronics Engineering and Computer Science, Fukuoka University, Fukuoka 814-0180, Japan*

Ability of atoms and molecules to self-order when deposited on surfaces brings possibility of spontaneous growth of well defined nanostructures, on which future electronic devices could be based. Organic molecules can be used as prefabricated building blocks with physical properties which can be tuned by modifying their chemical structure. The process of ordering also provides well-defined interface, required for implementation of multiple materials in electronic devices.

On weakly interacting surfaces, the ordering of organic molecules is usually a result of high on-surface mobility together with often intricate inter-molecular interactions [1]. Reactive surfaces such as those of semiconductors used in recent chip industry have high densities of dangling bonds. If not passivated [2–4], self-ordering of molecules on these technologically important surfaces is usually hindered by a limited diffusion of molecules covalently bonded to the surfaces.

The 3,4,9,10-perylenetetracarboxylic dianhydride (PTCDA) is a perylene derivative, often used as n-type organic semiconductor. On weakly interacting surfaces, PTCDA molecules typically form a herringbone structure, which is a result of quadrupole and hydrogen bond-like interactions [5,6]. As exception, surprisingly high mobility of PTCDA has been reported also on non-passivated Ge(111)-c(2×8) at room temperature [7], but the mobility did not result in ordering of the molecules.

In our previous works we studied low coverages of PTCDA on the Si(001)-2×1 [8] and Ge(001)-2×1 [9] surfaces. On the Si(001) surface, several configurations have been observed differing in orientation and position with respect to the Si dimer rows. In case of Ge(001) we demonstrated lower interaction of PTCDA with the substrate than on Si, resulting in adsorption of all molecules in a single configuration at room temperature. The molecules are adsorbed in a trough between dimer rows of the Ge(001) surface and four carboxylic O atoms form polar covalent bonds with Ge.

At first we will present scanning tunneling microscopy (STM) results obtained at low coverages and discuss in detail interaction of PTCDA with the Ge(001) surface. With help of the density-functional theory (DFT) we will separate different contributions to the adsorption energy – covalent bonding, dispersion forces, energy necessary to bend the molecule, and deformation of the surface dimers.

Next we will show STM results obtained by deposition of PTCDA at coverages forcing the molecules to interact together. Even though covalently bonded to the Ge(001) surface, the molecules are at elevated temperatures surprisingly mobile enough to rearrange and to form self-ordered structures. The morphologies observed by STM will be discussed with help of DFT calculations and Monte Carlo simulations.

In summary, we will report on exceptional self-ordering of PTCDA on germanium surface, allowing preparation of well defined interface between organic and inorganic semiconductor. The mechanism of ordering will be explained by considering energies of interactions and simplified kinetic aspects.

This work was supported in part by funds (Grant No. KD15078, No. 155008 and No. 157004) from the Central Research Institute of Fukuoka University and in part by Grants-in-Aid for Scientific Research (Grant No. 15K04630) from MEXT. P.K. acknowledges support from Czech Science Foundation (contract no. 16-15802S).

[1] F. S. Tautz,, Prog. Surf. Sci. 82, 479–520 (2007).

[2] A.A. Ahmad Zebari, M. Kolmer and J.S. Prauzner-Bechcicki, Appl. Surf. Sci. 332, 403–408 (2015).

[3] P. Matvija, F. Rozbořil, P. Sobotík, I. Ošťádal, B. Pieczyrak, L. Jurczyszyn and P. Kocán, Sci. Rep. 7, 7357 (2017).

[4] N. Nicoara, J. Méndez, and J.M. Gómez-Rodríguez, Nanotechnology 27, 365706 (2016).

[5] Y. Zhao and J.J. Wang, J. Phys. Chem. C 121, 4488–4495 (2017).

[6] M. Mura, X. Sun, F. Silly, H.T. Jonkman, G.A.D. Briggs, M.R. Castell and L.N. Kantorovich, Phys. Rev. B 81, (2010).

[7] A.J. Martínez-Galera, Z. Wei, N. Nicoara, I. Brihuega and J.M. Gómez-Rodríguez, Nanotechnology 28, 095703 (2017).

[8] T. Suzuki, Y. Yoshimoto, K. Yagyu and H. Tochihara, J. Chem. Phys. 142, 101904 (2015).

[9] P. Kocán, Y. Yoshimoto, K. Yagyu, H. Tochihara and T. Suzuki, J. Phys. Chem. C 121, 3320–3326 (2017).

SurfaceNet

Crystals

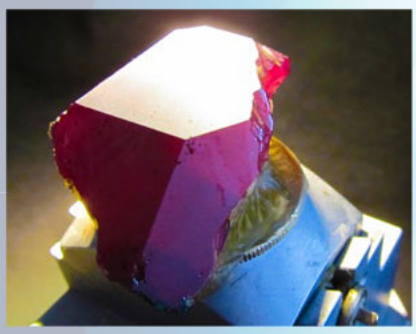

Crystal Puller

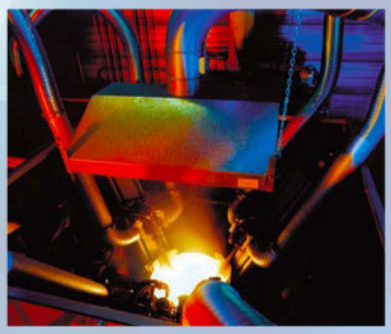

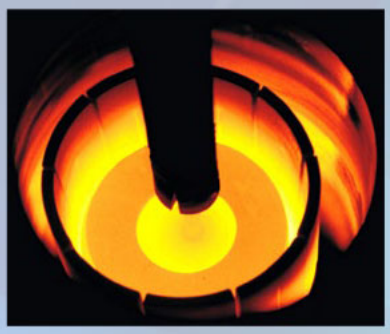

Wafers

Analytical Services

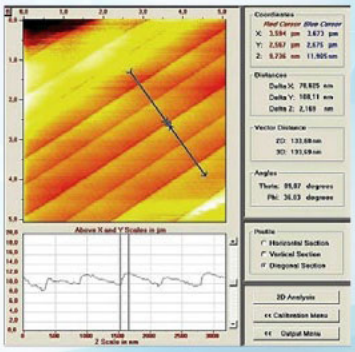

Substrates
Custom Parts

Sputter Targets
PLD Targets
Custom Crystal Growth

SurfaceNet GmbH
Oskar-Schindler-Ring 7 · 48432 Rheine – Germany
Fon +49 (0)5971 4010179 · Fax +49 (0)5971 8995632
sales@surfacenet.de · www.surfacenet.de

Wednesday

"Surface Attophysics"

P.M. Echenique

Dpto. de Física de Materiales UPV-EHU, Donostia International Physics Center (DIPC) and Material Physics Center (MPC), P. Manuel de Lardizabal 4, 20018 San Sebastián, Basque Country, Spain

Femtosecond and subfemtosecond time scales typically rule electron dynamics at surfaces. I will analyze briefly electron dynamics at surfaces and nanostructures with emphasis on surface attophysics, namely streaking experiments.

Attosecond lifetimes of excited electronic states in solids---determined without an attosecond laser

F. Roth[1,2], T. Arion[2], H. Kaser[3], A. Gottwald[3], and W. Eberhardt[2,4]

[1] *TU Bergakademie Freiberg, Institute of Experimental Physics, Leipziger Straße 23, D-09599 Freiberg, Germany*

[2] *Center for Free Electron Laser Science (CFEL), DESY, Notkestr. 85, D-22607 Hamburg, Germany*

corresponding author: wolfgang.eberhardt@desy.de

[3] *Physikalisch Technische Bundesanstalt (PTB), Abbestr. 2-12, D-10587 Berlin, Germany*

[4] *Inst. for Optics and Atomic Physics, TU Berlin, Strasse des 17. Juni 135, D-10623 Berlin, Germany*

The determination of excited electron lifetimes in solids and on surfaces is of high current interest. Knowledge about these excited states is of great importance for the understanding and control of photophysical processes, ranging from charge generation in solar cells to photochemistry as for example photo-activated splitting of water. We here use conventional angle resolved photoelectron spectroscopy to determine these lifetimes (1,2). This experimental technique has been very successfully employed to determine the occupied bandstructure of solids (3) to the extend that the results are by now incorporated into basic solid state physics textbooks. Angle resolved photoemission also reveals the excited state lifetime as originally shown for Cu (4). This is based upon monitoring the intensity of well identified interband transitions as the energy of the photons is changed. As this requires some careful calibrations, this has not been widely used so far. However as the interest in these lifetime measurements is growing, there are no obstacles to use this technique. Moreover, as we will demonstrate below, the quality of the data is better than the data obtained by direct techniques so far.

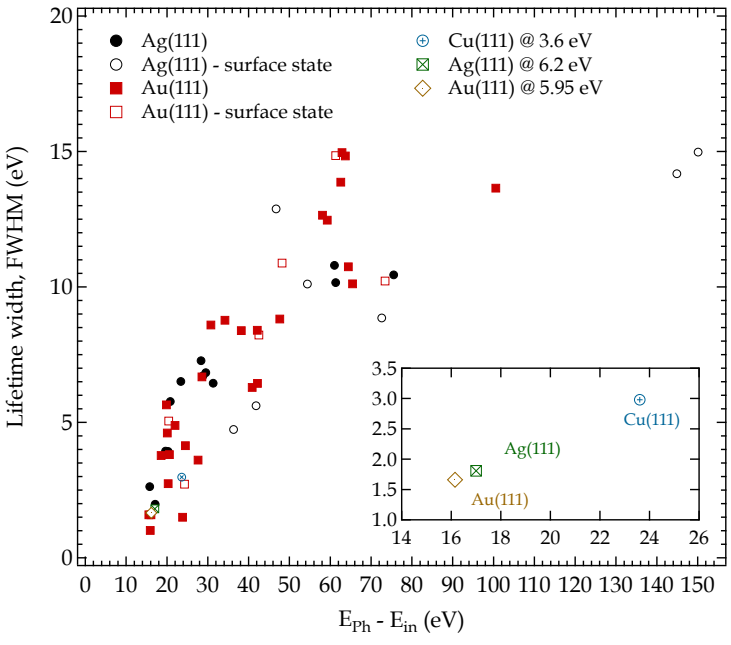

The Figure shown on the left displays an overview of the lifetime widths of transitions observed for Cu, Ag and Au. The most dominant transitions observed are attributed to f-derived final states located about 16 to 17 eV above E_F for Ag and Au and 24 eV above E_F for Cu. Especially these lower energy transitions exhibit very distinct resonance phenomena. The excited electron lifetime is in the *as* range as determined from the energy width of the observed transitions.

Concentrating on the strongest transitions observed, shown as inset in the figure above, we observe a width of 1.6 eV for Au, 1.9 eV for Ag and 3.0 eV for Cu. Making use of the energy-time uncertainty relation

$$(\Delta E)*(\Delta t) \geq \hbar/2,$$

we can get an estimate of the excited electron lifetimes at these energies. The ΔE in the uncertainty equation corresponds to the half width Γ/2 of our measured Lorentzians. The numerical lifetime values thus derived are 410 *as* for Au, 350 *as* for Ag, and 220 *as* for Cu.

The generation of attosecond UV pulse trains by harmonic generation of high power short pulse lasers has also enabled to access these timescales directly for pump-probe electron spectroscopy (5,6,7). The special technique employed to determine the lifetimes of excited states in Ni(5) or Au(7), called attosecond streaking or RABBIT, has been summarized by Cavallieri et al. (6). It is based upon superposition of an IR laser pulse with the HHG-as-pulse on the target and observing the electrons that actually have absorbed one photon each from the two laser fields while the phase shift between the two laser fields is varied. Originally this technique had been developed using isolated atoms in gas phase and for these the interpretation is quite straightforward. For solids this however is not the case---one of the difficulties hinges upon the location where the IR pulse is actually absorbed. This is viewed to be near the surface of the solid, but the relevant length scale is the wavelength of the IR pulse and what near the surface means on that scale is not clear. Accordingly, the results have to be taken with large uncertainties. Tao et al. 5 nevertheless quote a value of a lifetime on the order of >200 *as* for an excited electron at 25 eV in Ni, whereas Locher et al. 7 try to also take the transition time for the photon absorption into account in their interpretation/modeling of the data. They derive a combined lifetime/transition time of these states in Ag and Au with values between 200 *as* and 100 *as*.

Acknowledgment

We thank the staff of the Metrology Light Source of the PTB, for experimental and technical support. This research was funded through the research program ‘Structure of Matter’ of the Helmholtz Association of Research Centers in Germany.

References:

1. F. Roth, C. Lupulescu, E. Darlatt, A. Gottwald, and W. Eberhardt, J. Electron. Spectrosc. **208**, 2 (2016).
2. F. Roth, T. Arion, H. Kaser, A. Gottwald W. Eberhardt, J. Electr. Spectrosc. (2017) accepted
3. E. W. Plummer and W. Eberhardt, Advances in Chemical Physics **49**, 533 (1982).
4. F. J. Himpsel and W. Eberhardt, Solid State Comm. **31**, 747 (1979).
5. Z. Tao, C. Chen, T. Szilvasi, M. Keller, M. Mavrikakis, H. Kapteyn, M. Murnane, Science **353**, 62 (2016).
6. A. L. Cavalieri, N. Müller, T. Uphues, V. S. Yakovlev, A. Baltuska, B. Horvath, B. Schmidt, L. Blümel, R. Holzwarth, S. Hendel, M. Drescher, U. Kleineberg, P. M. Echenique, R. Kienberger, F. Krausz, and U. Heinzmann, Nature **449**, 1029 (2007).
7. L. Locher, L. Castiglioni, M. Lucchini, M. Greif, L. Gallmann, J. Osterwalder, M. Hengsberger, U. Keller, Optica **2**, 405 (2015)

Advanced ARPES Analyzer and Electron Detection Concepts – KREIOS energy analyzer with CMOS detector

T. Stempel, M. Wietstruk, S. Böttcher

SPECS Surface Nano Analysis GmbH, 13355 Berlin, Germany
(corresponding author: T. Stempel, e-mail: Thomas.stempel@specs.com)

Modern ARPES analyzers provide a high degree of parallelization in data acquisition, recording hundreds of energy and angle channels simultaneously. Additionally, integrated deflectors enable users to perform angle scanning perpendicular to the analyzer's entrance slit to record (k_x, k_y, E) data sets without sample rotation. However, the design of conventional analyzers implies a limited acceptance angle and corresponding accessible momentum space volume. Due to the trade-off between acceptance angle and angle resolution multiple changes in sample position and lens modes are necessary during a typical high resolution ARPES experiment. The new KREIOS 150 Energy Analyzer uses an extractor zoom lens design which was developed at MPI Halle and Johannes Gutenberg University in Mainz, overcoming these limitations.

This new lens provides a full 2π solid acceptance angle with highest angular resolution. In contrast to standard ARPES measurements with conventional hemispherical analyzers, electronic structure data from and beyond the 1st Brillouin zone is recorded without any sample movement. In addition the lens of such an instrument can work in a lateral imaging mode for microscopy as well. This enables navigation on the sample and reduces the size of the area under investigation in ARPES down to a few micrometers in diameter. This combination of large acceptance angle, high angular resolution and small acceptance area, makes this instrument the ideal tool for electronic structure studies on small samples or sample areas. The design is compact with a straight optical axis.

The capabilities of this instrument were tested at the UE 56/2 at the Bessy II synchrotron in Berlin. Specification tests show excellent angle and lateral resolution as well as small spot capability down to 2µm FOV. Subsequently real live samples like Graphene on Germanium were measured. Even on macroscopically rough surfaces like Graphene on $NbSe_2$ excellent ARPES and X-PEEM results could be obtained. By taking advantage of the small spot capability of the KREIOS 150 meaningful band structure data has been recorded on such patchy samples.

Like the vast majority of all ARPES analyzers in the world the KREIOS 150 was operated with a twodimensional MCP/CCD detector. These detectors allow for excellent lateral (=angle and energy) resolutions. It can be operated in an analog mode in which the integrated light intensity is used for counting, or in pulse counting mode in which individual light blobs are

detected. Both modes have disadvantages. In pulse counting mode conventional CCD detectors show saturation at high count rates. In analog mode the detection is non-linear at low count rates. To overcome these limitations we present a new generation of 2D imaging detectors based on CMOS camera technology. It features a superior dynamic range and extremely low noise level, resulting in an unprecedented dynamic range.

We will present specification and laser ARPES data taken with this new detector type mounted on a PHOIBOS analyzer.

Acknowledgements: We thank Yu. Dedkov (University of Shanghai, China) and M. Fonin (University Konstanz) for providing beamtime and samples for the measurements with KREIOS 150 at BESSY II.

The TESLA JT SPM

M. Maier, D. Stahl, A. Pirou, M. Fenner, T. Roth

Scienta Omicron GmbH
(corresponding author: M. Maier, e-mail: markus.maier@scientaomicron.com)

The TESLA JT SPM provides access to more than 5 days SPM measurement time at temperatures down to 1K (^{4}He operation) with magnetic fields larger than B > 3T. Careful thermal design of the bath cryostat and JT cooling stage as well as the integrated UHV magnet lead to exceptionally low LHe consumption, specifically during magnet operation. The external JT Helium supply allows for ^{3}He operation and significantly lower temperatures.

The microscope head is a proven, highly stable design developed specifically for high magnetic field environments. It offers the full range of SPM measurements modes, including Scienta Omicron's leading QPlus AFM technology.

Safe and independent tip/sample exchange under optical control is one of several key ease-of-use features delivering dependable high performance SPM and successful scientific work.

In contrast to a conventional wet magnet concept, the dry split-pair magnet provides for optical access enabling various optical experiments and even in-situ evaporation into the SPM at low temperatures.

We will discuss the technical concept and will show performance evaluation measurements at T=1K that prove stability below 1pm, energy resolution on superconductors, continuous STM imaging and spectroscopy during magnetic field variation.

Postersession

Exploring the Relation Between Intramolecular Conjugation and Band Dispersion in One-Dimensional Polymers

C. García-Fernández[1], Emil Sierda[2,3], Mikel Abadía[4], Bernhard Bugenhagen[5], Marc Heinrich Prosenc[5,6], Roland Wiesendanger[2], Maciej Bazarnik[2,3], José Enrique Ortega[1,4,7], Jens Brede[4], Eduard Matito[1,8,9], and Andrés Arnau[1,4,10]

(corresponding author: Andrés Arnau, e-mail: andres.arnau@ehu.eus)

[1] *Donostia International Physics Center (DIPC), Paseo Manuel de Lardizabal 4, 20018, Donostia-San Sebastián, Spain*
[2] *Department of Physics, University of Hamburg, Jungiusstrasse 11, D-20355, Hamburg, Germany*
[3] *Institute of Physics, Poznan University of Technology, Piotrowo 3, 60-965, Poznań, Poland*
[4] *Centro de Física de Materiales CSIC/UPV-EHU-Materials Physics Center, Manuel Lardizabal 5, 20018, San Sebastian, Spain*
[5] *Institute of Inorganic and Applied Chemistry, University of Hamburg, Martin-Luther-King-Platz 6, D-20146, Hamburg, Germany*
[6] *Department of Chemistry, Technical University Kaiserslautern, Erwin-Schroedinger-Strasse 52, D-67663, Kaiserslautern, Germany*
[7] *Departamento Física Aplicada I, Universidad del País Vasco, 20018, San Sebastián, Spain*
[8] *IKERBASQUE, Basque Foundation for Science, 48011, Bilbao, Spain*
[9] *Faculty of Chemistry, University of the Basque Country UPV/EHU P.K. 1072, 20080 Donostia, Euskadi Spain*
[10] *Departamento Física de Materiales, Universidad del País Vasco, 20018-San Sebastian, Spain*

Making use of the inherent surface anisotropy of different high index surface planes vicinal to the low index Au(111) orientation, one-dimensional polymers have been synthesized following established procedures from two different precursor molecules. The successful polymerization of both 4,4″-dibromo-*p*-terphenyl and 5,5′-dibromo-salophenato-Co(II) precursors into poly(*p*-phenylene) and poly[salophenato-Co(II)], respectively, has been confirmed by scanning tunneling microscopy and low energy electron diffraction. Angle-resolved photoemission spectroscopy data reveal a highly dispersive band in the case of poly(*p*-phenylene) while no significant dispersion is resolved for poly[salophenato-Co(II)]. On the basis of density functional theory calculations, we explain this observation as a result of a high conjugation along the aromatic phenyl groups in poly(*p*-phenylene) that is absent in the case of poly[salophenato-Co(II)], where intramolecular conjugation is interrupted in the salophenato-Co(II) unit. Furthermore, we make use of multicenter and delocalization indexes to characterize the electron mobility (corresponding to a high band dispersion) along different paths associated with individual molecular orbitals.

Development and Integration of a Universal SPM head for Low Temperature SPM measurements

B. Guenther, A. Feltz, and A. Bettac

Sigma Surface Science GmbH, 65594 Taunusstein, Germany
(corresponding author: A.Bettac, e-mail: andreas.bettac@sigma-surface-science.com)

Recently we have developed an SPM microscope head that merges the needs for high resolution STM/QPlus-AFM [1] and at the same time satisfies the requirements for integration into different cryogenic environments including in situ tip and sample handling.

So far the new SPM head was integrated into different platforms, e.g. in a Pulse Tube Cryostat environment (T<10K), in a UHV Helium Flow Cryostat (<10K) and in a 3He Magnet Cryostat UHV system for high magnetic fields (±12T) and temperatures <400mK. Furthermore we have successfully integrated the SPM head in a very compact in-house developed bath cryostat with superconducting magnet (B_Z=5T).

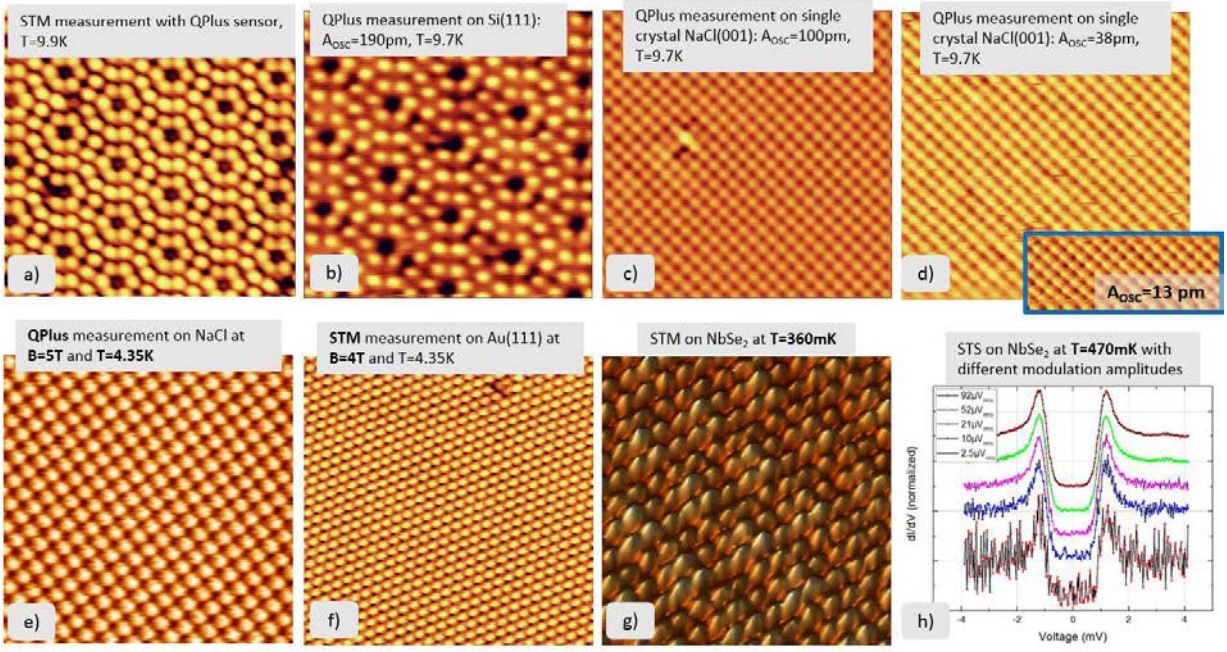

Figure: SPM results with new developed SPM head
Upper row: STM and NC-AFM result obtained with the Pulse Tube cryostat platform at a temperature of T<10K
Bottom row: e) and f) QPlus and STM measurement results (obtained with new developed bath cryostat); g) and h) STM and STS measurements obtained in a 3He bottom loader cryostat

This contribution focuses on design aspects and challenges for the new SPM head with respect to QPlus and STM signal shielding as well as on first results (STM, STS and QPlus)

obtained with the different instrumental setups. In detail we will present first QPlus results that have been measured with the Pulsed Tube cooler platform. With a very efficient acoustic and mechanical noise cancellation, it is possible to measure with oscillation amplitudes as low as 13pm. Furthermore we will present QPlus and STM measurements in a static and dynamic magnetic field of up to 5T that have been obtained with the new in-house-developed bath cryostat platform.

[1] F. J. Giessibl, Applied Physics Letters 73, 3956 (1998)

Modifying the surface stability of perovskite oxide cathode materials: Polarization and metal adsorption

Roland Bliem, Dongha Kim, Bilge Yildiz

Institute for Nuclear Science and Engineering, Massachusetts Institute of Technology, Cambridge, USA (Corresponding author: R.Bliem email: rbliem@mit.edu)

Highly active doped ternary oxides, including perovskites, are common functional materials in energy conversion, catalysis, and information processing applications [1]. At elevated temperatures related to synthesis or operation, however, surface segregation of dopant cations is a common problem of state-of-the-art materials, such as the Sr-doped La-based transition metal perovskites (La,Sr)CoO_3, (La,Sr)FeO_3, and (La,Sr)MnO_3, used for example as solid oxide fuel cell cathodes. In these oxides, Sr segregation under operating conditions leads to degradation via the formation of an inactive surface oxide [2,3], blocking the oxygen reduction reaction [4]. This dopant segregation occurs due to two driving forces: strain and electrostatics [5]. While the size mismatch between Sr and La cations causes strain that can be released via segregation, the electrostatic driving force originates in the interaction of positively charged oxygen vacancies at the surface with negatively charged dopants in the lattice. Here we aim to identify critical descriptors of this electrostatic effect, which may unveil strategies to tackle dopant segregation.

We modify the electrostatic driving force of segregation by changing the oxygen chemical potential at the surface of model cells using two approaches: polarization and chemical modification of the surface. Using *in-situ* ambient-pressure x-ray photoelectron spectroscopy (APXPS) at high temperatures and oxygen pressures close to operating conditions as well as *ex-situ* scanning probe microscopy, electron microscopy, and nano-Auger spectroscopy, we compare the properties of pristine and modified $La_{0.8}Sr_{0.2}MnO_3$ (LSM) thin films on (100)-oriented yttria-stabilized zirconia (YSZ) single crystals. The extent of segregation is determined based on the deconvolution of the Sr3*d* XPS peak into two species (Sr in pristine LSM and a segregated SrO_x species) and its intensity compared to La4*d* and Mn3*p*. In the polarization experiments, negative bias is applied between the model cathode and a grounded anode layer of porous Pt. An experimental setup that creates a polarization gradient across the surface [6] allows probing a range of different bias voltages on a single sample at equivalent experimental conditions. In the study of the effect of metal deposition, we employ APXPS and scanning probe microscopy to investigate how vapor-deposition of Hf affects the segregation behavior close to operating conditions. A nominal coverage of 4Å of Hf (as calibrated by a quartz crystal microbalance) is deposited *ex situ* on one half of an LSM thin-film sample at room temperature, followed by APXPS and microscopy experiments, in which we can compare pristine and Hf-modified LSM on one sample.

The effect of polarization is studied by applying a negative bias voltage of -600mV to an LSM thin-film model cathode. The applied voltage modifies the oxygen chemical potential at the surface, resulting in a lower effective oxygen pressure for negative polarity. APXPS spectra acquired in five spots of the LSM film, corresponding to five different bias voltages, show an enhancement of Sr segregation with increasing values of negative polarization. Electron microscopy images show precipitates attributed to SrO_x that increase in coverage and size in the regions modified by higher negative polarization. These

observations emphasize the relation of Sr segregation to the surface oxygen vacancy concentration, which is expected to increase substantially under negative polarization.

In the second approach to influence the electrostatic driving force of segregation, we modify the surface by Hf deposition. Hf was selected, since a previous study demonstrates that the deposition of metals with low reducibility such as Zr, Ti, and in particular Hf stabilize thin films of $La_{0.8}Sr_{0.2}CoO_3$ (LSC), another state-of-the-art SOFC cathode material [7]. Even though LSM is an intrinsically different cathode material than LSC, we observe a similar enhancement of the surface stability of LSM in the presence of Hf. Hf is expected to change the surface oxygen chemical potential of LSM, thus decreasing the overall reducibility of the surface. However, in contrast to LSC, we report changes in the surface stoichiometry of LSM, indicating a different stabilization mechanism, potentially involving the formation of a new type of surface phase.

The results of both studies identify the reduction state of the surface as an important factor in the segregation of Sr. Reducing the surface results in an enhancement of Sr segregation, in agreement with the observation that a decrease in reducibility can diminish this deactivation process. We present metal deposition as an effective way to tune the surface reducibility of LSM, offering a wide variety of options to optimize its stability and long-term activity.

Support by the Fonds zur Förderung der Wissenschaftlichen Forschung (FWF, project J4099) and the Air Force Office of Scientific Research (AFOSR) is gratefully acknowledged.

[1] N. Setter and R. Waser, Acta mater. 48, 151 (2000).
[2] S.P. Jiang J. Mater. Sci. 43, 6799 (2008).
[3] R. Bertacco, J.P. Contour, A. Barthélemy, and J. Olivier, Surface Science 511, 366–372 (2002).
[4] S.P. Jiang and J.G. Love, Solid State Ionics, 138, 183 (2001).
[5] W. Lee, J.W. Han, Y. Chen, Z. Cai, and B. Yildiz, J. Am. Chem. Soc. 135, 7909 (2013).
[6] T. Huber *et al.* J. Electrochem. Soc., 164 F809-F814 (2017).
[7] N. Tsvetkov, Q. Lu, L.Sun, E.J. Crumlin, and B. Yildiz, Nat. Mater. 15, 1010 (2016).

Surface chemistry of ruthenates

Ulrike Diebold[1], Daniel Halwidl[1], Wernfried Mayer-Schmözer [1,2], Martin Setvin[1], Florian Mittendorfer[1,2], Josef Redinger[1,2], and Michael Schmid[1]

[1]Institute of Applied Physics, TU Wien, A-1040 Wien, Austria
(corresponding author: U. Diebold, e-mail: diebold@iap.tuwien.ac.at)

[2]Center for Computational Materials Science, TU Wien, Vienna, Austria

Ternary oxides with a perovskite-type crystal structure are of increasing interest in energy-related applications such as solid oxide fuel/electrolysis cells and (photo-)electrocatalysis. Surface science studies can provide an atomic-scale understanding of relevant fundamental processes, but appropriate model systems with a well-defined surface structure are rare.

Here we report our results on the cleaved CaO and SrO-terminated surfaces of the Ruddlesden-Popper materials $Ca_3Ru_2O_7$ and $Sr_3Ru_2O_7$. Surfaces can easily be prepared by exfoliation in UHV, which provides large, defect-free terraces that are ideal for atomic-scale investigations [1, 2]. We used STM and nc-AFM in combination with XPS and DFT to investigate the adsorption of H_2O [2, 3] and O_2 [4]. We find that results on the related binary oxides give a good first guide for the adsorption behavior, while the tilting and rotation of the materials' octahedra strongly influence the ordering of overlayers.

This work was supported by the Austrian Science Fund (FWF projects F45 and Z 250-N27), the ERC Advanced Grant "OxideSurfaces" and the Vienna Scientific Cluster (VSC)

d

[1] B. Stöger, et al. Phys Rev B B, 90 (2014) 165438.
[2] B. Stöger, et al. Phys. Rev. Lett., 113 (2014) 116101.
[3] D. Halwidl, et al., Nature Mater. 15 (2016) 450.
[4] D. Halwidl, et al., Nature Comm. 8 (2017) 23.
[5] D. Halwidl, et al., submitted.

In-situ investigations of pulsed-laser-deposited Sr-doped lanthanum manganite thin films

Giada Franceschi, * *Michele Riva, Michael Schmid, and Ulrike Diebold*

Inst. Appl. Phys., TU Wien, Wiedner Hauptstraβe 8-10, 1040 Wien, Austria

*franceschi@iap.tuwien.ac.at

Sr-doped lanthanum manganite ($La_{0.8}Sr_{0.2}MnO_3$, or LSM) is a widely used material as a cathode in solid oxide fuel cells, and atomic-scale understanding of the reactions occurring at its surface is interesting from both fundamental and application-driven points of view. Atomic-scale investigations require a well-defined and well-ordered system, but LSM single-crystals are not available commercially. In the present contribution, I will show our efforts towards the establishment of a model system for LSM, in the form of a thin, pulsed-laser-deposited film onto $SrTiO_3$(110) substrates.
Combination of pulsed laser deposition with *in situ* surface sensitive techniques (STM, LEED, XPS, LEIS) allows to controllably tune the surface composition, and establish a relation with its structure.

Reactivity of Pt and Rh adatoms, dimers, and small clusters on Fe_3O_4 (001)

Jan Hulva[1], Matthias Meier[2], Martin Setvin[1], Zdenek Jakub[1], Roland Bliem[1], Michael Schmid[1], Ulrike Diebold[1], Cesare Franchini[2], Gareth S. Parkinson[1]

[1] TU Wien, Institute of Applied Physics, Vienna, Austria

[2] University of Vienna, Faculty of Physics and Center for Computational Material Science, Vienna, Austria

The rapidly emerging field of "single-atom catalysis" aims to drastically reduce the amount of precious metal required to catalyze chemical reactions by replacing nanoparticles with single-atom active sites. Although there are now many reports of active single-atom catalysts [1], the concept itself remains controversial because it is challenging to characterize real catalysts and determine the reaction mechanism. In our work, we study fundamental properties of supported single metal atoms using a surface science approach. We employ the Fe_3O_4 (001) surface as a model support, because it can stabilize dense arrays of single metal atoms to temperatures as high as 700 K [2,3]. In this contribution, we address the adsorption behavior and reactivity of the Pt and Rh adatoms, dimers, and small clusters using a combination of atomically resolved STM and non-contact AFM, high-resolution spectroscopy, and density functional theory. We conclude that Pt adatoms are inactive because CO adsorption results in mobility, and rapid sintering into Pt_2 dimers [5]. Pt dimers, on the other hand, are stable, and highly efficient CO oxidation catalysts. By isotopically labelling the oxide surface with ^{18}O, we unambiguously show that a Mars van Krevelen mechanism is responsible for the catalytic activity. Rh adatoms interact more strongly with the oxide, and do not sinter upon adsorption of CO. As a result, we find that Rh adatoms do catalyze CO oxidation, also via a MvK mechanism.

[1] – Acc. Chem. Res. 46(2013), pp.1740-1748.
[2] – Phys.Rev.Lett.108(2012): 216103
[3] – Science 346 (2014): 1215-1218.
[4] – Angew. Chem. Int. Ed. 54.47 (2015): 13999-14002.
[5] – PNAS 113.32 (2016): 8921-8926.

Babinet principle and localized surface plasmon resonances: HR STEM – EELS studies

Michal Horák[1], Vlastimil Křápek[1,2], Martin Hrtoň[1], Michael Stöger-Pollach[3], Tomáš Šamořil[1,2], Ondřej Metelka[2], Aleš Paták[4], Filip Ligmajer[1,2], Radek Kalousek[1,2], and Tomáš Šikola[1,2]

[1] *Central European Institute of Technology, Brno University of Technology, Purkyňova 123, 612 00 Brno, Czech Republic*
(corresponding author: R..Kalousek, e-mail: kalousek@fme.vutbr.cz)

[2] *Institute of Physical Engineering, Brno University of Technology, Technická 2, 616 69 Brno,Czech Republic*

[3] *University Service Centre for Transmission Electron Microscopy, TU Wien, Wiedner Hauptstraße 8-10, 1040 Wien, Austria*

[4] *Institute of Scientific Instruments, The Czech Academy of Sciences, Královopolská 147, 612 00 Brno, Czech Republic*

Localized surface plasmons (LSP) are collective oscillations of free electrons in metal nano- and microstructures of specific shapes and dimensions coupled to the local electromagnetic field. Such structures are often called the plasmonic antennas. A characteristic feature of LSP is a strong enhancement of electromagnetic field within the surrounding dielectric together with its confinement on the subwavelength scale, which can be utilized to control various optical processes in the visible- and near infrared spectral region even below the free space diffraction limit [1]. Significance of this feature is further increased by easy tunability of the optical properties of nanostructures via engineering their size, shape, or dielectric environment [2]. This design flexibility can be used for a large amount of optical functions, therefore plasmonic antennas have a wide field of applications. New discoveries with high application potential are often connected to implementation of new concepts into the field of plasmonics. Such an example is the Babinet principle of complementarity, which describes the correspondence between optical response of apertures and their complementary particles [3].

In the pioneering works about the Babinet principle in plasmonics, the main complementary characteristics of apertures and particles were identified [4,5,6], and methods of their evaluation were proposed [7]. In particular, the correspondence not only between reflectance and transmittance was verified, but also between effective permittivity resonances. The Babinet-complementary nanostructures were also discussed from the perspective of nonlinear optical processes [8], their sensing capabilities were evaluated both in the visible [9] and

infrared [10], and complementary metamaterials on their basis were demonstrated [11]. Seminal work by Hentschel et al. [12] provided a comprehensive survey of the important principles involved in coupled solid and hollow plasmonic nanostructures. Apart from identifying many open questions in the field, they stressed the importance of spatial and spectral overlap of the electric near-fields between coupled structures. Plasmonic nanostructures can be also used to direct radiation of nanoscale emitters, which was investigated in context of the Babinet complementarity [13], and the results demonstrated the immense potential of hollow plasmonic antennas for influencing magnetic resonances of both artificial and natural emitters [14].

We present an experimental study of the Babinet principle of complementarity in plasmonics. We show a set of elementary plasmonic antennas such as gold discs and apertures in a gold layer to investigate the basic properties of complementary structures and describe similarities and differences. Localized surface plasmon resonances in the antennas were measured by Electron Energy Loss Spectroscopy (EELS) and Cathodoluminescence (CL). We have focused on the main plasmon properties such as the plasmon resonance energy, the excitation efficiency, and the spatial distribution of the resonances.

This research has been supported by the Czech Science Foundation (17-25799S), CEITEC Nano RI (MEYS CR, LM2015041), CEITEC 2020 (MEYS CR, LQ1601), and Brno University of Technology (FSI/STI-J-17-4623).

[1] J. A. Schuller, E. S. Barnard, W. Cai, Y. C. Jun, J. S. White, and M. L. Brongersma, Nat. Mater. 9, 193 (2010)

[2] K. L. Kelly, E. Coronado, L. L. Zhao, and G. C. Schatz, J. Phys. Chem. B 107, 668 (2003)

[3] M. Born, E. Wolf, Principles of Optics: Electromagnetic Theory of Propagation, Interference and Diffraction of Light, Cambridge University Press, 2000

[4] F. Falcone, T. Lopetegi, M. A. G. Laso, J. D. Baena, J. Bonache, M. Beruete, R. Marqués, F. Martín, and M. Sorolla, Phys. Rev. Lett. 93, 197401 (2004)

[5] T. Zentgraf, T. P. Meyrath, A. Seidel, S. Kaiser, H. Giessen, C. Rockstuhl, and F. Lederer, Phys. Rev. B 76, 033407 (2007)

[6] H.-T. Chen, J. F. O'Hara, A. J. Taylor, R. D. Averitt, C. Highstrete, M. Lee, et al., Opt. Express 15, 1084 (2007)

[7] T. H. Hand, J. Gollub, S. Sajuyigbe, D. R. Smith and S. A. Cummer, Appl. Phys. Lett. 93, 212504 (2008)

[8] N. Feth, S. Linden, M. W. Klein, M. Decker, F. B. P. Niesler, Y. Zeng, W. Hoyer, J. Liu, S. W. Koch, J. V. Moloney, and M. Wegener, Opt. Lett. 33, 1975 (2008)

[9] T. Sannomiya, O. Scholder, K. Jefimovs, C. Hafner, and A. B. Dahlin, Small 7, 1653 (2011)

[10] C. Huck, J. Vogt, M. Sendner, D. Hengstler, F. Neubrech, and A. Pucci, ACS Photonics 2, 1489 (2015)

[11] X. Ni, S. Ishii, A. V Kildishev, and V. M. Shalaev, Light Sci. Appl. 2, e72 (2013)

[12] M. Hentschel, T. Weiss, S. Bagheri, and H. Giessen, Nano Lett. 13, 4428 (2013)

[13] J. Kim, Y.-G. Roh, S. Cheon, J.-H. Choe, J. Lee, J. Lee, H. Jeong, U. J. Kim, Y. Park, I. Y. Song, Q. H. Park, S. W. Hwang, K. Kim, C. W. Lee, Nano Lett. 14, 3072 (2014)

[14] T. H. Taminiau, S. Karaveli, N. F. van Hulst, and R. Zia, Nat. Commun. 3, 979 (2012)

Application of SPLEEM and highly performed strain-compensated super lattice photocathode

M. Suzuki[1)]*, T. Yasue[1)], E. Bauer[2)], X.G.Jin[3)] and Y.Takeda[4)], T. Koshikawa[1)]

1) Osaka Electro-Communication University Osaka, Japan,
2) Arizona State University, Tempe, USA,
3) KEK, Tsukuba, Japan
4) Aichi Synchrotron Radiation Center, Aichi, Japan

The current induced domain wall motion is a key phenomenon to realize novel spintronics devices. It has been indicated that domain in nanowires with perpendicular magnetic anisotropy can move with lower current density than those with in-plane magnetic anisotropy. Multilayer [CoNix] multi-layer is expected as the strong perpendicular magnetic anisotropy. We investigated magnetic property during growth of the [CoNix]y multi-layer with the SPLEEM. The magnetic domain images of SPLEEM results that the interface contribution between Ni and Co is dominant for the perpendicular magnetization. As shown in Fig.1 the experiments have been also carried out with the XMCD which can separate the contribution of Ni and Co, which showed the Ni contribution is dominant. These results show that the Ni layer at the interface could be big contribution.

The novel development has been performed on the photocathode, which is the strain compensated super lattice (SC-SL). This shows high quantum efficiency by factor 16 times compared from the strain SL and still keeps over 90% order of spin polarization. The beautiful TEM image is shown in Fig.2 [1]

Acknowledgement: The experiments were carried out with JST and JSPS research funds.

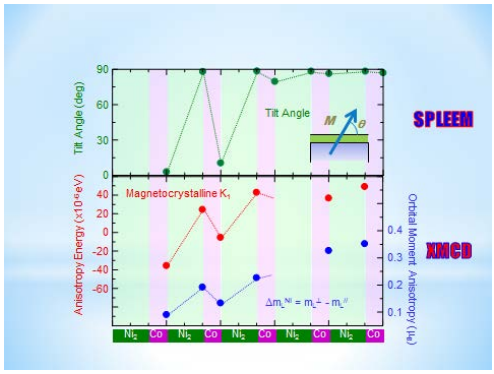

Fig.1 SPLEEM and XMCD results. They show the similar property. The positive anisotropy energy of XMCD suggests the perpendicular magnetization due to the contribution of orbital moment anisotropy which is the same of that SPLEEM.

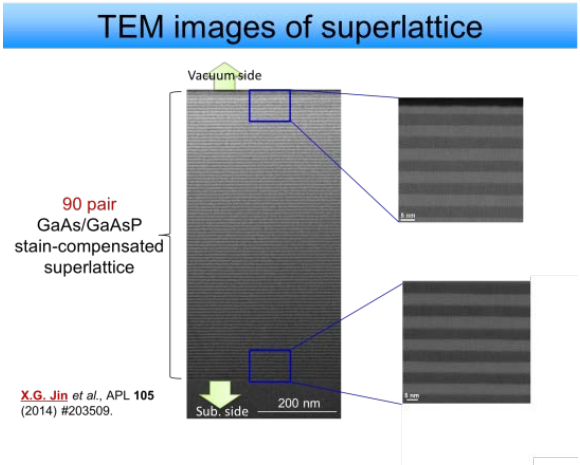

Fig.2 The TEM cross section image of the strain-compensated SL.

X.G. Jin et al., APL 105 (2014) 203509.

*Now He belongs to NIM, Tsukuba, Japan

Investigation of hydrogen isotope retention mechanisms in beryllium: High resolution TDS measurements

M. Eichler, T. Dittmar, D. Matveev, Ch. Linsmeier

Forschungszentrum Jülich GmbH, Institut für Energie- und Klimaforschung - Plasmaphysik, 52425 Jülich, Germany
(corresponding author: ch.linsmeier@fz-juelich.de)

During operation of the nuclear fusion experiment ITER hydrogen isotopes will be implanted in plasma facing components (PFC). The first wall of ITER will be made of beryllium while the divertor is made of tungsten. To predict the behavior of the PFC under the wide range of conditions that are to be expected in a fusion reactor, an understanding of the dominating mechanisms of hydrogen transport in the material and retention after implantation is required. In this work, the retained amount as well as the temperature dependent release of hydrogen after implantation in polycrystalline beryllium is investigated, which is of importance regarding the fuel balance in the plasma and possible changes of physical properties of the material caused by hydrogen uptake.

With this aim, the retention and temperature dependent release of hydrogen isotopes in beryllium is studied under well defined conditions using the ultra high vacuum experiment ARTOSS. With this facility, the in situ preparation and analysis of atomically clean surfaces at a base preassure of 2 x 10^{-11} mbar is possible. The sample surface is cleaned by Ar^+ sputtering and subsequent 1000 K annealing cycles. The chemical surface state is investigated by X-ray photoelectron spectroscopy. The ion bombardment caused by the hot plasma is simulated with a mass and energy separated ion source (0.6 - 6 keV/D, typically 10^{19} particles m^{-2} s^{-1}). Retained amounts of deuterium (D) are attained by nuclear reaction analysis (NRA). Additionally, information about the binding states of the retained D is accessed by thermal desorption spectroscopy (TDS). Different linear heating rates can be realized between 0.005 and 10 K/s up to 1000 K using an electron impact heater. Experiments have been carried out utilizing the described experimental procedure for pure polycrystalline Be surfaces. Deuterium ions are implanted with different fluences starting from 10^{18} m^{-2} up to 10^{22} m^{-2}, revealing low energy binding states in Be for higher fluences. Additionally, a variation of the used temperature ramps is performed. Especially using very slow ramps of 0.01 K/s makes it possible to resolve at least three low energy binding states of 0.43 eV, 0.67 eV and 0.82 eV for the first time. Comparable measurements are performed for oxidized Be surfaces after exposure to air. The high resolution TDS spectra are compared to older, already existing results [1]. Further investigation of the Be sample surfaces after implantation using SEM images shows that the low energy binding states seem to be not connected with the growth of Be-D dendrites on the surface [2]. Instead, the surface of our sample shows a fluence

dependent blistering effect, which is discussed as the reason for the low energy binding states. The experimental results are finally compared to coupled reaction-diffusion modeling including parameters, obtained from density functional theory calculations.

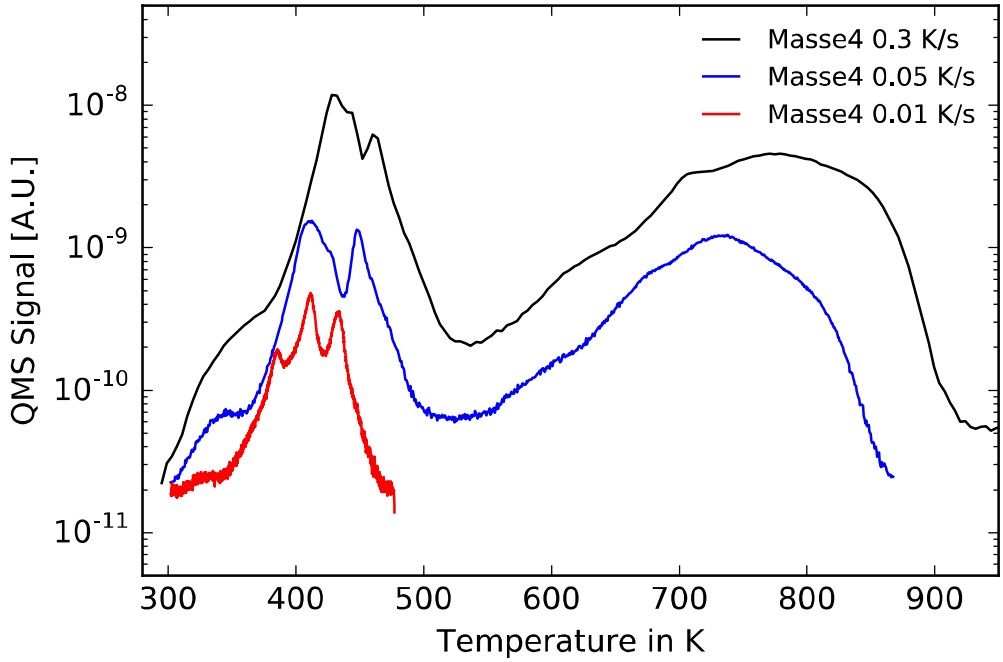

TDS spectra of deuterium implanted in polycrystalline beryllium using 1 keV/D and a fluence of $3x10^{21}$ D m^{-2}. As a consequence of the slow temperature ramps the low temperature peak is resolved and consists of at least three separate peaks.

[1] M. Reinelt, A. Allouche, M. Oberkofler and Ch. Linsmeier, New Journal of Physics 11 (2009) 043023.

[2] C. Pardanaud, M.I. Rusu, C. Martin, G. Giacometti, P. Roubin, Y. Ferro, A. Allouche, M. Oberkofler, M. Köppen, T. Dittmar and Ch. Linsmeier, Journal of Physics: Condensed Matter 27 (2015) 475401.

Electrochemical Surface Science of Magnetite Fe_3O_4 under Oxygen Evolution Conditions

Matthias Müllner, Michele Riva, Giada Franceschi, Gareth Parkinson, Ulrike Diebold, Stijn F. L. Mertens

TU Wien, Institut für Angewandte Physik, 1040 Vienna, Austria

Earth-abundant oxides such as magnetite Fe_3O_4, with the addition of dopants, are promising candidates for an effective but low-cost catalyst for the oxygen evolution reaction (OER), which is one of the remaining bottlenecks in electrolysis and artificial photosynthesis.

We report electrochemical surface science studies on well-defined magnetite single-crystal surfaces, with the aim of linking reactivity to atomic-level structural information. Preparation and characterisation in UHV (STM, LEED, XPS) are followed by transfer to the electrochemical environment (open-circuit potential measurements, cyclic voltammetry, impedance), using a new sessile-drop cell design. Post-measurement characterisation of the surface in UHV and by ambient AFM indicates stability of Fe_3O_4(001) towards electrolyte exposure (pH 7 up to 14) and during OER. Ongoing work aims to reveal the effects of surface orientation, whether transition-metal-doping of the surface is feasible and how this affects electrocatalytic activity.

Surface composition analysis of volatile species using Laser-Induced Ablation-Quadrupole Mass Spectroscopy (LIA-QMS) and Laser-Induced Breakdown Spectroscopy (LIBS)

J. Oelmann[1], S. Brezinsek[1], C. Li[1, 2], M. Rasinski[1], B. Turan[3], S. Haas[3], C. P. Dhard[4], T. Sunn Pedersen[4], R. König[4], Ch. Linsmeier[1] and the W7-X team[4]

[1] *Forschungszentrum Jülich GmbH, Institut für Energie- und Klimaforschung – Plasmaphysik, 52425 Jülich, Germany*
(Corresponding author: J. Oelmann, e-mail: j.oelmann@fz-juelich.de)
[2] *School of Physics, Dalian University of Technology, Dalian 116024, PR China*
[3] *Forschungszentrum Jülich GmbH, Institut für Energie- und Klimaforschung – Photovoltaik, 52425 Jülich, Germany*
[4] *Max-Planck-Institut für Plasmaphysik, 17491 Greifswald, Germany*

Laser-induced material analysis like LIBS [1] offer preparation-free sample composition analysis but cannot give a quantitative sample composition as it is based on a highly nonlinear ablation process. By using a quadrupole mass spectrometer for residual gas analysis after laser-induced ablation (LIA-QMS), the linearity of its signal to gas pressure simplifies the calibration and reduces uncertainties. The third harmonic (λ = 355 nm) of a Nd:YVO_4-laser with a pulse duration of τ_p = 35 ps is used in the presented setup, giving a depth resolution in the order of Δh =100 nm. A spot size diameter on the sample of x_{sp} = 0.7 mm with laser pulse energies of E_p = 30 mJ avoid significant matrix mixing effects but enables the simultaneous measurement of LIBS.
To show the capability of this method, a multilayer thin film solar cell is analyzed. LIA-QMS and LIBS signals are shown over laser ablation pulse number in Fig. 1. By analyzing the sample from its backside, at first a 1.6 µm thick µc-Si:H layer is p-i-n-junction is ablated in 8 laser pulses with an ablation rate of 200 nm/pulse. The electrode is a 0.5 µm thick ZnO:Al layer, which is partially transparent for the laser light. Thus, its ablation rate is lower than for the Si:H layer. The partial pressure of hydrogen and oxygen is detected by LIA-QMS with simultaneous measurement of Si and Zn with LIBS. The measured sample compounds in each layer show good agreement of LIA-QMS and LIBS signals (constant Si to H and Zn to O ratios). The hydrogen signal of LIBS is close to the noise level after the first laser pulse, which results in a sharp decay. Hence LIA-QMS is more efficient for hydrogen detection in this set-up, whereas LIBS can detect solid components.
Using this combined analysis technique, post mortem analysis of graphite limiter tiles from the stellarator Wendelstein 7-X (W7-X) after a hydrogen plasma campaign were performed. The aim is to study the impact of the plasma on the first wall surface and to measure the fuel (hydrogen) content at the surface quantitatively. This is essential to sustain the fuel cycle in a later reactor [2] as well as for safety reasons in long-term retained radioactive tritium. Previous surface studies of this samples with FIB, SEM and EDX measurement techniques could identify different interaction zones at the limiter: one zone where the graphite was purely eroded and zones with different kind

of deposition layers [3]. A lateral scan in toroidal direction of the limiter, analyzed with LIBS is in good agreement with these results [4].

In this work, LIA-QMS analysis additionally gives quantitative information about the hydrogen depth distribution of these tiles and a comparison to further poloidal and toroidal locations. The integrated hydrogen signal is compared with corresponding thermal desorption spectra, which provides an independent measure of the implanted and co-deposited hydrogen content.

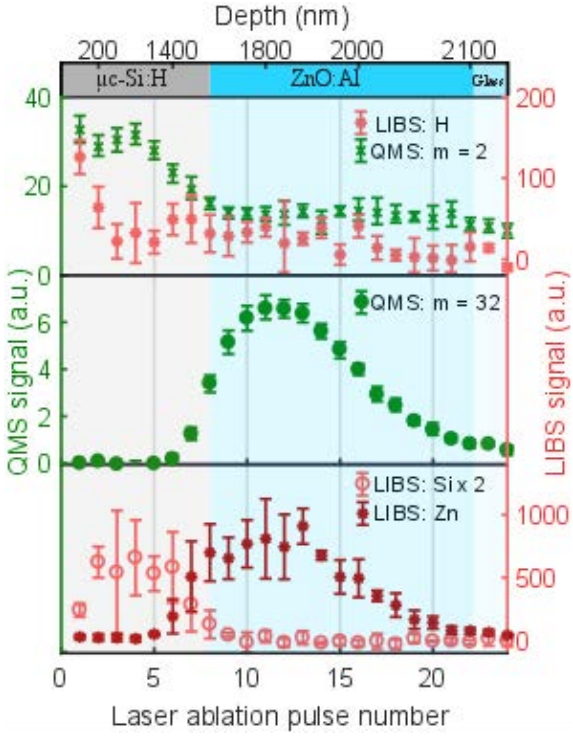

Fig. 1: LIA-QMS signal (green) and LIBS signal (red) over laser ablation pulse number and related average crater depth (top *x*-axis) of a thin film solar cell for laser-induced ablation with a pulse energy of E = 9 mJ and a laser spot diameter of x_{cr} = 800 µm.

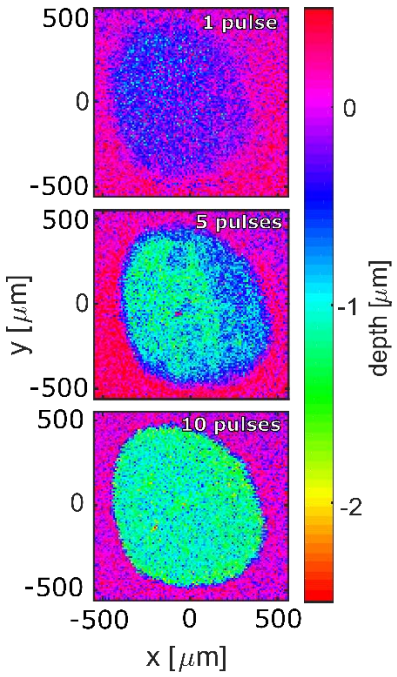

Fig. 1: Crater shape after one, five and ten laser pulses, measured by confocal microscopy.

[1] R. Noll, *Laser-Induced Breakdown Spectroscopy*, Springer Science & Business Media (2012).

[2] T.S. Pedersen et al., *Plans for the first plasma operation of Wendelstein 7-X,* Nuclear Fusion **55** *126001* (2015).

[3]. V.R. Winters et al., *Overview of the plasma-surface interaction on limiter surfaces in the startup campaign of Wendelstein 7-X.* Physica Scripta **T170** *014050* (2017).

[4]. C. Li et al., *Laser-induced breakdown spectroscopy for Wendelstein 7-X stellarator limiter tile analysis.* Physica Scripta **T170** *014004* (2017).

Femtosecond spectroscopic ellipsometry on optoelectronic materials and photonic structures

M. Rebarz[1], S. Espinoza[1], S. Richter[2], O. Herrfurth[2], J. Andreasson[1,3], R. Schmidt-Grund[2], and S. Zollner[4]

[1]*ELI Beamlines, Institute of Physics, Czech Academy of Science, 182 21, Prague, Czech Republic (corresponding author: M. Rebarz, e-mail: Mateusz.Rebarz@eli-beams.eu)*

[2] *Universität Leipzig, Institut für Experimentelle Physik II, 04103 Leipzig, Germany*

[3]*Condensed Matter Physics, Department of Physics, Chalmers University of Technology, SE-412 96 Gothenburg, Sweden*

[4]*Department of Physics, New Mexico State University, 88003-8001 Las Cruces, New Mexico,USA*

The ongoing progress in miniaturization and operational rates of electronic and optoelectronic devices obliges materials scientists to deeply understand the dynamics of the carriers upon external electromagnetic stimulus in very short time scale. Some phenomena such as scattering of excited carriers, their recombination as well as surface and bulk diffusion can happen in femto- and picosecond timescale. All these processes affect the temporal and local dielectric constants and determine many operational parameters of the devices. One of the most sensitive and non-invasive techniques for studying intrinsic dielectric properties of solid materials is ellipsometry i.e. the measurement of the changes in polarization upon the reflection of light from a surface. The experimental challenge is to make ellipsometry time-resolved technique useful in femtosecond timescale and operating in very broad spectral range. In this work, we report on recent progress in developing a spectroscopic ellipsometer for characterization of ultrafast dynamic changes of dielectric properties in materials and photonic structures technologically relevant in optoelectronics. Our time-resolved ellipsometer is based on pump-probe technique and offers monitoring the time evolution of the dielectric properties in range 0-5 ns with time resolution ~100 fs in broadband spectral range (340-750 nm).

This new instrument has been used to verify some theoretical predictions for Ge samples under femtosecond excitation [1]. Ultrafast phenomena such as excitation, relaxation and diffusion of charge carriers, band-gap renormalization and excitons screening have been investigated. Moreover the ultrafast ellipsometric measurements on undoped Ge revealed the existence of temporal phase-filling singularities which were observed before only in highly doped samples [2]. In addition we report on the first data obtained from a ZnO-based planar microcavity [3] especially on the temporal evolution of the microcavity modes. The time

evolution of the ellipsometric parameters in the spectral range around the exciton-polariton mode has been studied. It has been revealed that such modes disappear upon the excitation, possibly due to screening of the excitons and re-appear after a few hundreds of femtoseconds as blueshifted modes. The investigation of the short-time dynamics of such modes can stimulate new approaches for the description of exciton-polariton systems.

Support by the European Regional Development Fund: ELI Extreme Light Infrastructure Phase 2 (CZ.02.1.01/0.0/0.0/15_008/0000162) and ELIBIO (CZ.02.1.01/0.0/0.0/15_003/0000447) is gratefully acknowledged.

[1] S. Zollner, K.D. Myers, J.M. Dolan, D.W. Bailey, C.J. Stanton, Thin Solid Films 313-314, 568 (1998)

[2] C. Xu, N. Fernando, S. Zollner, J. Kouvetakis, J. Menendez, Phys. Rev. Lett. 118, 267402 (2017)

[3] H. Franke, C. Sturm, R. Schmidt-Grund, G. Wagner, M. Grundmann, New J. Phys. 14 013037 (2012)

X-ray investigation of Van der Waals Epitaxy of 2D diselenides and ditellurides

G. Renaud, R. Sant[1], A. Dimoulas[2,3], J. Coraux[1], S. A. Giamini[2], and P. Tsipas[2]

Univ. Grenoble Alpes, CEA INAC MEM, F-38000, Grenoble, France
(corresponding author: G. Renaud, e-mail: gilles.renaud@cea.fr)

[1] *Univ. Grenoble Alpes, Institut Néel CNRS, F-38000 Grenoble France*
[2] *Institute of Nanoscience and Nanotechnology, NCSR DEMOKRITOS, 1530 10, Athens, Greece*
[3] *LANEF Chair of Excellence, F-38000, Grenoble, France*

Atomically thin materials of the metal dichalcogenide family (MX_2, M=metal, X=S, Se, Te) are crystallized in stable 2D form and have been the subject of intense investigation due to a variety of physical properties **[1]**. Achievement of layered TMDs with large lateral dimensions is a pre-requisite for an easy implementation into devices and for the exploration of novel physics. For this purpose, molecular beam epitaxy is a viable approach for synthetizing large-scale TMDs thin films down to one monolayer with high uniformity and purity. In addition, as bulk Transition Metal Dichalcogenides (TMDs) exhibit out-of-plane van der Waals-type interactions between sandwiched layers, a van der Waals interaction between as-grown films with substrates is expected when growing TMDs films on inert substrates. Therefore, using Molecular Beam Epitaxy (MBE) allows to study impact of such short-range force on the growth dynamics of TMDs on different substrates [2].

Molecular beam epitaxy is used to synthetize a number of 2D materials and their van der Waals heterostructures [3-5] on crystalline AlN(0001)/Si(111), InAs(111)/Si(111) and on graphene on SiC(0001) substrates with the aim to obtain large area growth with good thickness uniformity [3]. The TMDs epilayers are fabricated by two-step growth processes which consists of depositing TMDs layers at a given temperature followed by a post-annealing around at a larger T. The growth rate and the substrate temperature of the first step play a key role in the growth dynamics of the TMDs. The post-annealing allows to improve the crystalline quality and to smooth the layers. The structure of the layers have been characterized by several techniques including RHEED, synchrotron X-ray diffraction, TEM and AFM.

Reciprocal space mapping obtained by synchrotron XRD (see e.g. the figure) and cross sectional HRTEM and STEM microscopy are used to investigate the epitaxial orientation, the microstructure and the crystalline quality of $MoSe_2$, $ZrTe_2$ [4] and $HfTe_2$ [5] layers. It is shown that there is a preferential in-plane alignment between the MX_2 layers and the substrate without 30 deg rotated domains, albeit with a sizeable in plane mosaicity. Defects due to heteroepitaxy (e.g. misfit dislocations or stacking faults) are not observed which is compatible with a vdW epitaxial growth mode, although the expected quasi-w.d.Waals gap at the interface could not be confirmed.

We will emphasize on the characterization of ZrTe2 semimetal evidencing massless Dirac fermions [4] and $HfTe_2$ [5] which also shows a semimetallic behavior with a very small overlapping between the conduction and valence bands. More interestingly, CB and VB disperse linearly near the center of the Brillouin zone (Γ point) and cross exactly at the Fermi energy exhibiting a Dirac cone-like behavior which is similar to the band dispersion of 3D topological Dirac semimetals, the so called "new 3D graphenes".

« This work is supported by French state funds ANR-10-LABX-51-01 (Labex LANEF du Programme d'Investissements d'Avenir) and by the French stat funds Equipex ANR-11-EQPX-0010 "

[1] G.R. Bhimanapati et al., *ACS Nano* 9, 11509 (2015);
[2] Koma et al., Thin Solid Films 216 (1992) 72
[3] Xenogiannopoulou et al., *Nanoscale* 7, 7896 (2015)
[4] S. A. Giamini *2D Mater* 4, 015001 (2017)
[5] P. Tsipas et al, ACS Nano, Just Accepted Manuscript Publication Date (Web): 09 Jan 2018

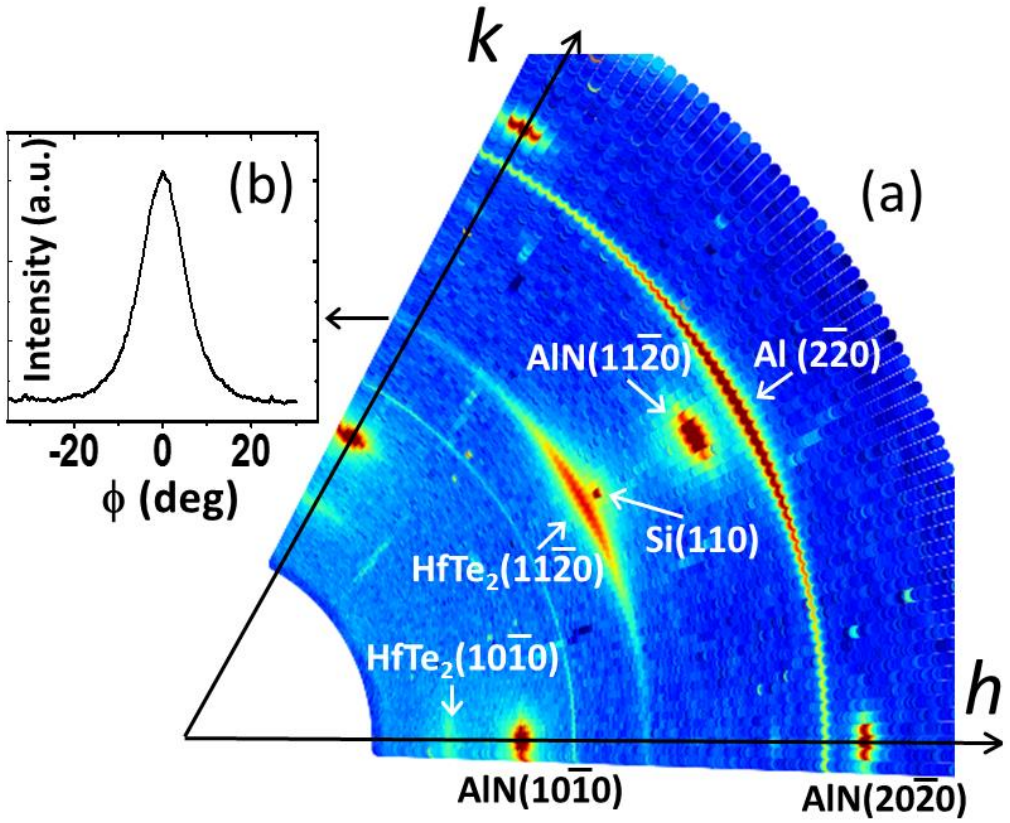

Figure: Extended in-plane reciprocal space map of a $HfTe_2$ layer grown on AlN(0001) on Si(111) [5].

Effects of surface structure on oxygen exchange on $SrTiO_3(110)$

M. Riva, M. Kubicek,[1] X. Hao,[2,3] S. Gerhold, G. Franceschi, M. Schmid, H. Hutter,[1] J. Fleig,[1] C. Franchini,[2] B. Yildiz,[4] and U. Diebold

Institut of Applied Physics, TU Wien, A-1040 Wien, Austria
(corresponding author: M. Riva, e-mail: riva@iap.tuwien.ac.at)

[1] *Institute of Chemical Technologies and Analytics, TU Wien, A-1060 Wien, Austria*

[2] *University of Vienna, Faculty of Physics and Center for Computational Materials Science, A-1090 Wien, Austria*

[3] *Key Laboratory of Applied Chemistry, Department of Chemical Engineering, Yanshan University, Qinhuangdao 066004, P. R. China*

[4] *Laboratory for Electrochemical Interfaces, Department of Nuclear Science and Engineering, Massachusetts Institute of Technology, Cambridge, MA 02139, United States*

Perovskite oxides are widely used and studied materials for enabling oxygen reduction and evolution reactions, which limit the efficiency of energy conversion technologies, including fuel cells, electrolyzers and photo-/electrochemical water splitting. In solid-state electrochemistry, most often the reactivity on perovskite oxides is interpreted in terms of the availability of surface oxygen vacancies, or the ease of electron transfer. Intriguingly, none of these standard reactivity models consider the role of the precise atomic structure of surfaces.

In the present contribution I will show that the surface atomic structure can play a crucial role in affecting oxygen exchange on the prototypical perovskite $SrTiO_3$ [1]. In doing so, we take advantage of our ability to reproducibly and reversibly prepare $SrTiO_3(110)$ with several different surface phases, by adjusting the chemical potential of Sr and Ti [2,3]. All the structures are based on families with $(n \times 1)$ and $(2 \times m)$ symmetries, with their surface layers composed of tetrahedrally- and octahedrally-coordinated Ti atoms, respectively [4,5]. Using a host of surface science techniques (STM, LEED, XPS, etc.) we find that these structures are remarkably stable under realistic conditions for oxygen-exchange reactions. We use two different ion-based spectroscopy techniques to quantify the ^{18}O exchange and find that the reactivity of these two reconstructions differs by a factor of three.

From DFT calculations and electron spectroscopic measurements we rule out that this difference is due to oxygen vacancies or the variations in work function or surface potential that would affect the availability of electrons on this material. Instead the structural details

determine the interaction with molecular oxygen: Our results reveal that the flexibility of coordination polyhedra of surface cartions is an important and new factor that governs the surface reactivity to oxygen exchange reactions on perovskite oxides [1].

Work supported by the Austrian Science Fund (Project F45, FOXSI) and the ERC Advanced Grant 'OxideSurfaces'.

[1] M. Riva, M. Kubicek, X. Hao, S. Gerhold, G. Franceschi, M. Schmid, H. Hutter, J. Fleig, C. Franchini, B. Yildiz, and U. Diebold, *submitted*.

[2] Z. Wang, J. Feng, Y. Yang, Y. Yao, L. Gu, F. Yang, Q. Guo, and J. Guo, Appl. Phys. Lett. **100**, 051602 (2012).

[3] Z. Wang, F. Li, S. Meng, J. Zhang, E. W. Plummer, U. Diebold, and J. Guo, Phys. Rev. Lett. **111**, 056101 (2013).

[4] J. A. Enterkin, A. K. Subramanian, B. C. Russell, M. R. Castell, K. R. Poeppelmeier, and L. D. Marks, Nature Mater. **9**, 245 (2010).

[5] Z. Wang, A. Loon, A. Subramanian, S. Gerhold, E. McDermott, J. A. Enterkin, M. Hieckel, B. C. Russell, R. J. Green, A. Moewes, J. Guo, P. Blaha, M. R. Castell, U. Diebold, and L. D. Marks, Nano Lett. **16**, 2407 (2016).

The atomic structure of a metal-supported two-dimensional Germania film

Adrian Lewandowski, Philomena Schlexer[1], Christin Büchner, Earl Davis, Hannah Burrall[2], Kristen M. Burson[2], Wolf-Dieter Schneider, Markus Heyde, Gianfranco Pacchioni[1], Hans-Joachim Freund

Fritz-Haber-Institut der Max-Planck-Gesellschaft, Faradayweg 4-6, 14195 Berlin, Germany
(e-mail: wolf-dieter.schneider@epfl.ch)

[1]*Dipartimento di Scienza dei Materiali, Università di Milano-Bicocca, Italy*
[2]*Taylor Science Center, Hamilton College, 198 College Hill Road, Clinton, NY 13323, USA*

Germanium oxide (GeO_2), or germania, is a highly insoluble thermally stable germanium source used in engineering optical materials such as windows and lenses of night-vision technology, luxury vehicles and thermographic cameras. Germania can be prepared in both crystalline and amophous forms [1]. It is mechanically stronger than other infrared (IR) transparent glasses, making it more reliable in harsh environmental conditions.

Analyzing the atomic structure of gemania plays a critical role in the understanding of its material properties. In the present study we investigated structures within a germania film on a ruthenium, Ru(0001), substrate. The samples were grown in an ultra-high vacuum chamber. A structure study by LEED-*IV* (Low energy electron diffraction) analysis was combinded with atomic-resolution real-space imaging by scanning tunneling microscopy (STM). Atomically flat monolayer (ML) germania films have been prepared allowing us to resolve in detailed STM images the individual network and domain boundary structures.

Throughout the structural analysis, LEED measurements were taken over an energy range of 60 and 550 eV with steps of 1 eV. 42 diffraction spots were recorded and averaged over 6 symmetry equivalent spots, leading to a total energy range of 2500 eV. The experimental curves were compared to modeled diffraction pattern intensities from suggested test structures based on density funtional theory (DFT) calculations. The individual preparation steps from the clean Ru(0001) substrate[2], the oxygen pre-covered Ru(0001)[3], and finally, the deposited gemania film on Ru(0001) were separately analyzed. For the germania monolayer film the best agreement has been achieved with DFT structures where the germanium atoms are located preferentially on atop and fcc hollow sites of the Ru(0001) substrate.

The STM images reveal a series of ring networks formed by the germanium and oxygen atoms present in this two-dimensional (2D) film. The size of a particular ring is defined by the number of germanium atoms in the ring. Ideal crystalline regions contain only six-membered rings, while domain boundaries and defects introduce other ring sizes. We identify a variety of domain boundaries with monolayer germania structures from STM data, discuss characteristic properties of the sample that result from these defects, and develop atomic models for the relationship between domain boundaries and the substrate. Initial results from germania films with coverages larger than one monolayer indicate that both, crystalline and amorphous configurations of germania might exist.

[1] M. Micolaut *et al*., J. Phys.: Condens. Matter **18**, R753 (2006)

[2] G. Mischalk *et al*., Surf. Sci. **129**, 92 (1983)

[3] M. Gsell *et al*., Isr. J. Chem. **38**, 339 (1998)

Interaction of highly charged ions with 2D materials

J. Schwestka[1], R.A. Wilhelm[1,2], S. Creutzburg[2], R. Heller[2], R. Kozubek[3], M. Schleberger[3], S. Facsko[2] and F. Aumayr[1]

[1]*TU Wien, Institute of Applied Physics, 1040 Vienna, Austria*

[2]*Helmholtz-Zentrum Dresden-Rossendorf, Institute of Ion Beam Physics and Materials Research, 01328 Dresden, Germany*

[3]*University Duisburg-Essen, Faculty of Physics and CENIDE, 47057 Duisburg, Germany*

Low dimensional materials have been in the spotlight of theoretical as well as experimental research for many years. They offer a broad range of unique properties and novel phenomena not found in bulk materials. Especially their electronic and optical properties and the already discovered ways to modify them, make 2D materials to promising candidates for future nano-devices [1–3].

A reliable tool for modification of those properties is found in making use of the high potential energy stored in a highly charged ion (HCI). With the usage of slow HCI projectiles, we can directly address the first few atomic layers of a target material, leading to a large energy deposition and distribution into the 2D material. Depending on the target's properties ion irradiation can result in modification of the material as well as damage formation.

For a better understanding of the nature of those effects on the material, we present a measurement technique, which allows a deeper insight in the charge transfer process between the projectile and the target. After the transmission through a freestanding two-dimensional membrane, the ion is still in a pre-equilibrium charge state, which we analyse by using a set of deflection plates in combination with a position sensitive microchannel plate (MCP) detector. From the mean exit charge state, we conclude the amount of captured and stabilised electrons during the interaction process. By measuring the time-of-flight of the projectile, we can calculate its energy loss during the transmission.

Recently the interaction of slow HCIs with the prototype 2D material, a single layer of graphene (SLG), has been studied by using an electrostatic analyser setup. The results show a surprisingly fast electronic response of SLG to a high local electric field of about 10^{11} V/m applied by slow HCIs [4]. With a new MCP detector setup, we extend our investigations on the material's response to other freestanding 2D candidates beyond graphene, like semiconducting molybdenum disulfide (MoS2).

[1] M.M. Furchi, D.K. Polyushkin, A. Pospischil, T. Mueller, *Nano Lett.* **14** (2014) 6165–6170.

[2] S. Schuler, D. Schall, D. Neumaier, L. Dobusch, O. Bethge, B. Schwarz, M. Krall, T. Mueller, *Nano Lett.* **16** (2016) 7107–7112.

[3] S. Wachter, D.K. Polyushkin, O. Bethge, T. Mueller, A microprocessor based on a two-dimensional semiconductor, *Nat. Commun.* **8** (2017) 14948.

[4] E. Gruber, R.A. Wilhelm, R. Petuya, V. Smejkal, R. Kozubek, A. Hierzenberger, B.C. Bayer, I. Aldazabal, A.K. Kazansky, F. Libisch, A. V Krasheninnikov, M. Schleberger, S. Facsko, A.G. Borisov, A. Arnau, F. Aumayr, *Nat. Commun.* **7** (2016) 13948.

Surface and quantum-well electronic states in ultra-thin Ir and Pt films on the Au(111) surface

I. V. Silkin[1], Y. M. Koroteev[2], E. V. Chulkov[3,4], P. M. Echenique[3,4], and V. M. Silkin[3,5]

Donostia International Physics Center (DIPC), 20018 San Sebastián, Spain
(corresponding author: V. M. Silkin, e-mail: waxslavas@ehu.es)

[1] *Tomsk State University, 634050 Tomsk, Russia*

[2] *Institute of Strength Physics and Materials Science, Russian Academy of Sciences, 634055 Tomsk, Russia*

[3] *Departamento de Física de Materiales, Facultad de Ciencias Químicas, Universidad del País Vasco, 20080 San Sebastián, Spain*

[4] *Material Physics Center MPC, Centro Mixto CSIC-UPV/EHU, 20018 San Sebastian, Spain*

[5] *IKERBASQUE, Basque Foundation for Science, 48011 Bilbao, Spain*

The heterostructures consisting of the noble metal substrates and the late d-metal adsorbates and other heavy atoms with the degree of coverage from one atom to several monolayers (MLs), have been actively studied for the last two decades [1-7]. The interest to these systems can be explained by the possibility of exploiting them in chemical industry, namely, in heterogeneous catalysis. It is known that the properties of two-dimensional systems can drastically differ from the properties of their bulk counterparts [8,9]. Moreover, frequently the degree of coverage plays a crucial role in these effects. An example of such situation is the Pt/Au(111) heterostructure with the Pt adsorbate thickness varying from one to several atomic layers. In general, favorable catalytic activity, resulting in strong enhancement in rates of certain oxidation reactions, of thin Pt films deposited on Au has been found [3,10-14]. All of this is making this and similar systems very attractive for experimental and theoretical research.

On the other hand, heterostructures containing as a substrate a heavy metal and several atoms/monolayers of metallic adsorbate demonstrate unique properties caused by spin-orbit interaction that may be attractive for spintronics, a research field experiencing nowadays explosive development. A well-known example is the Bychkov-Rashba splitting effect consisting in lifting of a spin degeneration in two-dimensional systems due to spin-orbit

interaction [14]. Large Bychkov-Rashba splitting is characteristic for surface states of both noble and late d metals such as Ir and Pt metals. Moreover the heterostructures based on light noble metals (Cu and Ag) and heavy metal adsorbate such as Bi and Pb have a giant spin-orbit splitting of surface states noticeably larger than in pristine materials. The main reason for this giant splitting is the occurrence of a local potential gradient at the surface of such heterostructures that does not exist inside the bulk materials with inversion symmetry.

In this work we investigate the formation of the surface and quantum-well states in thin Ir and Pt films deposited on the Au(111) substrate. From comparison of the electronic structure of Ir(111), Pt(111), and Au(111) surfaces [15] one can observe a strong mismatch between positions of the band gaps in the projected bulk electronic structures of these materials. As a result, the electrons related to iridium or platinum atoms are reflected from the gold substrate by its energy gaps. Together with scattering produced by the potential barrier from the vacuum side this introduces the necessary conditions for realization of the quantum-well states. Since the electronic states in Ir and Pt in the Fermi level vicinity are mainly of the d character they present strong localization at the surface. In turn, this produces strong modification in the density of states in the surface region. Studying Ir- and Pt-derived surface and quantum-well states at different regions of the surface Brillouin zone (SBZ) we find distinct formation character. We also investigate in these heterostructures the effect of spin-orbit interaction on the electronic states localized at the surface since despite many experimental and theoretical studies devoted to these systems with adsorbate thickness of several monolayers, the effect of the spin-orbit interaction on the electronic structure of these systems was not addressed.

[1] L. P. Nielsen, F. Besenbacher, I. Stensgaard and E. Laegsgaard, Phys. Rev. Lett. 74, 1195 (1995).
[2] C. S. Shern, J. S. Tsay and T. Y. Fu, Appl. Surf. Sci. 92, 74 (1996).
[3] K. Uosaki, S. Ye, H. Naohara, Y. Oda, T. Haba and T. Kondo, J. Phys. Chem. B 101, 7566 (1997).
[4] J. C. Bertolinn, Appl. Catal. 191, 15 (2000).
[5] F. Maroun, F. Ozanam, O. M. Magnussen and R. J. Behm, Science 293, 1811 (2001).
[6] H. F. Waibel, M. Kleinert, L. A. Kibler and D. M. Kolb, Electrochim. Acta 47, 1461 (2002).
[7] A. E. Baber, H. L. Tierney and E. C. H. Sykes, ACS Nano 4, 1637 (2010).
[8] T.-C. Chiang, Surf. Sci. Rep. 39, 181 (2000).
[9] E. V. Chulkov, A. G. Borisov, J. P. Gauyacq, D: Sanchez-Portal, V. M. Silkin, V. P. Zhukov and P. M. Echenique, Chem. Rev. 106, 4160 (2006).
[10] M. O. Pedersen, S. Helvig, A. Ruban, I. Stengaard, E. Laegsgaard, J. K. Norskov and F. Besenbacher, Surf. Sci. 426, 395 (1999).
[11] Y. Gohda and A. Gross, Surf. Sci. 601, 3702 (2007).
[12] M. Li, P. Liu and R. R. Adzic, J. Phys. Chem. Lett. 3, 3480 (2012).
[13] S. H. Ahn, Y. Liu and T. P. Moffat, ACS Catal. 5, 2124 (2015).
[14] Y. A. Bychkov and E. I. Rashba, JETP Lett. 39, 78 (1984).
[15] A. Dal Corso, Surf. Sci. 637-638, 106 (2015).

Sputtering of Fusion Relevant Materials and Comparison to SDTrimSP-2D and TRI3DYN

R. Stadlmayr, P.S. Szabo, D. Mayer, D. Thima, B.M. Berger,
D. Blöch and F. Aumayr

Institute of Applied Physics, TU Wien, Fusion@ÖAW
Wiedner Hauptstraße 8-10, A-1040 Wien, Austria
(corresponding author: R. Stadlmayr, e-mail: stadlmayr@iap.tuwien.ac.at)

In a future fusion reactor and in DEMO a stable and quiescent plasma can be assumed. With this presumption the lifetime of the plasma facing components (PFCs) will be mainly limited by plasma-induced erosion due to ion and neutral particle bombardment [1]. An improvement of our understanding in plasma surface interactions is therefore crucial in order to use nuclear fusion as an energy source. At the expected low ion energies in the near PFC surface region [2], the erosion rate of high-Z materials is significantly lower than the erosion of low-Z materials. Therefore the use of thin tungsten (W) armors as PFCs are foreseen in some DEMO design studies [2, 3]. Additionally, the presumed steady-state operation of a future fusion reactor brings new demands to the heat removal from the PFCs. Especially the bonding of the W armor to the cooling components is highly important and technologically challenging.

An attractive alternative to a full tungsten armor, especially for recessed areas in a fusion reactor, is the use of tungsten containing steels, like EUROFER [1, 3]. Investigations of Fe-W sample films (with 1.5 at% W), which can be seen as a model system for EUROFER, showed a strong decrease in the sputtering yield for low energetic D ion bombardment at high incident fluences [4, 5]. Sputtering of the wall material in addition causes modifications of the surface topography (i.e. roughening or smoothening, ripple or blister formation) of the PFCs which in turn will influence the sputtering behaviour [4, 5].

To separate the effect of surface structural modifications from the effect of surface enrichment of high Z materials, experiments were performed using pure Fe and W target films. Due to the fact, that Ar might be used as seeding gas in fusion reactors like ITER, to avoid local overheating of the PFCs by radiative cooling [6] and Ar – Fe,W sputtering yields are significantly higher than D – Fe,W sputtering yields, our investigations concentrated on Ar.

Hence we have investigated the influence of surface morphology modifications on the sputtering of fusion relevant materials by using a highly sensitive quartz crystal microbalance (QCM) technique. The morphology changes are induced by prolonged irradiation of 400 nm thick Fe and W films (up to 25% roughness), by mono-energetic Ar ions at various angles of incidence. Atomic force microscopy measurements are performed to analyse the sample topography before and after irradiating up to a fluence of 10^{22} Ar/m2 and to determine surface

roughness parameters. Numerical modelling with dynamic and morphology including Monte-Carlo BCA codes, like SDTrimSP-2D and TRI3DYN are performed for comparison [7-9].

Our investigations show that by including the local distribution of projectile impact angles, as derived from AFM measurements, as well as the elemental depth profile of the samples as an input to SDTrimSP-2D the agreement between experiment and simulation is substantially improved [5]. Further investigations with 3D Monte-Carlo BCA codes like TRI3DYN gave deeper insight into the dynamics of surface morphology changes and its influence to sputtering.

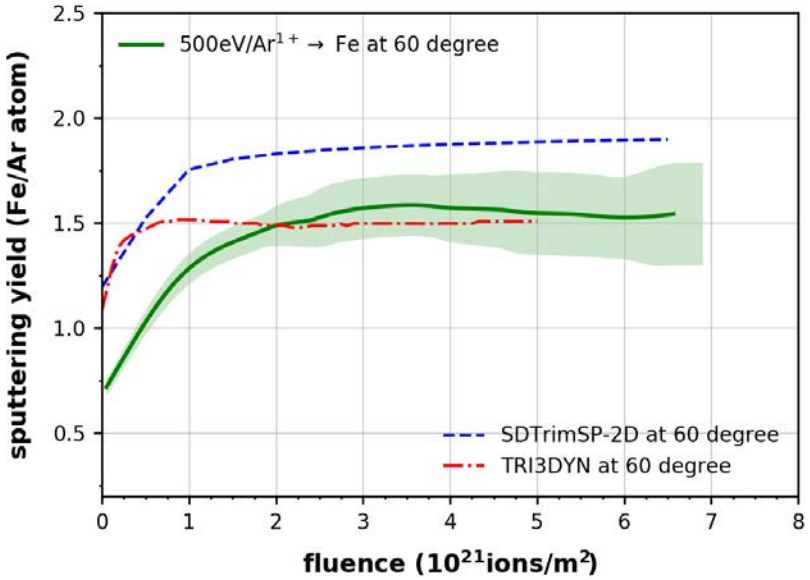

Fig. 1 Sputtering yield of an Fe sample under monoenergetic Ar ion bombardment (500eV/Ar^{1+}) as a function of fluence, under 60 degree impact angle (with respect to the surface normal) in comparison to SDTrimSP-2D and TRI3DYN simulation.

The authors are grateful to M. Oberkofler (IPP Garching) for preparation of the Fe and W model films, to A. Mutzke (IPP Greifswald) for his support in SDTrimSP-2D, to W. Möller (HZDR Dresden) for his support in TRI3DYN and to M. Schmid (TU Wien) for his continued support with the QCM electronics. This work has been carried out within the framework of the EUROfusion Consortium and has received funding from the Euratom research and training programme 2014-2018 under grant agreement No 633053. The views and opinions expressed herein do not necessarily reflect those of the European Commission. Financial support has also been provided by KKKÖ.

[1] S. Brezinsek et al., Nucl. Fusion **57** (2017) 116041
[2] H. Bolt et al., J. Nucl. Mat. **43** (2002) 307-311
[3] R. Lindau et al., Fusion Eng. Design **989** (2005) 75-79
[4] B.M. Berger et al., Nucl. Mat. Energy **12** (2017) 468-471
[5] R. Stadlmayr et al., Nucl. Instrum. Meth. Phys. Res. B, submitted
[6] A. Kallenbach et al., Plasma Phys. Control. Fusion **55** (2013) 124041
[7] A. Mutzke et al., Techn. Report IPP 12/11, (2013)
[8] U. von Toussaint et al, Physica Scripta, **T167** (2016) 014023
[9] W. Möller et al., Nucl. Instrum. Meth. Phys. Res. B, **322** (2014) 23

Low Temperature UHV STM
& micro Raman Spectroscopy

UNISOKU

USM1400-TERS

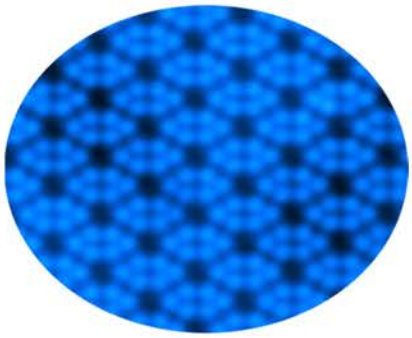

High Resolution STM

Precise Optical Tip Navigation

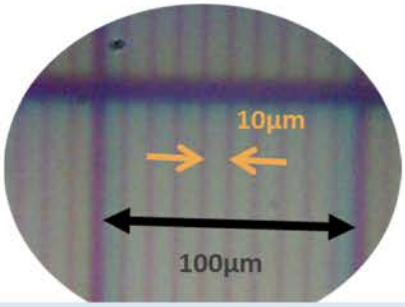

High Effiency Collection

Perfect Focussing

True Single Molecule Resolution in TERS

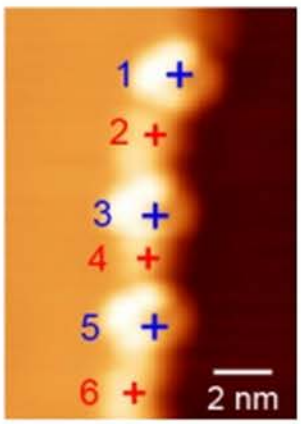

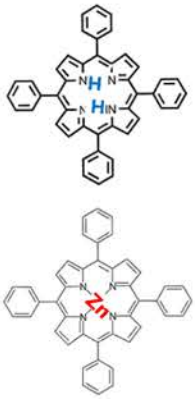

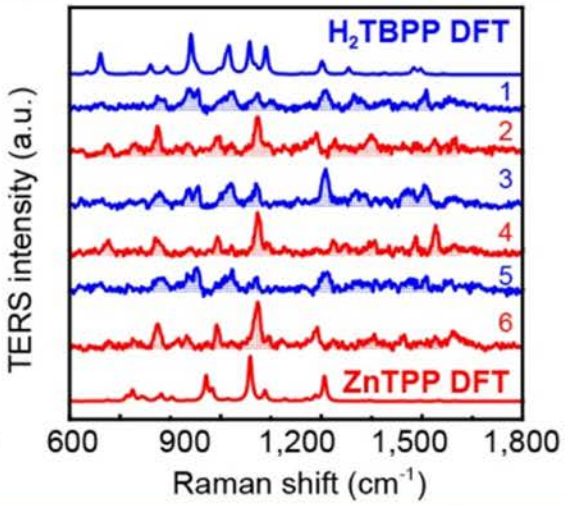

ZnTPP+H2TBPP on Ag, Z.Dong + et al. Nature Nanotechnology 10, 865–869 (2015)

nanoscore gmbh Distributor for UNISOKU and BihurCrystal in Europe

Maisebachstr. 3
61479 Glashütten
Germany

www.nanoscore.de

Thursday

SPM discrimination of the spin-state in organometallic complex and its control by positioning on N-doped graphene

Bruno de la Torre[1,2], Martin Švec[1,2], Prokop Hapala[1], Jesus Ruben[1], Ondřej Krejčí[1], Rabindranath Lo[3], Debashree Manna[3], Amrit Sarmah[3], Dana Nachtigallova[3], Jiri Tucek[2], Piotr Błoński[2], Michal Otyepka[2], Radek Zboril[2], Pavel Hobza[2,3], Pavel Jelínek[1,2]

[1] *Institute of Physics of the Czech Academy of Sciences, Cukrovarnická 10, Prague 6, Czech Republic.*
(corresponding author: P. Jelinek, e-mail: jelinekp@fzu.cz)

[2] *Regional Center of Advanced Technologies and Materials, Palacký University, Olomouc, Czech Republic.*

[3] *Institute of Organic Chemistry and Biochemistry, Czech Academy of Sciences, Flemingovo nám. 2, 16610 Prague 6, Czech Republic.*

Possibility to control electronic and magnetic states of single molecules represents a big challenge towards miniaturization of electronic devices on molecular scale. So far modification of spin states of single molecules was achieved applying various external stimuli including temperature, light, magnetic and electric field [1]. Here, we introduce additional emerging strategy based on a cooperative effect of a weak non-covalent interaction of iron(II) phtalocyanine (FePc) with graphitic N-doped graphene [2] and electron density rearrangement between iron(II) d-orbitals and the singly occupied p_z orbital of the N atom of doped graphene. The interaction is characterized by sharp variations in the sub-molecular contrast over molecules located on bare graphene and in vicinity of the graphitic N-dopant. High-resolution atomic force microscopy (AFM) experiments with functionalized CO-tip [3], supported by theoretical calculations, show a reorganization of the electron density distribution within molecule corresponding to singlet and triplet spin states, respectively. This work demonstrates capability of the technique to discriminate between different spin states of single molecules. This opens the doors towards control of their electronic properties via non-covalent interaction and positioning, by means of molecular manipulation, onto suitably functionalized graphene.

[1] P. Gutlich, et al, Chem. Soc. Rev. 29, 419-427 (2000); S. Ohkoshi, et al, Nat. Chem. 3, 564-569 (2011).
[2] M. Telychko, et al, ACS Nano 8, 7318–7324 (2014).

[3] L. Gross, et al, Science **325**, 1110-1114 (2009); P. Jelinek J. Phys. Cond. Mat. 29 343002(1) - 343002(18) (2017).

Surface-adsorbed magnetic materials: A challenge for first-principles theory

G. S. Michelitsch, K. Reuter

Lehrstuhl für Theoretische Chemie, Technische Universität München, 85747 Garching b. München, Germany

(corresponding author: G.S. Michelitsch, e-mail: georg.michelitsch@ch.tum.de)

Single, heavy-metal atoms are an appealing ultimate unit in the quest for an ever more miniaturized information storage. Core-level spectroscopies are among the most established methods of characterization in modern material science, providing information about the chemical interaction and magnetic properties of an atomic species embedded in a composite material matrix. A reliable interpretation of the experimental signatures of such newly designed materials requires the support by computational modeling. Parametrized, effective models are routinely used to explain main features or isolated resonances based on generalized assumptions [1,2]. First-principles theory, on the other hand, gives a unique insight in the internal makings which lead to the macroscopically observed and measured variable, such as core-level spectroscopies or scanning-tunnenling microscopic (STM) signatures. Having obtained a sound electronic structure, many more interesting physical properties of the studied system become readily available. For extended systems, density-functional-theory (DFT) has become the method of choice to determine the electronic structure and study the quantum realm of newly developed materials. However, the intricate electronic structure of rare earth metals are a challenge to the established methodologies which were developed and are routinely used mainly for light elements.

We present systematic density-functional theory (DFT) calculations of Dy atoms on corrugated graphene. As was observed experimentally [3], adsorption occurs in a regular 2-dimensional pattern without an initially obvious reason for the site-specificity. We asses the situation through DFT calculations [4] on the screened-hybrid functional (HSE06) [5] and the Hubbard-corrected (DFT+U) [6] level and discuss how minor changes in the electronic level alignment due to strong local coulomb interaction of the partially filled 4*f*-states effectuate intricate consequences in the makeup of the material favoring one adsorption site over another. Furthermore, spectroscopic signatures such as x-ray absorption (XAS) or x-ray magnetic circular dichroism (XMCD) are heavily influenced by changes in the electronic structure. Owing to the extensive system size of experimentally accessible lengthscales, the simulation has to adapt an approximate treatment of the electronic structure through the introduction of the DFT+U methodology including perturbative spin-orbit coupling [7]. We discuss how this approximate electronic structure can still be used to reproduce the main features of an experimentally recorded M-edge XAS and XMCD signature.

[1] A. Uldry, F. Vernay, and B. Delley, Phys. Rev. B 85, 125133 (2012)

[2] E. Stavitski, F. M. de Groot, Micron 41(7), 687 (2010)

[3] R. Baltic, M. Pivetta, F. Donati, C. Wäckerlin, A. Singha, J. Dreiser, S. Rusponi, and H. Brune, Nano Lett. 6 (12), 7610 (2016)

[4] V. Blum, R. Gehrke, F. Hanke, P. Havu, V. Havu, X. Ren, K. Reuter, M. Scheffler, Comp. Phys. Comm. 180(11), 2175 (2009)

[5] A. Krukau, O. A. Vydrov, A. F. Izmaylov, and G. E. Scuseria, J. Chem. Phys. 125, 224106 (2006)

[6] S. L. Dudarev, G. A. Botton, S. Y. Savrasov, C. J. Humphreys and A. P. Sutton, Phys. Rev. B 57, 1505 (1998).

[7] Huhn, W. P., and Blum, V. ArXiv: 1705.01804 [cont.-mat.mtrl.-sci] (2017)

The misfit structure between the Pd(100) and PdO(101) under reaction conditions

M. Shipilin[1], A. Stierle[2,3,4], L. R. Merte[1], J. Gustafson[1], U. Hejral[1], N. M. Martin[5], C. Zhang[1], D. Franz[3], V. Kilic[4], E. Lundgren[1]

1 Division of Synchrotron Radiation Research, Lund University, Lund, Sweden
2 Physics Department, University of Hamburg, Hamburg, Germany
3 Deutsches Elektronen-Synchrotron (DESY), Hamburg, Germany
4 Physics Department, University of Siegen, Siegen, Germany
5 Competence Centre for Catalysis, Chalmers University of Technology, Göteborg, Sweden
(corresponding author: E. Lundgren, e-mail: Edvin.lundgren@sljus.lu.se)

The details of the oxygen induced (√5×√5)R27° structure on Pd(100) [1-3] was studied by Surface X-Ray Diffraction (SXRD) during the catalytic oxidation of CO using a pressure of 200 mbar and a temperature of 300°C. It is shown that the misfit of the PdO(101) layer on the Pd(100) gives rise to a diffraction pattern deviating from that of a perfect (√5×√5)R27° due to a lattice mismatch between the PdO(101) and the Pd(100) in essentially one direction. The presence of four rotated domains significantly complicates the high resolution SXRD diffraction pattern, a pattern not observed in standard Low Energy Electron Diffraction (LEED) due to the lower resolution. To reproduce the observed diffraction pattern, we constructed a number of different models of larger PdO(101) unit cells including various types of mismatch. By comparing the calculated diffraction patterns to the observed pattern, we find that only a model including a periodic rigid shift of the Pd and O atoms in the PdO(101) in the incommensurate direction (the [011] substrate direction) explains the experimental diffraction pattern [4]. Surprisingly, despite the fact that the SXRD data is recorded under harsh reaction conditions, the results are in qualitative agreement with Scanning Tunneling Microscopy (STM) observations performed under Ultra High Vacuum (UHV) conditions.

References:

[1] M. Todorova, et al., Surf. Sci. **541** (2003) 101.
[2] P. Kostelnik, et al., Surf. Sci. **601** (2007) 1574.
[3] M. Shipilin et al, Surf. Sci. **630** (2014) 229.
[4] M. Shipilin et al, Surf. Sci. **660** (2017) 1.

Vicinal Ag(111) surfaces with fully-kinked steps

J. Enrique Ortega[1,2,3], Guillaume Vasseur[2], Ignacio Piquero[3], Sonia Matencio[4], Julien Raoult[5], Frederik Schiller[2,3], Martina Corso[3,6], Aitor Mugarza[4], Jorge Lobo-Checa[7]

[1]*Departamento de Física Aplicada I, Universidad del País Vasco (UPV/EHU), San Sebastian, Spain*

[2]*Donostia International Physics Center (DIPC) San Sebastian, Spain*

[3]*Centro de Física de Materiales (CSIC-UPV/EHU), San Sebastian, Spain*

[4]*Institut Catalá de Nanociencia i Nanotecnologia (ICN2), Barcelona, Spain*

[5]*Synchrotron SOLEIL, Saint-Aubin-Gif sur Yvette, France*

[6]*IKERBASQUE, Basque Foundation for Science, E-48011 Bilbao, Spain*

[7]*Instituto de Ciencia de Materiales de Aragón (ICMA), CSIC-Universidad de Zaragoza, Spain*

Vicinal surfaces with arrays of atomic steps have important applications in catalysis, nanostructure growth, or electronic band engineering, since steps are active sites for chemical reactions, as well as nucleation and electron scattering centers. Given the infinite possibilities for the orientation of a vicinal surface, it is important to perform systematic investigations, in order to identify optimal substrates for specific functions. Using macroscopically curved crystal samples one can systematically probe entire families of vicinal planes with standard surface science techniques [1-4]. This is done here for vicinal Ag(111) surfaces featuring the so-called fully- or 100%-kinked steps. Fully-kinked monatomic steps (height h=2.35 Å) run parallel to the $[11\bar{2}]$ direction and have six-fold atomic coordination, as compared with the seven-fold coordinated close-packed steps, which are oriented along the $[1\bar{1}0]$ direction. In such fully-kinked Ag(111) vicinals we investigate electronic and structural properties with STM, LEED and Angle-Resolved Photoemission (ARPES), and test both the growth of $BiAg_2$ alloys and the on-surface synthesis of zig-zag polymers.

The sample is a Ag single crystal curved around the (645) direction, such that the vicinal angle α can be tuned from the Ag(111) plane, beyond the Ag(423) surface, up to α=18º. As done in previous works on close-packed Ag(111), Cu(111) and Au(111) vicinals [1], we study the probability distribution of the terrace size d as a function of the vicinal angle from STM images, and probe the scattering of the Shockley state at the fully-kinked step by ARPES. We find that fully-kinked vicinals exhibit exceptional ordering, allowing one to visualize the universal, structural transformation of vicinal metal surfaces [2-3] with unprecedented precision. This opens the way to a fine test of statistical models of step-lattices largely debated in the past [5]. As shown in the Figure, the Shockley state analysis reveals a much stronger scattering strength at the fully-kinked step when compared to the closed-packed, leading to a dramatic decrease of the surface electron density in vicinal surfaces, that is, to a complete electron depletion of Ag(111) terraces with d <1.6 nm.

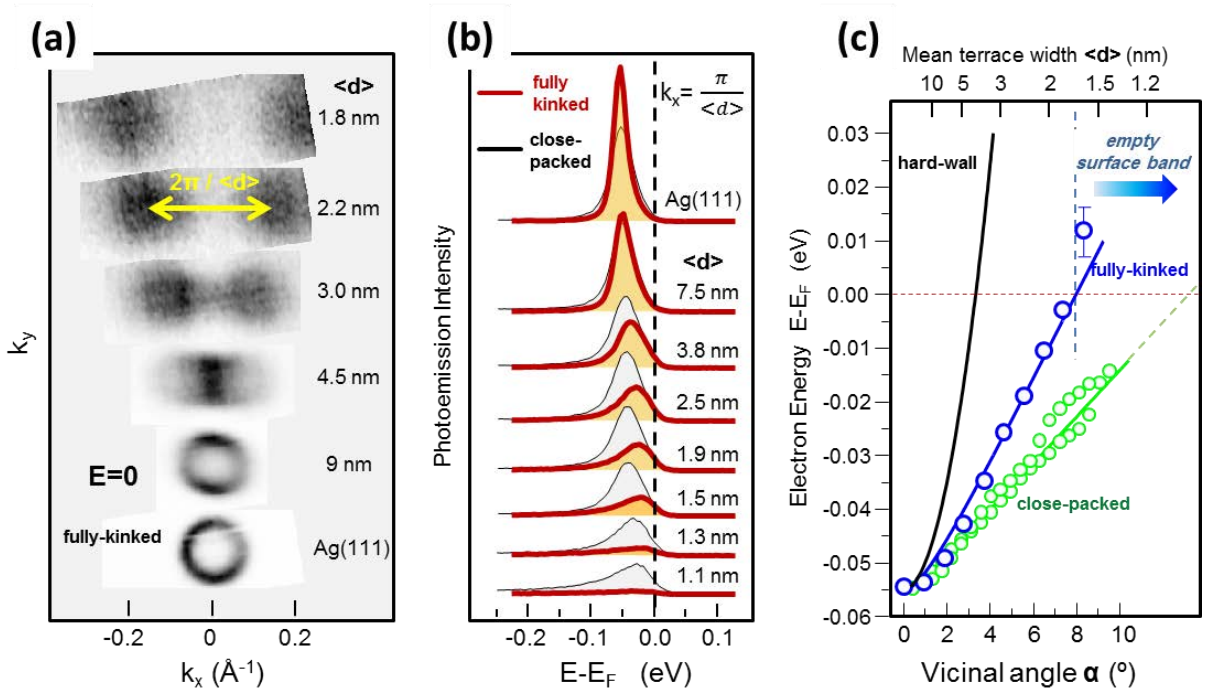

Figure 1. *(a) Shockley Fermi surface scanned across the curved Ag(111) sample with fully-kinked steps.* $2\pi/< d >$ *umklapps reveal scattering at the step lattice. (b) <d>-dependent surface state shift for fully-kinked Ag(111) vicinals (orange), as compared to that of the close-packed vicinals. The surface band is electron-depleted for d <1.6 nm. (c) Fit of the <d>-dependent surface state shift (data points) with a 1D Kronig-Penney model (lines), indicating a barrier strength for fully-kinked steps that is twice as big as for close-packed steps.*

Next we tested the growth of the $BiAg_2$ monolayer, and observed the presence of magic vicinal angles at which one can achieve atomically sharp $BiAg_2$ step grids, ideal to explore spin scattering properties. Finally we explored the on-surface synthesis of DMTP zig-zag polymers, where we also found optimal crystal orientations to template well-oriented one-dimensional chains, such as to facilitate spectroscopic characterization by ARPES.

We acknowledge financial support from the Spanish Ministry of Economy (grant MAT2017-88374-P) and the Basque Government (grant IT621-13).

[1] J. E. Ortega et al., Phys. Rev. B **83**, 085411 (2011).
[2] A. L. Walter et al., Nature Commun. **6**, 8903 (2015).
[3] M. Ilyn et al., J. Phys. Chem. C **121**, 3880–3886 (2017).
[4] L. A. Miccio et al., Nanoletters **16**, 2017–2022 (2016).
[5] T. L. Einstein, Appl. Phys. A **87**, 375 (2007)

Structure Determination Considering Surface Dynamics: The O/Rh(100) System revisited

L. Hammer, T. Kißlinger, P. Ferstl, and M. A. Schneider

Lehrstuhl für Festkörperphysik, Universität Erlangen-Nürnberg, Germany
(corresponding author: L. Hammer, e-mail: lutz.hammer@fau.de)

In this study we combine quantitative LEED-IV, STM and DFT calculations to reinvestigate the ordered phases of oxygen on the Rh(100) surface up to a coverage of 0.67 ML. In this regime three distinct phases are observed: A (2x2)-O [1], a (2x2)-2O [2] and a (3x1)-2O structure [3]. Their appearance in LEED and room temperature STM as well as ball models of the best-fit structures are summarized in Fig.1.

Regarding the (3x1)-2O phase our LEED analysis (Pendry R-factor $R_P = 0.095$) validates the "shifted-row" model with oxygen atoms in quasi-threefold coordination proposed by Gustafson *et al.* [3]. The resulting structural parameters coincide almost quantitatively to those obtained for the $Pt_{25}Rh_{75}$(100)-(3x1)-2O structure [4]. DFT calculations yield a total energy gain of 0.27 eV per oxygen atom compared to adsorption on the unreconstructed surface. This by far overcompensates the energetic penalty of 0.10 eV per oxygen atom for shifting the Rh-row and thus drives the substrate reconstruction [5].

For the (2x2)-O phase our LEED re-analysis ($R_P = 0.072$) corroborates the hollow site adsorption revealed by the very early analysis of Oed *et al.* [1] and refines their structural model by the determination of 13 additional parameters. This finding, however, contrasts to the appearance in room temperature STM, where non-primitive (2x2), (2x1) and (1x1) areas are imaged (*cf.* Fig.1). We interpret these features as a time average of rapidly fluctuating light domain walls which is corroborated by an oxygen diffusion barrier of only 240 meV calculated by DFT.

In case of the (2x2)-2O structure our LEED analysis confirms the principle model of a clockwise-/anticlockwise reconstruction of the substrate. We also confirm the quasi-threefold coordinated adsorption site of oxygen sites created by the reconstruction as proposed by Baraldi *et al.* [2] and corroborated by DFT calculations of by Alfè *et al.* [6]. However, their static model with oxygen occupying just one of the two adjacent sites clearly violates the glide symmetry of the structure, which is obvious from the LEED pattern. In our LEED analysis, in contrast, we assume a statistical 50 : 50 occupation of neighboring oxygen adsorption sites, which correctly accounts for all symmetry elements observed in experiment. This dynamic model improves the best-fit R-factor from $R_P = 0.13$ for the static model to a final value of $R_P = 0.098$.

Such a dynamic model is corroborated by DFT calculations which determines the barrier between these two adjacent sites to be as low as 25 meV. Thus, every single oxygen atom

fluctuates with close to phonon frequency leading to an equal population of both sites on shortest time scales. This also seems to prevent the substrate from a complete, symmetry-breaking local relaxation as is also predicted by DFT calculations for a static model. Of course, STM can only see the mean positions of the hopping atoms and therefore pretends a simple c(2x2) configuration.

Support by the Deutsche Forschungsgemeinschaft (DFG) through project "COMCAT" is gratefully acknowledged.

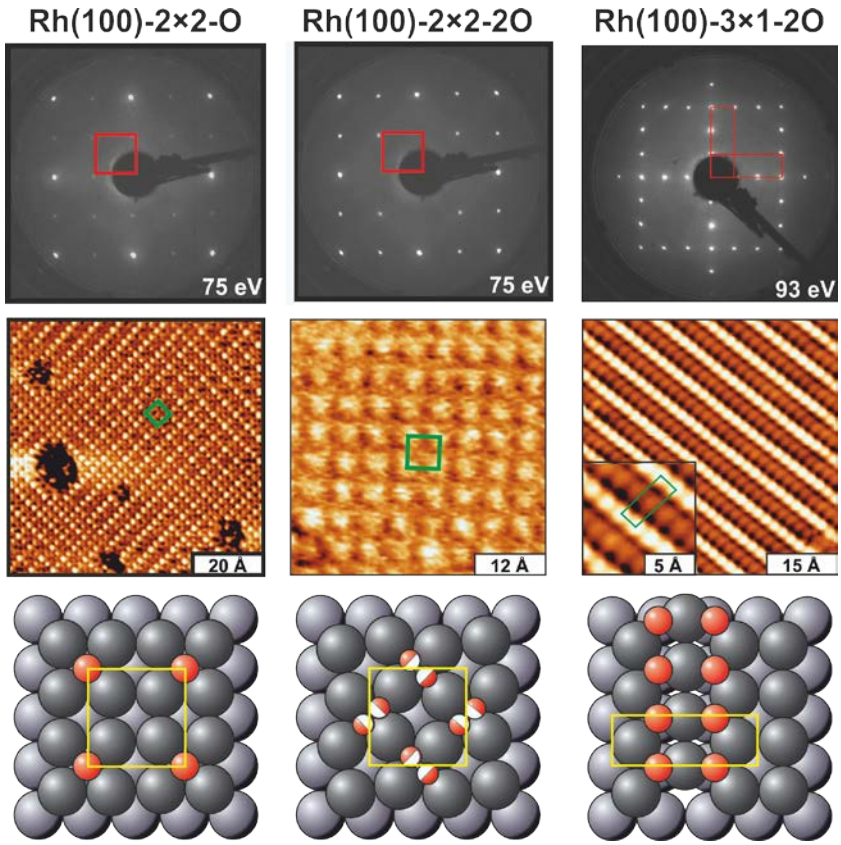

Fig.1: Summary experimental results for the different adsorption phases of oxygen on Rh(100). Top: LEED images. Center: room-temperature STM images. Bottom: ball models for the best-fit structures of the LEED intensity analyses. Red balls stand for oxygen, whereby half-filled symbols indicate a 50 % site occupation on time average.

[1] W. Oed, B. Dötsch, L. Hammer, K. Heinz, and K. Müller, Surf. Sci. **207** (1988) 55.

[2] A. Baraldi, J. Cerdá, J.A. Martín-Gago, G. Comelli, S. Lizzit, G. Paolucci, and R. Rosei, Phys. Rev. Lett. **82** (1999) 4874.

[3] J. Gustafson, E. Lundgren, A. Mikkelsen, M. Borg, J. Klikovits, M. Schmid, P. Varga, and J.N. Andersen, J. Phys.: Condens. Matter **24** (2012) 225006.

[4] M. Sporn, E. Platzgummer, E. Gruber, M. Schmid, W. Hofer, and P. Varga, Surf. Sci. **416** (1998) 384.

[5] T. Kißlinger, P. Ferstl, M.A. Schneider, and L. Hammer, J. Phys.: Condens. Matter **29** (2017) 365001.

[6] D. Alfè, S. de Gironcoli, and S. Baroni, Surf. Sci. **410** (1998) 151.

LEEM and STM - a valuable combination for the study of organic-inorganic interface heterostructures

P. Procházka[1,2], L. Kormoš[1,2], J. Čechal[1,2], and T. Šikola[1,2]

[1]*Inst. of Physical Engineering, Brno University of Technology, Technická 2, 616 69 Brno, Czech Rep. (corresponding author: T. Šikola, e-mail: sikola@fme.vutbr.cz)*

[2]*CEITEC BUT, Brno University of Technology, Technická 10, 61669 Brno, Czech Republic*

Low Energy Electron Microscopy (LEEM) was invented some 25 years ago by Ernst Bauer [1] and since that time has become a well known technique suitable for a study of surfaces. It provides microscopic observation of surfaces at electron energies within the typical range of 0 - 100 eV and enables observations of dynamic processes at surfaces, namely thin-film growth, etching and adsorption, and phase transitions in real time. In principle, four different imaging modes can be applied [2]: a) *photo-electron emission microscopy (PEEM)*, *mirror-electron microcopy* sensitive to topography as well as work function, *bright-field imaging* utilizing a specular (0, 0) LEED diffraction spot only while all other spots are blocked by a contrast aperture, and finally *a dark-field imaging* based on a diffracted beam other than (0, 0). In contrast to classical LEED, enhanced imaging optical properties of LEEM make it possible to take diffraction patterns from areas slightly below 200 nm (so called *the μ-diffraction mode*), and thus the atomic structure analysis of small objects can be carried out. In addition, utilizing the dark-field imaging mode, specific domains of surface structures can be distinguished, as demonstrated in Fig. 1.

However, the ultimate lateral resolution of LEEM real-space imaging modes is 2 – 5 μm and thus is not sufficient enough for revealing the atomic structure of surfaces. Hence, one would find beneficial to combine LEEM studies with complementary atomically resolved methods, namely Scanning Tunneling Microscopy (STM).

In the contribution we will report on such in situ studies combining LEEM and STM methods in our complex ultrahigh vacuum (UHV) system installed at CEITEC Nano Research Center and aiming at organic-inorganic interface heterostructures. LEEM experiments were carried out by a SPECS FE-LEEM P90 instrument with a base pressure of 2×10^{-8} Pa, STM images were recorded by a commercial system Aarhus 150 (SPECS) equipped with the KolibriSensor featuring a tungsten tip.

We will show that the strong interaction of 4,4’ biphenyl dicarboxylic acid (BDA) with the step edges on Cu(001) results in the formation of a densely packed molecular step decoration causing the step edge passivation. The step edge passivation limits the BDA diffusion over the

step edges and inhibits the attachment of additional BDA molecules preventing nucleation and growth of molecular islands on the step edges. Our results thus provide fundamental insight in the anomalous growth behavior exhibited by certain organic/inorganic systems, which allows the development of models enabling the control of growth of organic heterointerfaces.

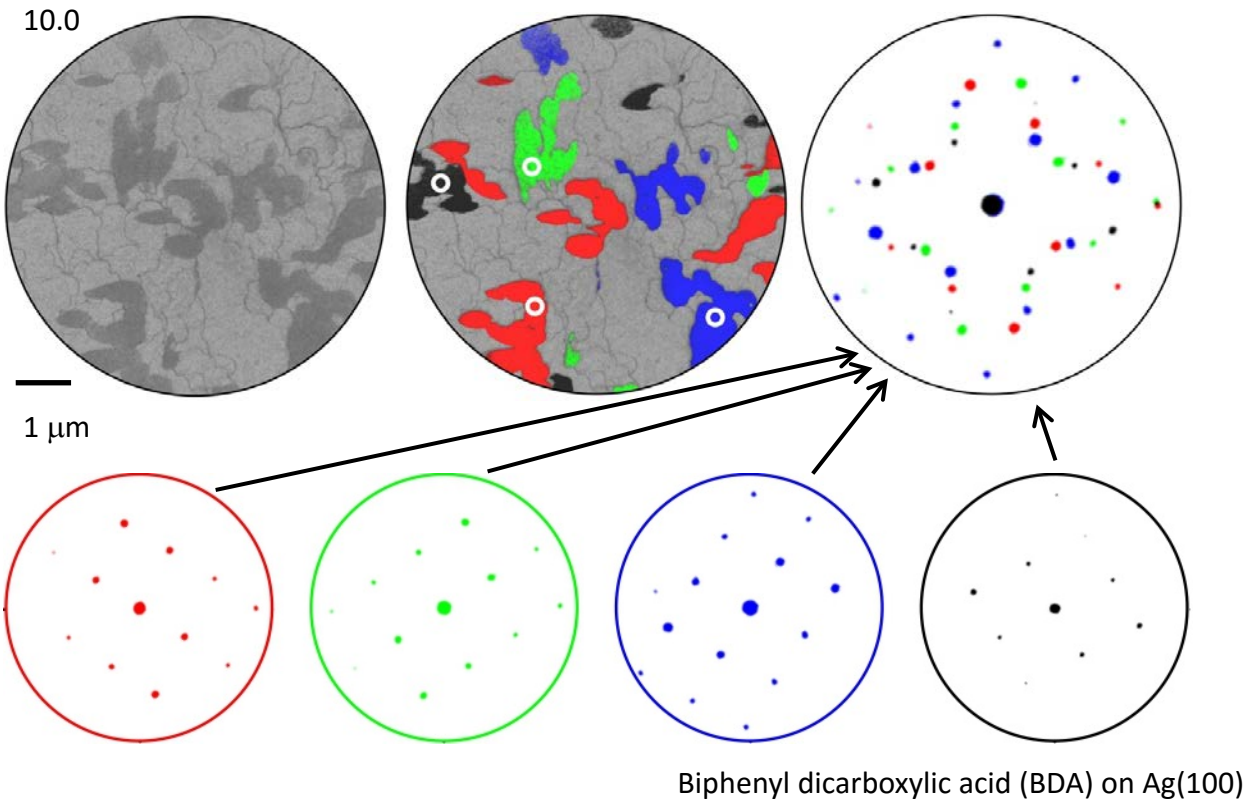

Fig. 1: Dark-field imaging of individual surface domains and related diffraction patterns obtained by the μ-diffraction mode.

We acknowledge the support by the Technology Agency of the Czech Republic (grant No. TE01020233), European Regional Development Fund (project No. CZ.1.05/1.1.00/02.0068), and MEYS CR (project No. LQ1601 – CEITEC 2020).

[1] E. Bauer, in Electron Microscopy, Vol. 1, S. S. Breese, Ed., Academic Press, Inc., New York, 1962, p. D-11

[2] R. M. Tromp, IBM J. Res. Develop., 44 (4), 503 (2000)

Dome-shaped µm-sized curved Rh crystals as a playground for H_2 oxidation

Y.Suchorski[1], J. Zeininger[1], S. Buhr[1], M. Stöger-Pollach[2], J. Bernardi[2], G. Rupprechter[1]

[1]*Institut für Materialchemie, Technische Universität Wien, 1060 Vienna, Austria*
(corresponding author: Y. Suchorski,, e-mail: yuri.suchorski@tuwien.ac.at)
[2]*USTEM, Technische Universität Wien, A-1060 Wien, Austria*

Recently, a new type of spatio-temporal behaviour in a catalytic surface reaction was observed: multifrequencial reaction rate oscillations on differently oriented domains of a polycrystalline Rh surface [1]. Despite of the effective spatial coupling between the neighbouring domains, the reaction oscillates with its „own" frequency on each individual domain. The factor governing the particular frequencies is the surface structure of the corresponding domains: „rougher" surfaces exhibit, in general, higher frequencies. The above study exploited the applicability of µm-sized domains of a polycrystalline metal foil for revealing the structure sensitivity in catalysis, as established by our previous studies [2]. Such applicability is based on the simultaneous presence of regions with different terrace structures, step types and step densities within the same sample, creating a kind of the surface structure library, as well as on the possibility to define the local surface structure by EBSD [3] and to observe simultaneously and *in situ* processes on different domains by PEEM [4].

An alternative possibility to benefit from a surface structure library is to use a curved single crystal. In this case a continuous variation of surface structure is possible which offers many benefits for studying structure sensitivity. Mostly, cylindrical curved crystals are used [5], where the surface orientation varies by one degree of freedom, but comprehensive studies of structure sensitive processes across a wide range of structures require an access to all possible orientations. This is feasible by combination of spherically curved, dome-shaped crystal surfaces with spatially resolved methods for surface analysis [6].

Mostly, mm-sized curved crystals are used, which simplifies the experimental handling, but limits the curvature and thus the number of structures in the library. In the present contribution, we use a µm-sized, highly curved spherically shaped Rh crystal which allows simultaneous visualisation of the whole spherical apex using field emission microscopy (FEM). Usually, tips with nm-sized hemispherical apexes are used as specimens in FEM, in order to minimize the applied imaging voltage. Using the catalytically active nanotips, many interesting aspects in surface reactions were revealed [7]. However, the reaction-induced fluctuations occurring on the nanofacets of such tips [8] mimic well the processes on real nanoparticles, but lead to deviations from the mean-field theoretical simulations and make any comparisons with the µm-sized domains of polycrystalline foils difficult. In turn, a significantly bigger, µm-sized spherically shaped Rh crystal used in present study, allows a direct comparison with the µm-sized domains of the polycrystalline Rh foil. Figure 1 shows an SEM micrograph of such curved crystal Rh specimen and an FEM image of its clean apex surface. The known

crystallographic symmetry (from FEM) and the exact shape (from SEM) allow a detailed crystallographic characterisation of the spherical apex.

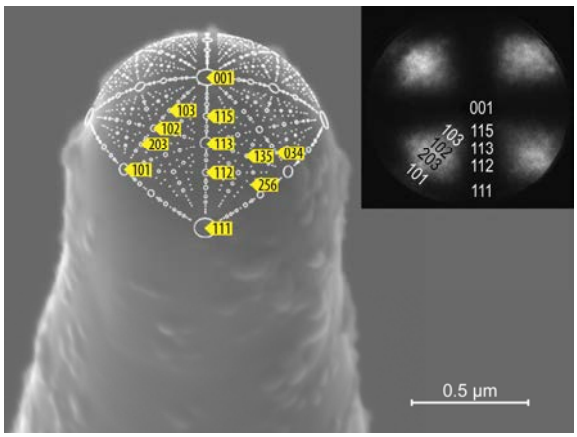

Fig.1. An SEM micrograph of a curved µm-sized crystal Rh specimen. The net of crystallographic orientations of individual differently oriented Rh(hkl) facets is introduced as an overlayer. The inset shows the corresponding FEM image of the apex surface after cleaning in UHV with marked orientations.

Using the model system described above, H_2 oxidation on Rh was studied using the FEM as imaging method with a nm-resolution and the *kinetics by imaging* approach for the evaluation of the reaction kinetics [9]. Bistable and oscillating modes of the reaction were studied, kinetic transitions were monitored and kinetic phase diagrams were constructed. An effect of the temperature dependent paths of the surface propagation of the reaction was detected and is discussed in view of the adsorption induced surface reconstruction of Rh surfaces [10].

This work was supported by the Austrian Science Fund (FWF) [SFB F45 FOXSI]

[1] Y. Suchorski, M. Datler, I. Bespalov, J. Zeininger, M. Stöger-Pollach, J. Bernardi, H. Grönbeck, G. Rupprechter, Nature Comm. 2018, in press
[2] D. Vogel, C. Spiel, Y. Suchorski, A. Trinchero, R. Schlögl, H. Grönbeck, G. Rupprechter, Angew. Chem. Intern. Ed. 51, 10041 (2012)
[3] M. Datler, I. Bespalov, S. Buhr, J. Zeininger, M. Stöger-Pollach, J. Bernardi, G. Rupprechter, Y. Suchorski, Cat. Lett. 146, 1867 (2016)
[4] Y. Suchorski, C. Spiel, D. Vogel, W. Drachsel, R. Schlögl, G. Rupprechter, ChemPhysChem 11, 323 (2010)
[5] M. Ilyn, A. Magaña, A.Walter, J. Lobo-Checa, D.G. de Oteyza, F. Schiller, J.E. Ortega, J. Phys. Chem. C 121, 3880 (2017)
[6] T.J. Lawton, V. Pushkarev, E. Broitman, A. Reinicker, E.C.H. Sykes, A.J. Gellman, J. Phys. Chem. C 116, 16054 (2012)
[7] Y. Suchorski, W. Drachsel, Top. Catal. 46, 201 (2007)
[8] Y. Suchorski, J. Beben, E.W. James, J.W. Evans, R. Imbihl, Phys. Rev. Lett. 82, 1907 (1999)
[9] Y. Suchorski, G. Rupprechter, Surf. Sci. 643, 52 (2016)
[10] V. Medvedev, Y. Suchorski, C. Voss, T. Visart de Bocram, T. Bär, N. Kruse, Langmuir, 14, 6151 (1998)

Shifting from reactant to substrate engineering in the selective synthesis of graphene nanoribbons

N. Merino-Díez,[1,2,3] J. Lobo-Checa,[4,5] P. Nita,[1,2] A. Garcia-Lekue,[1,6] J. Li,[3] E. Carbonell-Sanromà,[3] A. Basagni,[7] G. Vasseur,[1,2] L. Colazzo,[7] F. Tiso,[7] F. Sedona,[7] M. Corso,[1,2] M. Sambi,[7,8] D. Sánchez-Portal,[1,2] J. I. Pascual,[3,6] J. E. Ortega,[1,2,9] D. G. de Oteyza [1,2,6]

[1] *Donostia International Physics Center (DIPC), 20018 San Sebastián, Spain.*
[2] *Centro de Física de Materiales (CSIC-UPV/EHU) - MPC, 20018 San Sebastián, Spain.*
[3] *CIC nanoGUNE, 20018 San Sebastián-Donostia, Spain.*
[4] *Instituto de Ciencia de Materiales de Aragón (ICMA), CSIC-Universidad de Zaragoza, 50009 Zaragoza, Spain.*
[5] *Departamento de Física de la Materia Condensada, Universidad de Zaragoza, 50009 Zaragoza, Spain.*
[6] *Ikerbasque, Basque Foundation for Science, 48011 Bilbao, Spain.*
[7] *Dipartimento di Scienze Chimiche, Università Degli Studi Di Padova, Padova, Italy.*
[8] *Consorzio INSTM, Unità di Ricerca di Padova, Padova, Italy*
[9] *Departamento de Física Aplicada I, Universidad del Pais Vasco, 20018 San Sebastián, Spain.*
(corresponding author: D. G. de Oteyza, e-mail: d_g_oteyza@ehu.es)

The challenge of synthesizing graphene nanoribbons (GNRs) with atomic precision is currently being pursued along a one-way road, based on the synthesis of adequate molecular precursors that react in predefined ways and form GNRs through self-assembly processes. Adding a new direction to this readily successful approach, the synthetic options for GNRs are expected to multiply, especially if both approaches can be combined. We show here how, still based on self-assembly to maintain the atomic precision not yet achievable with top-down methods, selectivity in the GNR synthesis can be guided, instead of by designed reactants, by an adequately nanotemplated substrate. This new strategy´s proof-of-concept compares experiments using 4,4´´-dibromo-para-terphenyl as molecular precursor on flat Au(111) and stepped Au(322) substrates.

On Au(111), the reactant first polymerizes into poly-para-phenylene (PPP) at moderate temperatures below 200 ºC. Annealing to higher temperatures drives the lateral fusion of PPP chains through cyclo-dehydrogenation, ending up with graphene nanoribbons of varying width depending on the number of polymers involved. The resulting samples are thus interesting to study width-dependent properties and phenomena in GNRs. We have used such samples to characterize the width-dependent band gap of GNRs and, most importantly, the associated evolution of the energy level alignment of frontier bands. Doing so, a Fermi level pinning scenario of the valence band has been found for GNRs displaying band gaps below ~1.7

eV.[1] However, from the synthetic point of view, selectivity towards particular GNRs is completely missing.

A completely different scenario is found on Au(322). The polymerization and cyclo-dehydrogenation reactions occur in a similar way. However, the periodic steps of Au(322) limits the number of fusing polymers to two, resulting in the selective synthesis of 6 atom-wide armchair GNRs (6-aGNRs). In addition, all GNRs being uniaxially aligned along the substrate´s steps, we have been able to characterize the sample´s valence band properties by angle resolved photoemission spectroscopy. Complemented with scanning tunneling spectroscopy measurements and density functional theory calculations, we end up with a fully coherent and complete picture of the electronic properties of 6-aGNRs.

Support by the European Research Council (ERC) under the European Union's Horizon 2020 research and innovation programme (grant agreement No 635919), from the Spanish Ministry of Economy, Industry and Competitiveness (MINECO, Grant No. MAT2016-78293-C6), and from the Basque Government (Grant No. IT-621-13) is gratefully acknowledged.

[1] N. Merino-Díez, A. Garcia-Lekue, E. Carbonell-Sanromà, J. Li, M. Corso, L. Colazzo, F. Sedona, D. Sanchez-Portal, J. I. Pascual, D. G. De Oteyza, ACS Nano 11, 11661 (2017)

Long acenes generated by on-surface dehydrogenation

R. Zuzak, R. Dorel[1], M. Krawiec[2], B. Such, M. Kolmer, M. Szymonski, A. M. Echavarren[1,3] and S. Godlewski

Centre for Nanometer-Scale Science and Advanced Materials, NANOSAM, Faculty of Physics, Astronomy and Applied Computer Science, Jagiellonian University, Łojasiewicza 11, PL 30-348 Krakow, Poland
(corresponding author: S. Godlewski, e-mail: szymon.godlewski@uj.edu.pl)

[1] *Institute of Chemical Research of Catalonia (ICIQ), Barcelona Institute of Science and Technology, Avenida Països Catalans 16, 43007 Tarragona, Spain*

[2] *Institute of Physics, Maria Curie-Sklodowska University, Pl. M. Curie-Skłodowskiej 1, 20-031 Lublin, Poland*

[3] *Departament de Química Orgànica i Analítica, Universitat Rovira i Virgili, C/Marcel·lí Domingo s/n, 43007 Tarragona, Spain*

In recent years we observe rapid development of organic electronics. This has prompted the researcher attention toward detailed characterization of single molecules, which are the building blocks of novel devices. Among different families of organic species, the members of the acene family, linearly fused benzene rings, hold the special position being one of the most often studied families in the context of the organic semiconductor applications [1,2]. Acenes belong to the family of arenes, for which the electronic properties strongly depend on the size (both lateral dimensions) and the edge morphology [3]. They are attracting considerable attention due to the outstanding electronic properties originating from only one Clar π-sextet regardless of the molecule length. For instance, it is predicted that the HOMO-LUMO (highest occupied – lowest unoccupied molecular orbital) gap decreases when the number of annealed rings grows and importantly the gap value is relatively small when compared to other arenes with a similar number of fused rings [3-5]. It is also expected that for linear acenes with increased number of fused rings the contribution of the open-shell configuration to the ground state raises [6]. However, the unique π-electron system causes the molecules to be more reactive and less stable with increased length and consequently makes their synthesis, detailed characterization and functionalization a very challenging task [5]. In recent years a few successful strategies toward fabrication of acene-based molecules have been reported, e.g. a number of acene derivatives have been synthesized and some long acenes were stabilized and detected within noble gas matrices or in polymers [7-10]. However, it was only recently when the on-surface chemistry approach based on chemical reactions transforming "chemically protected" acene derivatives into parent acenes directly on a crystalline surfaces

allowed for synthesis and characterization of higher acenes [3, 5, 11, 12]. Furthermore acenes could be regarded as the narrowest graphene nanoribbons with zig-zag edge topology, which makes them promising candidates for applications in spintronics and plasmonics [13-14].

Herein we present the on-surface generation of long acenes (Figure 1) as well as the detailed study of their electronic structure on the Au(111) surface. Our method is based on the two-step dehydrogenation of a stable tetrahydroacene precursors, assisted by the tip of a combined STM/AFM instrument. High-resolution NC-AFM imaging was applied for the detailed visualization of the internal structure of the generated long acenes. Details on the electronic structure of final molecules, as well as the intermediate dihydroacenes, were revealed using high resolution dI/dV mapping. Our measurements showed that not only frontier molecular orbitals (i.e., HOMO and LUMO) but also deeper lying ones could be imaged with submolecular resolution. Additionally, we demonstrate that the surface-assisted dehydrogenation process that leads to the generation of parent acenes could also be induced thermally, constituting a highly efficient method for the preparation of increased amounts of final molecules. We show that in this case the hydrogen abstraction process is accompanied by a series of hydrogen shifts over the dihydroacene species, resulting in a variety of isomers with the nonaromatic ring located at different positions within the internal structure of the molecule, which therefore allows also the electronic characterization of a range of isomers.

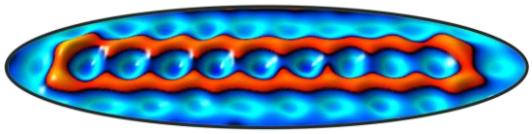

Figure 1. 3D NC-AFM image of on-surface generated nonacene.

The research was supported by the National Science Center, Poland (2014/15/D/ST3/02975), European Research Council (Advanced Grant No. 321066), MINECO/FEDER, UE (CTQ2016-75960-P), MINECO-Severo Ochoa Excellence Acreditation (2014-2018, SEV-2013-0319), and CERCA Program/Generalitat de Catalunya. M.Kr. acknowledges the support of the National Science Centre (Poland), project no. DEC-2014/15/B/ST5/04244. M.Ko. acknowledges financial support received from the Foundation for Polish Science (FNP).

[1] J. E. Anthony, Chem. Rev. 106 (2006) 5028-5048.
[2] R. Dorel, A.M. Echavarren, Eur. J. Org. Chem. 2017, 14-24.
[3] M. Zugermeier, et al., Nanoscale 9 (2017) 12461.
[4] J.E. Anthony, Angew. Chem. Int. Ed. 47 (2008) 452.
[5] J. I. Urgel, et al., J. Am. Chem. Soc. 139 (2017) 11658−11661.
[6] Y. Yang, E. R. Davidson, W. Yang, Proc. Natl. Acad. Sci. U. S. A. 113 (2016) E5098−E5107.
[7] C. Tönshoff, H. F. Bettinger, Chem., Int. Ed. 49 (2010) 4125−4128.
[8] X. Shi, C. Chi, Chem. Rec. 16 (2016) 1690−1700.
[9] H. F. Bettinger, C. Tönshoff, Chem. Rec. 15 (2015) 364−369.
[10] S. S. Zade, M. Bendikov, Angew. Chem., Int. Ed. 49 (2010) 4012−4015.
[11] R. Zuzak, et al., ACS Nano (2017) 11, 9321−9329.
[12] J. Krüger, et al., Angew.Chem. Int.Ed. 56 (2017) 11945 –11948.
[13] Y. -W. Son, M. L. Cohen, S. G. Louie, Nature 444 (2006) 347−349.
[14] L. Bursi, A. Calzolari, S. Corni, E. Molinari, ACS Photonics 1 (2014) 1049−1058.

Wannier Stark localisation and Rashba splitting in ferroelectrics and multiferroics

Stefan Muff, Juraj Krempasky, Milan Radovic, and Hugo Dil

Institute of Physics, Ecole Polytechnique Fédérale de Lausanne, Switzerland
Swiss Light Source, Paul Scherrer Institut, Switzerland
(corresponding author: H. Dil, e-mail: hugo.dil@epfl.ch)

Ferroelectrics are the electrical analogue to ferromagnets in the sense that they retain a polarization in the absence of any applied electric field. Because of their non-volatile properties ferroelectrics are expected to play an important role in modern electronics and their material properties are extensively studied. The presence of free carriers will directly diminish the ferroelectric properties and the systems thus need to be dielectrics with very low free carrier densities. This is one of the reasons that the electronic structure of ferroelectrics has not received much attention until recently. However, many interesting electronic structure effects can result from ferroelectric properties and in this presentation I will give some prime examples.

The large local fields associate with the intrinsic polarization of the materials will act upon the electrons in the solid. The most obvious example occurs when the surface of a ferroelectric with in-plane domains hosts a free electron-like surface state. In this case the electrons in the surface state will be accelerated due to the (ferro)electric field of the bulk. If this field is large enough, scattering off the crystal planes of the unit cell will become more important as scattering off random defects. As a result the electrons will be localised in the unit cell in the direction of the domain polarisation, which is referred to as Wannier-Stark localisation. This localisation in real space results in a smearing in reciprocal space which is directly visible in angle-resolved photoemission spectroscopy (ARPES) as streaks. When a mixture of domains is present the Fermi surface as measured by ARPES will show a checkerboard pattern as shown in Figure 1 for the 2D state at the surface of ferroelectric $BaTiO_3$(001) [1].

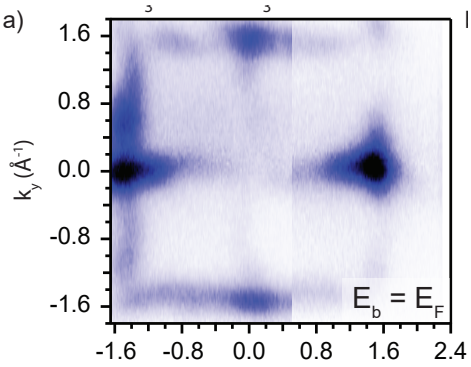

Fig. 1: Fermi surface of 20 unit cells of $BaTiO_3$(001) grown on $SrTiO_3$(001). The checkerboard pattern results from the Wannier Stark localization.

When the polarization direction is along the out-of-plane direction with regard to the surface or a thin film the effect on the states in a ferroelectric semiconductor is markedly different. In this case the inversion symmetry is broken in the bulk and is associated with a strong dipole

moment and the situation is similar to crystals with a polar stacking order such as BiTeX (X=Br, Cl, I). In these systems the inversion symmetry breaking causes a Rashba-type spin splitting also of the bulk states, resulting in a spindle torus shaped constant energy surface [2,3]. Indeed theory predicted such an effect for room temperature ferroelectric GeTe along the (111) direction with a record high spin splitting at the Z-point [4]. Using spin-resolved and also soft X-ray ARPES in combination with first principles calculations we have been able to verify the full 3D electronic structure and spin texture of thin GeTe(111) films [5].

Upon doping with Mn the GeTe films become ferromagnetic while retaining their ferroelectric properties with a reduced ordering temperature. This means that the system becomes multiferroic as a single crystalline thin film. In our experiments we could show that the Mn is incorporated in the GeTe lattice and strongly hybridizes with the GeTe bands opening up a Zeeman-type gap around the Z-point [6]. This results in a single spin-polarized constant energy sheet in the 3D electronic structure.

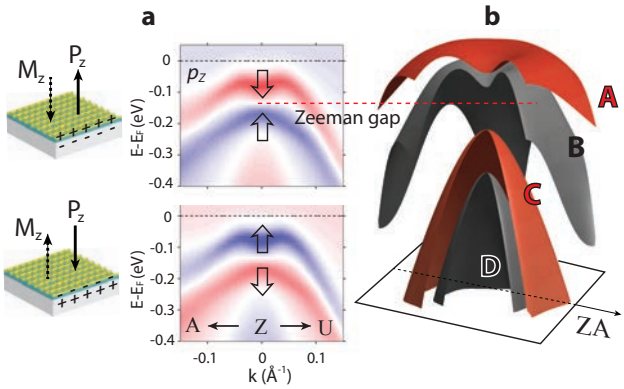

Fig. 2: Illustration of the generic band structure and of the reversal of the magnetization direction by applying an electric field for $Ge_{1-x}Mn_xTe(111)$ thin films

The main interest in of ferroelectric or multiferroic systems is the possibility to influence their properties by external fields. Using a prototypical set-up we have performed *operando* spin-resolved ARPES measurements to follow the switching of the spin texture with applied electric field. We found that the switching is strongly influenced by ferroelectric fatigue effects after the first cycle, but that switching is feasible [7]. Furthermore, the magnetisation direction can be reversed by the applied electric field as illustrated in Figure 2, indicating that the system is not just multiferroic, but truly magnetoelectric with strong coupling between ferroelectric and ferromagnetic degrees of freedom.

[1] Stefan Muff, Nicolas Pilet, Mauro Fanciulli, Andrew P. Weber, Christian Wessler, Zoran Ristic, Zhiming Wang, Nicholas C. Plumb, Milan Radovic, and J. Hugo Dil; arXiv:1710.02421

[2] K. Ishizaka et al. Nat. Mater. 10, 521 (2011)

[3] G. Landolt et al. Phys. Rev. Lett. 109, 116403 (2012)

[4] D. Di Sante, P. Barone, R. Bertacco, and S. Picozzi, Advanced Materials 25, 509 (2013)

[5] J. Krempasky et al. Phys. Rev. B 94, 205111 (2016)

[6] J. Krempasky et al. Nat. Commun. 7, 13071 (2016)

[7] J. Krempasky et al. arXiv:1707.08431

VUV Magneto-Optical Transient Ellipsometer: ELIps

S. Espinoza[1], M. Rebarz[1], S. Richter[1], J. Andreasson[1,2]

[1]*ELI Beamlines, Institute of Physics, Czech Academy of Science, 182 21, Prague, Czech Republic (corresponding author: S. Espinoza, e-mail: Shirly.Espinoza@eli-beams.eu)*

[2] *Condensed Matter Physics, Department of Physics, Chalmers University of Technology, SE-412 96 Gothenburg, Sweden*

Spectroscopic ellipsometry measurements performed on the millisecond time scale are widely used for real-time monitoring of thin-film growth and for the investigation of surface phenomena such as adsorption or modification. Ellipsometry is the determination of the optical properties of a material based on the changes in the state of polarization of the light upon its reflection on the material sample.

In solid state materials, the VUV radiation has a low penetration depth which might be translated as a high optical contrast for a thickness of a few atomic layers. A VUV ellipsometer, then, is an excellent tool for the investigation of surfaces and very thin films. The ELIps instrument being built at the European Extreme Light Infrastructure Beamlines (ELI Beamlines). will combine three advanced techniques of ellipsometry: VUV ellipsometry, Transient (Pump-probe) ellipsometry, and Magneto-optical ellipsometry [1] The working range of energies in the VUV is between 12 eV and 40 eV, this VUV radiation comes from a High Harmonics Generation (HHG) source driven by a high-power femtosecond-laser.

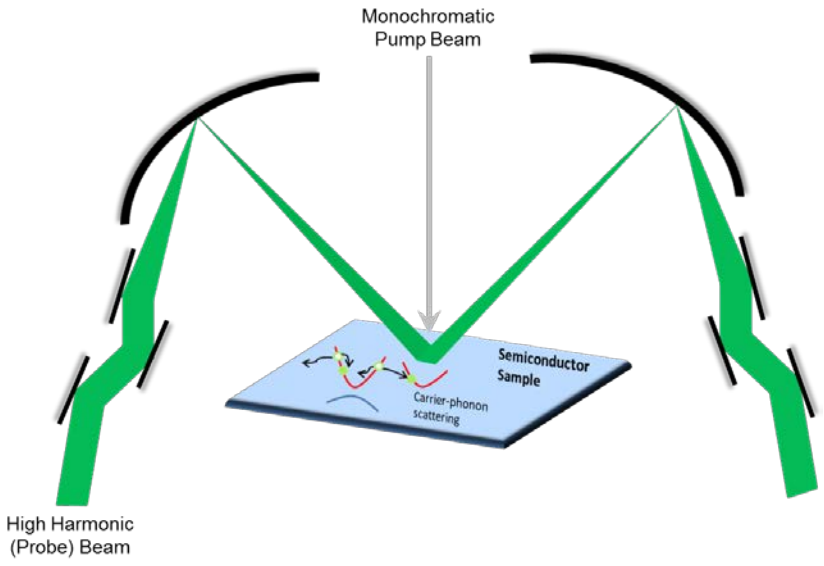

Fig. 1. Schematic representation of the ELIps transient ellipsometer

The instrument differs from already established VUV ellipsometers at synchrotron light sources [2] in that it is a transient pump-probe ellipsometer (Figure 1). It can measured processes with a time-resolution of a few picoseconds. The pump pulse from a laser hits the sample first, triggering e.g. charge transfer processes; these processes can be observed and quantified by measuring

the changes on the optical properties of the material by a probe pulse. The pump beam is a single wavelength beam that can be chosen from 180 nm – 20 um.

A Helmholtz coil is also installed in the instrument, which can deliver a field of up to 1.5 T at a rate of up to1 kHz. It would be possible to obtain the transverse magneto-optical Kerr Effect and probe e.g. the excitation of spin-polarized states.

All the components are contained within a single UHV chamber (with a target pressure lower than 10^{-8} mbar) designed with several additional ports to support future upgrades such as a sample preparation chamber (e.g. different ambient gases). Furthermore, the sample chamber is designed with a cryostat for temperature dependent studies.

Additional to the VUV ellipsometer, at ELI Beamlines, there is table top system for time-resolved ellipsometry utilizing super-continuum white-light pulses ranging from 350 nm – 750 nm.

Support by the European Regional Development Fund: ELI Extreme Light Infrastructure Phase 2 (CZ.02.1.01/0.0/0.0/15_008/0000162) and ELIBIO (CZ.02.1.01/0.0/0.0/15_003/0000447) is gratefully acknowledged.

[1] S. Espinoza, G. Neuber, C.D. Brooks, B. Besner, M. Hashemi, M. Rübhausen, J. Andreasson. Appl. Surf. Sci. 421, 378-382 (2017)

[2] M.D. Neumann, C. Cobet, H. Kaser, M. Kolbe, A. Gottwald, M. Richter, N. Esser. Rev. Sci. Instrum. 85, 55117 (2014)

DC to 500 kHz / 5 MHz

MFLI Lock-in Amplifier
MFIA Impedance Analyzer

starting at
$5,940

$10,230

All Instruments include

- Spectrum Analyzer
- Parametric Sweeper
- Oscilloscope with FFT
- Imaging Module
- Threshold Unit Tip Protection
- MATLAB®, LabVIEW®, .NET, C, and Python interfaces

Upgrade options

4 PID/PLL Controllers

- PID Advisor suggests initial set of parameters
- Auto-tune automatically minimizes residual PID error
- PLL Mode with ±1024 π phase unwrap for robust locking

AM/FM Modulation

- Generation and analysis of AM/FM modulated signals
- Single and higher order sideband analysis
- Adjustable filter settings for each frequency

Get in touch
www.zhinst.com
info@zhinst.com
Intl. +41 44 515 0410
USA 617 765 7263

Zurich Instruments

Your Application. Measured.

Friday

Two-probe STM/STS experiments performed on atomic wires and single molecules supported on Ge(001) surface

Marek Kolmer, Pedro Brandimarte[1], Łukasz Zając, Rafał Zuzak, Szymon Godlewski, Hiroyo Kawai[2], Thomas Frederiksen[1], Mads Engelund[1], Aran García-Lekue[1], Nicolas Lorente[1], Jakub Lis, Antonio M. Echavarren[3], Christian Joachim[4], Daniel Sanchez-Portal[1], Marek Szymoński

Centre for Nanometer-Scale Science and Advanced Materials, NANOSAM, Faculty of Physics, Astronomy and Applied Computer Science, Jagiellonian University, Łojasiewicza 11, 30-348 Kraków, Poland
(corresponding author: M. Kolmer, e-mail: marek.kolmer@uj.edu.pl)

[1] *Centro de Física de Materiales CSIC-UPV/EHU and DIPC, Paseo Manual de Lardizabal 5, E-20018, Donostia-San Sebastián, Spain*

[2] *Institute of Materials Research and Engineering, IMRE,, 2 Fusionopolis Way, Innovis, #08-03, 138634 Singapore*

[3] *Institute of Chemical Research of Catalonia (ICIQ), Barcelona Institute of Science and Technology, Avenida Països Catalans 16, 43007 Tarragona, Spain*

[4] *Nanoscience Group & MANA Satellite, CEMES/CNRS, 29 rue Marvig, BP 94347, 31055 Toulouse, France*

Due to unprecedented precision reaching sub-picometers scanning probe microscopy (SPM) methods are currently the most popular and reliable tools for local characterization of atomic and single-molecule systems supported on surfaces of solids. However, direct determination of many functional properties, including especially electronic transport in prototypical planar atomic-scale devices, lies beyond the single-probe SPM approach. Recent technical advances provide multi-probe SPM instruments, which are able to operate on the same surface simultaneously with stability comparable to best cryogenic single-probe SPMs [1].

In this work, we describe the full methodology behind atomically defined two-probe scanning tunneling microscopy [2] and spectroscopy (STM/STS) experiments performed on model systems on the germanium (001) surface. Firstly, we discuss our methodology for fine relative positioning of two STM probes on Ge(001) and Ge(001):H surfaces with exact atomic precision and lateral probe to probe distances below 50 nm (Fig.1). That technical results

opens possibility of direct testing of on-surface electron transport in a planar geometry. It is realized by a novel two-probe STS (TP-STS) methodology, in which both STM tips are kept in tunneling conditions above a grounded sample. By applying a small AC component to a varied DC bias voltage on one of the probes and by demodulation of resulting current signals on both of the probes, we extract corresponding dI_1/dV_1 (single-probe, vertical) and dI_2/dV_1 (two-probe, planar) STS signals. In this case of Ge(001) we show that the detection of TP-STS signal is related to quasi-ballistic hot-electron transport through one-dimensional π* states of Ge dimer-row wires located within bulk bang gap of the surface [3-5]. Our two-probe experimental results are corroborated by first-principles calculations combining the non-equilibrium Green's function (NEGF) formalism with density function theory (DFT) in a four-terminal setup.

Finally, we present a non-local switching of single trinaphthylene molecule adsorbed on Ge(001) surface. The switching is induced by hot electrons injection into discussed π* states of Ge dimer-rows. Here by taking the advantage of two-probe STM configuration we observe "in-situ" non-local molecule switching using one of the probes as a source of hot electrons injected into surface states and the other as a detector of a molecule motion.

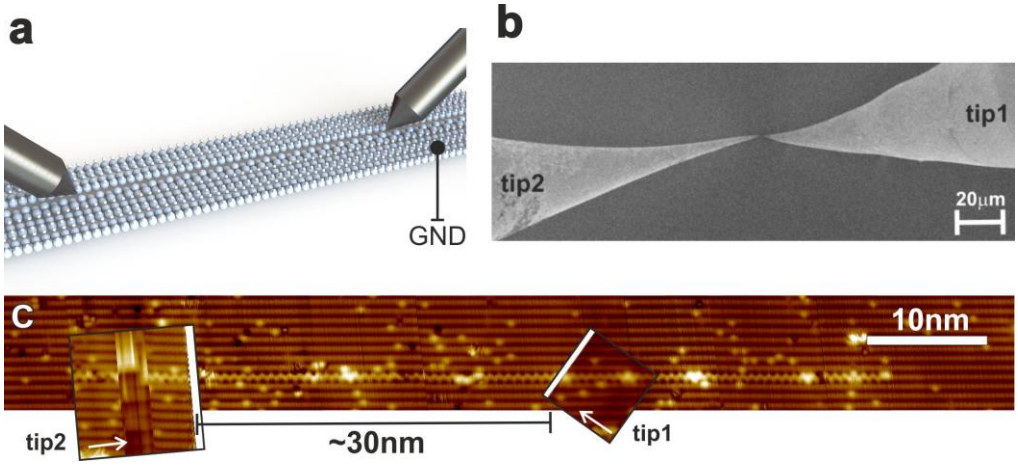

Fig.1 Two-probe STM characterization of atomic wire on Ge(001):H surface [2]. (a) Schematic presentation of the experiment: both STM probes approach the same atomic-scale wire of bare Ge dimers along Ge(001):H reconstruction rows. (b) SEM image of two tungsten tips approached to Ge(001):H surface. Both tips have a diameters below 50 nm, what also enables two-probe experiments on probe to probe distances below 50 nm. (c) STM image of DB dimer wire (−0.5 V, 50 pA). Insets: two STM images obtained *simultaneously* by two different tips in the geometry shown in (a) and (b). White arrows point the slow STM scan direction. White bars present on the insets are due to retraction of the tips after their contact on probe to probe distance of about 30 nm.

Support by the European Commission under PAMS project (contract no. 610446) and by the Polish Ministry of Science and Higher Education (contract no. 0341/IP3/2016/74) are gratefully acknowledged.

[1] J.S. Yang et al., Eur. Phys. J. Appl. Phys. 73, 10702 (2016)
[2] M. Kolmer et al., J. Phys.: Condens. Matter 29, 444004 (2017)
[3] K. Nakatsuji et al., Phys. Rev. B, 72(24), 241308 (2005)
[4] K. Sagisaka and D. Fujita, Phys. Rev. B, 72(23), 235327 (2005)
[5] M. Kolmer et al., Phys. Rev. B 86 125307 (2012)

Coulomb's law at the nanoscale: imaging CaF2(111) with atomically engineered tips

Alexander Liebig, Angelo Peronio, Daniel Meuer, Alfred J. Weymouth, and Franz J. Giessibl

Institute of Experimental and Applied Physics, University of Regensburg, D-93053 Regensburg, Germany

e-mail: Franz.Giessibl@ur.de

We probed the polar $CaF_2(111)$ surface by non-contact atomic force microscopy, using qPlus sensors with a bare metal tip and with a CO-terminated tip. In contrast to ionic crystals of the rocksalt structure, $CaF_2(111)$ exposes only one ionic type at the surface of its natural cleavage plane (F, see Fig.1) [1]. Far from the surface, where the contrast is entirely determined by electrostatics, we can resolve individual atoms with force contrast down to the fN-regime. The images taken with the two tips are inverted with respect to each other, which indicates that the local charge at the tip apex points is opposite for metal versus CO tips.

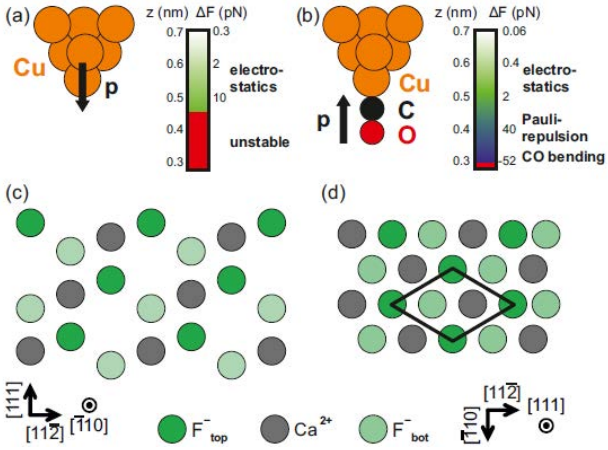

Fig.1 (a) A metallic tip presents a dipole moment pointing towards the surface due to the Smoluchowski effect. (b) CO-terminated tips have been modeled with a dipole moment pointing away from the surface. The color bars illustrate the evolution of the force contrast ΔF with tip- sample distance z. The red region indicates the height at which stable imaging is no longer possible. The shading represents distances at which electrostatics (green) and Pauli repulsion (blue) dominate the imaging mechanism. (c) Side view of the $CaF_2(111)$ surface, formed by electrically neutral triple layers of $F^-/Ca^{2+}/F^-$ ions spaced by $a_0/3^{\wedge 0.5}$ = 315pm [11]. The individual layers within a triple layer are separated by 79 pm. (d) Top view of the $CaF_2(111)$ surface. The surface is a triangular lattice of F^--ions spaced by 386pm. The surface unit cell presents three inequivalent sites, corresponding to the different ions of the topmost triple layer.

We compare the experimental data to an electrostatic model and find excellent agreement between experiment and the inverse power law that was found in 1784 by Charles-Augustin de Coulomb [2]. The contrast changes when imaging with the CO tip at closer distances, which we can explain in terms of Pauli repulsion and subsequent CO bending. As the electric field decays exponentially with distance, the main origin of contrast is the charge of the front atom. The COFI method [3] allows us to determine the structure and orientation of the tip on the atomic scale.

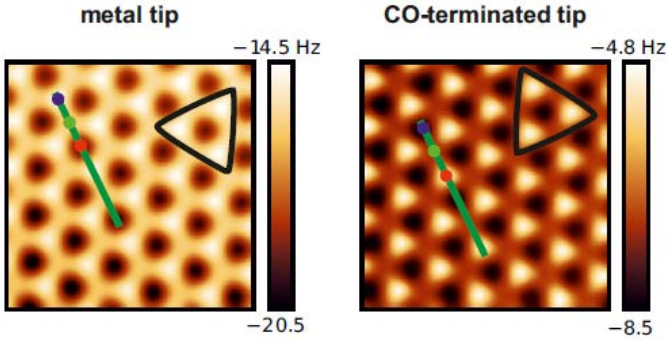

Support by the DFG (SFB1277 and GRK1570) is gratefully acknowledged.

[1] C. Barth, A. S. Foster, M. Reichling, and A. L. Shluger, J. Phys. Condens. Matter 13, 2061 (2001)
[2] J. E. Lennard-Jones and B. M. Dent, Trans. Faraday Soc. 24, 92 (1928)
[3] J. Welker and F. J. Giessibl, Science 336, 444 (2012)

Surface science and DEMS studies of electrochemical CO and ethanol oxidation on TiOC supported Pt catalysts

Niusha Shakibi Nia[1], Celine Rüdiger[1], Andrea Paduano[2], Gonzalo García[3], Alessandro Martucci[2], Elena Pastor[3], and Julia Kunze-Liebhäuser[1]

Institut für Physikalische Chemie, Leopold-Franzens-Universität Innsbruck, 6020 Innsbruck, Austria (corresponding author: J. Kunze-Liebhäuser, e-mail: julia.kunze@uibk.ac.at)

[1] *Institut für Physikalische Chemie, Leopold-Franzens-Universität Innsbruck, Innrain 52c, 6020 Innsbruck, Austria*

[2] *Department of Industrial Engineering, University of Padova, Via Marzolo 9, 35131 Padua, Italy*

[3] *Instituto de Materiales y Nanotecnología, Universidad de La Laguna, 38071 La Laguna, Spain*

Direct Ethanol Fuel Cells (DEFCs) have been subject of numerous studies in recent years. However, the complete oxidation of ethanol to CO_2 at the anode side is still one of the main challenges. Efficient electro oxidation of ethanol (EOR) requires the use of elevated temperatures >60°C [1]. Moreover, the catalysts that are usually platinum (Pt) based alloys, are mainly supported on carbon, which can corrode under these conditions resulting in detachment and agglomeration of catalyst nanoparticles.

In this study, titanium oxycarbide (TiOC) is investigated as innovative support for Pt based nanoparticles during the EOR [2,3]. The chemical composition of the TiOC surface is characterized *in-situ* during its conversion from TiO_2 to $TiO_{0.5}C_{0.5}$ using X-ray photoelectron spectroscopy (XPS). For this, a surface science approach is followed, where compact anodic TiO_2 films are first converted via an *ex-situ* emersion treatment to test the influence of exposure to air and oxygen on the chemical composition of the surface [4]. An *operando* study of the same conversion procedure is then conducted under UHV conditions which revealed that TiOC is thermodynamically less stable than anatase TiO_2 and carbon, and that it therefore always decomposes at the surface [4]. This decomposition and the formation of a TiO_2 surface film upon exposure to ambient air protect the material from further oxidation when it is used in an electrochemical environment, without majorly influencing its electronic conductivity. To understand the role of TiOC as catalyst support, its surface chemistry is monitored during the EOR using *ex-situ* emersion XPS in combination with electrochemistry, where the electrochemical cell is directly connected to the XPS [5].

The activity of the catalysts is determined using cyclic voltammetry, and current transients recorded at temperatures up to 70 °C in acidic electrolytes with ethanol concentrations varying from 0.1 to 1 M. For a quantitative evaluation of the EOR products, differential

electrochemical mass spectrometry (DEMS) is employed. CO oxidation and EOR studies are conducted to evaluate the CO_2 efficiencies of Pt nanoparticles supported on TiOC and on carbon (C). The results show that Pt/TiOC is less prone to poisoning than Pt/C which is most likely due to a stronger interaction of TiOC with ethanol, when compared to carbon [6]. This explanation is based on electrochemical findings that reveal in combination with *ex-situ emersion* XPS and subtractively normalized interfacial Fourier Transform infrared spectroscopy (SNIFTIRS), an infrared technique that can probe the solid/liquid interface during electrochemical reactions, that ethanol adsorbs on TiOC and suppresses its oxidation at anodic potentials [5]. The reaction pathway of the EOR at Pt/TiOC can be quantitatively followed and compared to that of Pt/C using DEMS in combination with electrochemistry and *ex-situ emersion* XPS [6].

Financial support by the EU-FP7 program (DECORE, NMP4-SL-2012-309741) and the University of Innsbruck is gratefully acknowledged.

[1] S. Sun, M.C. Halseid, M. Heinen, Z. Jusys, R.J. Behm, J. Power Sources 190, 1 (2009).

[2] C. Rüdiger, F. Maglia, S. Leonardi, M. Sachsenhauser, I. D. Sharp, O. Paschos, J. Kunze, Electrochimica Acta, 71, 1 (2012).

[3] C. Rüdiger, J. Brumbarov, F. Wiesinger, S. Leonardi, O. Paschos, C. Valero-Vidal, J. Kunze-Liebhäuser, ChemCatChem, 5, 3219 (2013).

[4] L. Calvillo, D. Fittipaldi, C. Rüdiger, S. Agnoli, M. Favaro, C. Valero-Vidal, C. Di Valentin, A. Vittadini, N. Bozzolo, S. Jacomet, L. Gregoratti, J. Kunze-Liebhäuser, G. Pacchioni, G. Granozzi, J. Phys. Chem. C 118, 22601 (2014).

[5] L. Calvillo, G. Garcia, A. Paduano, O. Guillen-Villafuerte, C. Valero-Vidal, A. Vittadini, M. Bellini, A. Lavacchi, S. Agnoli, A. Martucci, J. Kunze-Liebhäuser., E. Pastor, G. Granozzi, Appl. Mat. Interf. 8, 716 (2016).

[6] N. Shakibi Nia, J. Kunze-Liebhäuser, in preparation.

In-situ X-ray observations of Sn electrodeposition into two-step anodized alumina

W. Linpé[1], G.S Harlow[1], J. Evertsson[1], U. Hejral[1], Filip Lenrick[1], Soenke Seifert[3], Nikolay A. Vinogradov[2], E. Lundgren[1]

[1]*Division of Synchrotron Radiation Research, Lund University, SE-22100 Lund, Sweden (corresponding author: W. Linpé, e-mail: weronica.linpe@sljus.lu.se)*

[2]*MAX IV Laboratory, SE-22594, Lund, Sweden*

[3]*Argonne National Laboratory, 9700 South Cass Avenue, Argonne, Illinois 60439-4838 USA*

Aluminium is a material widely used for different products and applications, this is due to the excellent material characteristics of aluminium such as high strength, low density and good corrosion resistance. When aluminium is exposed to air a native oxide is formed on it's surface, and will provide protection of the aluminium from corrosion [1,2]. The native oxide can be grown thicker by electrochemical means, where a method called anodization can be used [3]. Using acidic electrolytes for the anodization a nano-porous anodic aluminium oxide (NP-AAO) can be formed. This porous oxide can be grown into an ordered oxide by the use of a two step anodization process [4]. The ordered NP-AAO is useful in applications such as templated growth of nano-wires and colouring of aluminium in a wide range of colours. The metal Sn can be deposited into the porous oxide and is used in industry for colouring aluminium products black.

We have studied *in-situ* electro-deposition of Sn into Nano porous anodic aluminium oxide (NP-AAO) by using Grazing Transmission Small Angle X-ray Scattering (GTSAXS), X-Ray Fluorescence (XRF) spectroscopy and X-Ray Absorption Near Edge Structure (XANES) spectroscopy, at Beamline 12-ID-C at APS, Chicago. The ordered NP-AAO was created by a two step anodization process, where the sample is anodized in acidic electrolytes in two steps with a chemical etch between the two anodization steps, this will lead to an ordered porous aluminum oxide.

For the second anodization step, GTSAXS was used to continuously image the sample as the porous oxide was grown on the aluminum substrate. After the second anodization two different methods, pore widening or barrier layer thinning, were used to facilitate the deposition of Sn into the porous oxide. The pore widening is a chemical etch that etches away some of the pore wall materials, which is achieved by leaving the sample in a heated acid. The barrier layer thinning will decrease the thickness of the barrier layer at the bottom of the pores by step-wise decreasing the anodization potential in a controlled manner to a lower potential than the one used for the anodization. This method will decrease the barrier layer

thickness as the thickness is dependent on the anodization potential. These two methods were imaged continuously with GTSAXS.

Deposition of Sn into the NP-AAO was achieved by the use of an alternating voltage and an electrolyte solution containing Tin sulfate. This deposition was studied *in-situ* with GTSAXS, XRF and XANES. For the measurements a photon energy of 29.4keV was used. The GTSAXS measurements show an increase in intensity during deposition indicating Sn being deposited in the sample. From our XRF measurements an increase of the fluorescence signal at the position of the sample surface can be seen, showing a deposition of Sn at the sample. XANES is used to determine the chemical state of the deposited Sn and by comparison with reference samples these measurements indicate a deposition of Sn^{4+} into the porous oxide.

Ex-situ measurements with FIB-SEM, conducted at the Lund Nano Lab, supports the *in-situ* measurements as rods of Sn can be seen within the pores of the porous oxide. A change in color of the sample, from metallic to black, could also be observed after the electrodeposition.

References:

[1] L.P.H. Jeurgens, W.G. Sloof, F.D. Tichelaar, C.G. Borsboom, E.J. Mittemeijer, Determination of thickness and composition of aluminium-oxide overlayers on aluminium substrates, *Appl. Surf. Sci*. **144**, 11 (1999)

[2] J. Evertsson et al, The thickness of native oxides on aluminum alloys and single crystals, *Appl.Surf. Sci*. **349**, 826 (2015)

[3] F. Bertram et al, In situ anodization of aluminum surfaces studied by x-ray reflectivity and electrochemical impedance spectroscopy, *J. Appl. Phys*. **116**, 034902, (2014)

[4] W. Lee. and S.-J. Park, Porous Anodic Aluminum Oxide: Anodization and Templated Synthesis of Functional Nanostructures, *Chem. Rev*. **114**, 7487 (2014)

Unusual and stable Ga bonding at its solid-liquid interface with GaN

V. Vonk[1], A.E.F. de Jong[2,3], V. Honkimäki[3], E. Vlieg[2]

[1] *Deutsches Elekronen-Synchrotron (DESY), Hamburg, Germany*
(corresponding author:V. Vonk, e-mail: vedran.vonk@desy.de)

[2] *Radboud University Nijmegen, The Netherlands*

[3] *European Synchrotron Radiation facility (ESRF), Grenoble, France*

Here we present the first results of a study which targets the atomic-scale understanding of GaN crystal growth from solution. GaN has become the second most important semi-conductor after silicon, in particular due to its use in blue LED applications. The growth of large nearly perfect GaN single crystals is a challenge, because of the high temperatures and pressures of the gaseous nitrogen feedstocks. Wafers, on the other hand, which are typically grown by chemical vapour deposition, suffer from too high defect densities. There is a continuing effort to optimize any of these growth methods, preferably from solution since this gives the highest quality material. The aim is to investigate the solid-liquid interface and to uncover features in the atomic structure which are relevant for the crystallization process. Such an approach has for example uncovered preferential ordering of metal solute atoms at hollow sites of the InP(111) surface, which can sterically hinder the growth of zinc-blende crystals and results in unwanted wurtzite stacking sequences [1].

Modern X-ray scattering methods enable the study of surfaces and interfaces under non-vacuum conditions, which are relevant in for example catalysis and crystal growth. Such studies pave the way for obtaining atomic-scale insights into industrially relevant processes, which can take place at high temperature and at pressures in the range of several hundred bars. This technique therefore offers unique capabilities when trying to bridge the so-called pressure gap, i.e. extending the fundamental insights obtained by traditional vacuum-based surface science.

Dissolution of N in liquid Ga is difficult, since the dissociation of N_2 or NH_3 requires high temperature and high pressure. For our study, a special furnace was designed, built and tested, which can hold a crucible for liquid Ga in contact with a GaN substrate up to 800 deg C and gas pressures up to 50 bar [2]. This setup was used in combination with high-energy synchrotron radiation for a number of studies [3]. X-rays with an energy of 70 keV can penetrate the chamber walls and Ga in order to reach and scatter off the deeply buried interface.

The most important result is that the solid-liquid interface is formed by several stacked 2D Ga layers, which contain both ordered and more disordered atoms with a well-defined height above the substrate. The more ordered Ga atoms form for example a c(2x2) lattice, with the Ga atoms at substrate hollow sites, whereas the more disordered atoms surround these in a more liquid-like fashion. Such a geometry also implies that a small number (a few %) of the Ga-Ga bonds have to be as short as 0.23 nm, much shorter than the distance within a dimer of approx. 0.275 nm. At the same time, we find that about 20-30% vacancies exist in these layers, as determined by the available substrate lattice sites. These interface layers are found to exist over the whole investigated temperature and pressure range, see Figure 1, and therefore seem to represent a particularly stable configuration.

We argue that such an interface, which consists of anchor atoms at high symmetry positions as determined by the substrate, in combination with a more liquid-like component will play an important role for the energetics and kinetics which control the transition from liquid to solid. This is important for the growth of GaN at this interface, but possibly also for the melting and solidification of Ga at this interface. In the case of Au droplets on Si(111), it has been found that a stable (6x6) reconstruction can induce huge supercooling of the metal [4].

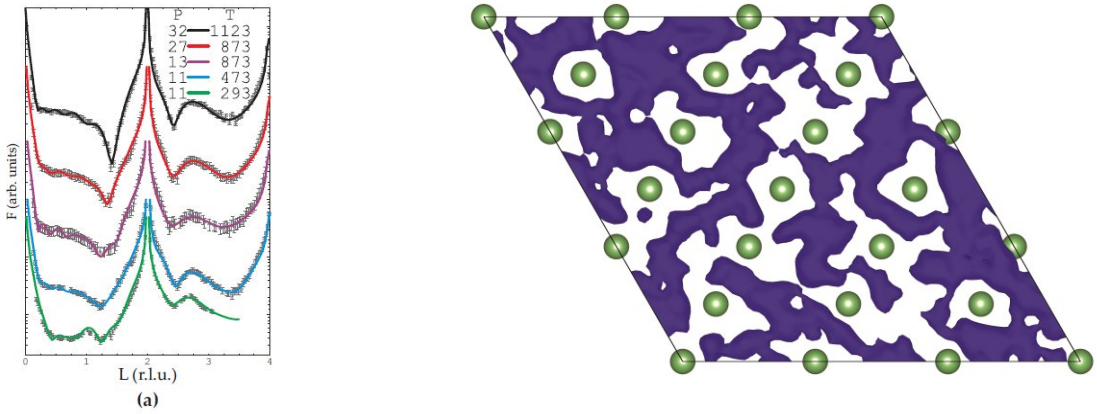

Fig 1 a) Specular CTR data for the different investigated pressures and temperatures. The solid lines present fits, which all contain a 2D Ga layer as shown in b) and as discussed in the text. b) Schematic view of the 2D interface layer which contains Ga (green) anchor atoms in a c(2x2) lattice and more disordered liquidlike atoms (blue).

Supported by the Netherlands Organization for Scientific Research (NWO) through a VENI grant.

[1] R.E. Algra, V.Vonk, E.P.A.M. Bakkers, E. Vlieg et al., Nano Lett. 11 (2011) 44

[2] A.E.F. de Jong, V. Vonk, V. Honkimaki, B. Gorges, H. Vitoux and E. Vlieg, J. Cryst. Growth 420 (2015) 84

[3] A.E.F. de Jong, PhD. *Ordering at the GaN-Ga solid liquid interface*, Thesis Radboud University Nijmegen (2016)

[4] T.U. Schülli, R. Daudin, G. Renaud, A. Vaysset, O. Geaymond and A. Pasturel Nature 464 (2010) 1174

Dynamics of Si surface nanostructures under electromigration

S. Curiotto, A. El-Barraj, F. Cheynis, P. Müller, and F. Leroy

Aix Marseille Univ, CNRS, CINAM, Marseille, France
(corresponding author: S. Curiotto, e-mail: curiotto@cinam.univ-mrs.fr)

Mass transport processes play an important role in nano devices. They determine the morphology and the stability of a working device, and eventually its lifetime. When a direct electric current is applied to a material, it affects the mass transport by adding a bias to the atomic diffusive motion. This effect, called electromigration, can play an important role on the dynamics and the morphological stability of nanostructures at surfaces.

Electromigration has been intensively studied to improve the stability of electronic devices [1,2]. Indeed, it can be responsible for hillocks or voids that may disrupt electronic circuits. Electromigration can also change the surface morphology modifying steps arrangement, leading to instabilities of step meandering and step bunching [3]. Theoretical works have also addressed the kinetics of motion of 2D surface nanostructures under electromigration [4,5]. The electromigration force is extremely small and therefore biases the diffusion of the atoms without changing the fundamental transport mechanisms limiting the motion of a nanostructure. These can be periphery diffusion, terrace diffusion or attachment-detachment. According to the prevailing mechanism, different scaling laws are predicted for the velocity of a nanostructure as a function of its size [6].

These theoretical studies need to be addressed by experimental results, as only scarce data (see for instance [7] and [8]) are available. We have recently undertaken the investigation by LEEM of the motion of monoatomic islands and holes at Si surfaces with orientations (100) and (111), under electromigration. In order to obtain very large step free areas, we have patterned holes (300 μm diameter, 7 μm depth) in the wafers by lithography, following the procedure suggested by Lee and Blakely [9]. The samples are mounted on a specific sample holder allowing to apply an electric field across their long axis, are introduced in the Ultra High Vacuum (UHV) chamber and degassed for some hours then flashed at high temperature to remove the surface oxide. In order to study electromigration dynamics, we have observed in real time the motion of surface nanostructures by low energy electron microscopy (LEEM).

On Si(100), single-step holes have been made by evaporation, increasing the current through the sample and therefore increasing the temperature (above 1340 K) and observing in real time by LEEM their formation. When the desired hole size is reached, the temperature is lowered to stop evaporation and the sample is kept at a certain temperature and observed to study the hole motion dynamics. Islands can also be created by Si deposition, their number and size can be tuned by changing the substrate temperature, the flux or the deposition time.

The Si(100) surface reconstruct forming dimer rows oriented along the [011] or the [0-11] directions, alternatively on successive terraces. Under a same current, holes with different dimer orientations displace in opposite directions. The same applies for islands. Their shape depends on the dimer orientations and their velocity does not depend on the size. This suggests that the main mechanism controlling the motion is diffusion on terraces, while periphery diffusion and attachment-detachment play only a minor role. The details of the motion depend on the strong diffusion anisotropy of the Si dimer rows. The holes or islands velocity increases with temperature, as it depends on diffusion. The motion of islands and holes is characterized by the same activation energy.

Holes and islands on Si (111)-1×1 do not move or move only very slowly under electromigration, because diffusion is isotropic on this orientation and the Schwoebel barrier at step edges is very small [10]. However, if the nano-structure has a different structure from the rest of the surface, a motion can be observed. This is obtained in very specific conditions, at a temperature corresponding to the 7×7 ↔1×1 surface transition, where 1×1 holes can be formed under a metastable state surrounded by a 7×7 reconstructed terrace. In this case the difference of diffusion on the 7×7 from the 1×1 is at the origin of the motion. Velocity measurements of holes under electromigration as a function of their size allows to put in evidence that the limiting mechanism changes from attachment-detachment below 500 nm radius to terrace diffusion at larger sizes.

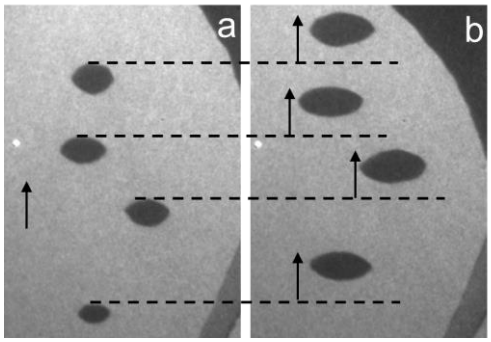

Figure 1: Dark field LEEM images of 2x1 islands on a 1x2 Si terrace. The images show the position of four dark islands moving by electromigration (image b is taken 278 s after a). The size of the islands has increased from a to b

This work was supported by the ANR grant HOLOLEEM (ANR-15-CE09-0012). We thank Igor Ozerov for the technical support.

[1] A. Blech and E.S. Meyeran, J. Appl. Phys. 40, 485 (1969)

[2] A. Blech, J. Appl. Phys. 47, 1203 (1976)

[3] F. Leroy, D. Karashanova, M. Dufay, J.M. Debiere, T. Frisch, J-J. Métois, P. Müller, Surf Sci 603, 507 (2009)

[4] O. Pierre-Louis and T.L. Einstein, Phys Rev. B. 62, 13697 (2000)

[5] P. Khun, J. Krug, F. Hausser and A. Voigt, Phys Rev Lett. 94, 166105 (2005)

[6] K. Morgenstern, Phys. Rev. Lett. 74 2058 (1995)

[7] J-J. Métois, J-C Heyraud, A. Pimpinelli, Surf. Sci. 420 250 (1999)

[8] C. Tao, W.G. Cullen, E.D. Williams, Science 328 736 (2010)

[9] D. Lee and J. Blakely, Surf. Sci. 445, 32 (2000)

[10] Thin Film Growth: Physics, Materials Science and Applications, Z Cao editor, WoodHead publishing, Cambridge UK

Iron-based magnetic nanoparticles with tuned composition and crystal structure

C. Preger, C. Bulbucan[1], L. Ludvigsson, M. Muntwiler[2], R. Westerström[1], and M. E Messing

Solid State physics and NanoLund, Lund University, Box 118, 221 00 Lund, Sweden
(corresponding author: M. E. Messing, e-mail: maria.messing@ftf.lth.se)

[1] *Synchrotron Radiation Research, Lund University, Box 118, 221 00 Lund, Sweden*

[2] *Paul Scherrer Institut, WSLA/122, CH-5232, Villigen PSI, Switzerland*

Macro scale iron-based alloys have since a long time been used extensively in myriads of different applications due to its profitable price and accessibility and combination with its interesting properties such as corrosion resistance and magnetic behavior. In recent years, also nanoscale iron-based alloys have started to gain attention, due to the possible new properties that arises on this scale. Although there is ongoing work to understand these materials on the nanoscale, a complete understanding on how particle properties are linked to for example magnetic behavior is still not obtained. One reason for this is that very few generation methods where size, composition and number of particles can be fully controlled exist.

One promising route for production of metal alloy nanoparticles with tuned size and composition is aerosol-based physical generation. Previously, low yield of particles has been a limitation with physical methods but recently particle production rates of g/hour has been foreseen [1]. Here, we report on fabrication of size-selected iron-based alloy nanoparticles with tuned composition and crystal structure, using spark discharge generation [2]. The particles are thoroughly characterized by high resolution transmission electron microscopy (TEM), x-ray photoemission spectroscopy (XPS) and SQUID magnetometry. We also report on the influence of particle properties on the corrosion resistance and magnetic behavior of the as-produced nanoparticles.

Nanoparticle generation by spark discharge where the formation of a plasma channel between two conducting electrodes leads to a spark discharge that evaporate material [3] is reasonably energy efficient. Other advantages with this method includes a continuous generation process, high cleanliness of the nanoparticles, avoidance of chemical precursors and the possibility to easily manufacture alloy and mixed metal particles including particles of materials that are immiscible in bulk form [4].

To generate iron-based nanoparticles pre-alloyed electrodes with different chromium content, as well as an iron and manganese alloy was used, and resulted in particle formation. To reach a stable continuous generation an electrode gap distance of 2 mm and an output current of 10 mA

was found to be optimal settings. The as-produced particles are in the form of agglomerates and to form compact particles, useful for further characterization, sintering of the as-produced particles was performed.

It was shown that compact particles could be formed from all electrodes and that the crystal structure and composition could be tuned by a combination of the carrier gas, the sintering temperature and the composition of the electrodes. To form a single crystalline iron chromium/iron manganese particle, pure nitrogen was used as carrier gas, whereas a core-shell particle with a single crystalline core surrounded by an amorphous shell could be formed by mixing in a small amount (5%) of hydrogen to the nitrogen carrier gas. From XEDS measurements it was confirmed that the formed particles have the same composition as the starting electrodes, in most cases. For iron manganese generated with a small amount of hydrogen in the carrier gas, the amount of manganese can be reduced by increasing the sintering temperature.

From TEM, XEDS and XPS measurements it is clear that the single crystalline particles are oxidized iron chromium and iron manganese whereas the core-shell particles consist of a pure metal core surrounded by a protective oxide shell (see figure 1 for iron chromium). Although the measured oxygen levels in the SDG system is below ppm levels it is clearly enough to oxidize the formed iron-alloy particles. The hydrogen can likely act both as oxygen scavenger and a reducing agent and is clearly key if formation of metallic particles is desired. The oxygen shell is most likely formed after deposition when the particles are exposed to air before characterization, as a self-passivating layer. One sample with iron chromium core-shell particles where analyzed with TEM twice, with more than 6 months between the analysis. It was seen that the shell-thickness had not increased during this time period, hence a sign of good stability in air.

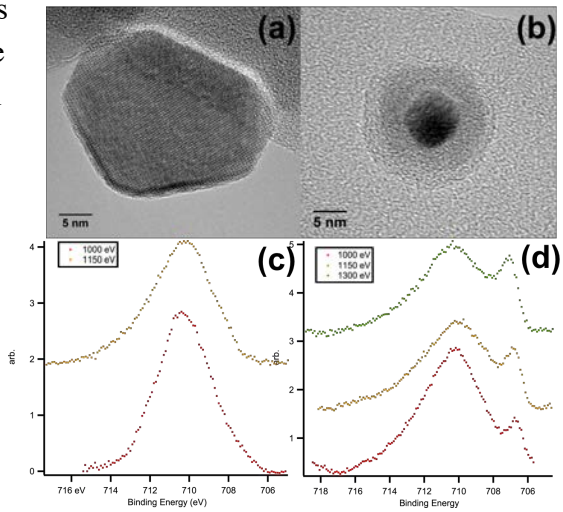

Figure 1: TEM images of (a) single crystalline oxidized iron chromium nanoparticle and (b) core-shell iron chromium nanoparticle and (c-d) Fe $2p_{3/2}$ XPS spectra from (c) single crystalline oxidized iron chromium and (d) core-shell iron chromium nanoparticles (d). Metallic iron (~707 eV) is detected in (d) whereas only oxidized iron (~710 eV) is present in (c).

This work has been performed with financial support from NanoLund and the Swedish Research Council. Part of the work has been performed within Lund Nano Lab and we acknowledge the lab staff for their support. We also acknowledge the Paul Scherrer Institut, Villigen, Switzerland for provision of synchrotron radiation beamtime at the PEARL beamline of the SLS.

[1] J. Feng, G. Biskos and A. Schmidt-Ott, Sci. Rep. 5, 15788 (2015)

[2] B. O. Meuller et al., Aerosol Sci. Technol. 46, 1256 (2012)

[3] M. E. Messing, J. Green Eng. 5, 83 (2016)

Hydrophilicity and microsolvation of organic molecules resolved on the sub-molecular level by scanning tunneling microscopy

Karsten Lucht[1], Dirk Loose[2], Maximilian Ruschmeier[1], Valerie Strotkötter[1], Gerald Dyker[2], and Karina Morgenstern[1]

Ruhr-Universität Bochum, Universitätsstraße 150, D 44801 Bochum, Germany
(corresponding author: K. Morgenstern, e-mail: E-mail: karina.morgenstern@rub.de)

[1]Chair of physical chemistry I

[2]Chair of organic chemistry II

Solute-solvent interactions play an important role in chemistry. Chemical reactions are highly sensitive towards changes in the solvation environment.[1,2] The most abundant solvent on our planet is water. Therefore, it is of utmost significance to investigate the interactions between water and the substances it solvates. Recently, detailed insight into the microsolvation environment of ions and small organic molecules was gained by ab-initio calculations and the spectroscopy of water doped helium nanodroplets.[3,4] However, the geometrical arrangement of the resulting solvation shells for e.g. for the chloride ion is only known theoretically.[5-7] Solvation of organic molecules is even more complex because their spatial extend as well as the varying charge density of functional groups need to be considered. Consequently, they offer more potential attachment sites, which complicate the interpretation of spectra and increase the computational effort. Scanning tunneling microscopy performed at UHV conditions and low temperature is a valuable tool to address this issue. In a recent study, we co-adsorbed 4,4‘-dihydroxy-azobenzene with small amounts of water.[8] The water molecules were found to attach exclusively to the hydroxyl groups, but as they are identical no conclusion about relative hydrophilicity of the endgroups could be drawn.

Here, we used low-temperature scanning tunneling microscopy to follow the formation of a solvation shell around an adsorbed functionalized azo dye, 5-(4-Nitrophenylazo)salicylic acid (hereafter designated NPAS) with groups of different water affinity (carboxyl, hydroxyl, and nitro group) from the attachment of the first water molecule to a fully solvated molecule (see Fig. 1). Specific functional groups bind initially one water molecule each, which act as anchor points for additional water molecules. Further water attachment occurs in areas close to these functional groups even when the functional groups themselves are already saturated. In contrast, water molecules surround the hydrophobic parts of the molecule only, when the two-dimensional solvation shell closes around them. Our study thus traces hydrophilic and hydrophobic properties of an organic molecule down to a sub molecular length scale.

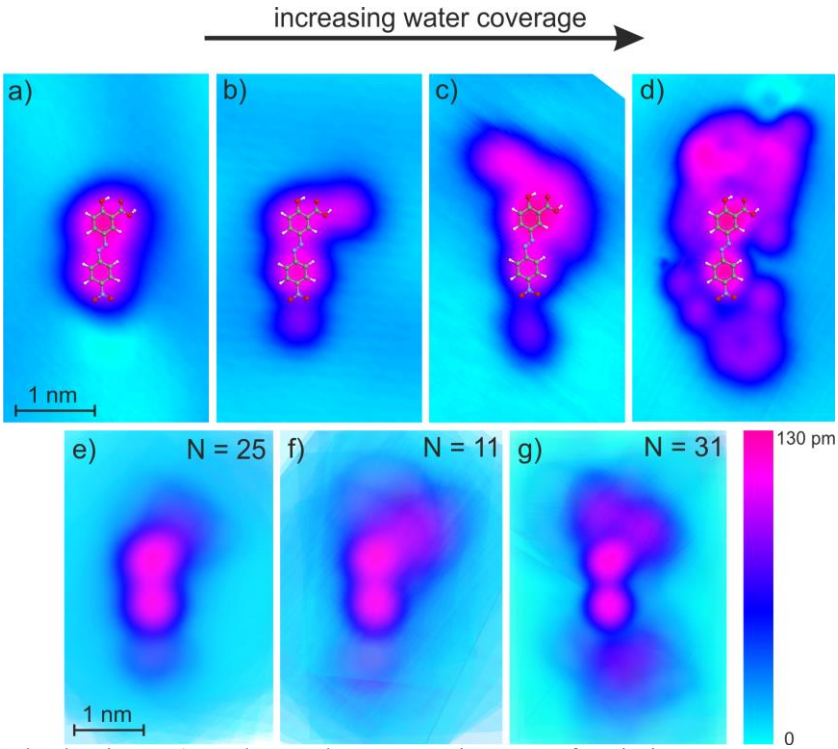

Figure 1. NPAS hydration. a) False color STM image of pristine NPAS molecule with calculated gas-phase structure of NPAS superimposed. (b - d): STM images of NPAS/water complexes for three preparations with D_2O/NPAS ratios of: a) 2:1, b) 18:1, c) 70:1 with calculated gas-phase structure of NPAS superimposed. Features differing from a) are caused by the presence of water. (e – g): Stacked semi-transparent STM images for the three preparations in (b – d). Number of stacked STM images is given by N. Diagonal lines in the images are stacking artifacts.

Support by the Deutsche Forschungsgemeinschaft (DFG) through the Cluster of Excellence RESOLV (EXC 1069).

[1] R. Otto, J. Brox, S. Trippel, M. Stei,T. Best, R. Wester, Nat. Chem. 2012, 4, 534

[2] G. Balakrishnan, S. K. Sahoo, B. K. Chowdhury, S. Umapathy, Faraday Discuss. 2010, 145, 443

[3] A. Gutberlet, G. Schwaab, Ö. Birer, M. Masia, A. Kaczmarek, H. Forbert, M. Havenith, D. Marx, Science 2009, 324, 1545

[4] D. Leicht, M. Kaufmann, N. Pal, G. Schwaab, M. Havenith, J. Chem. Phys. 2017, 146, 114306

[5] A. M. Morrison, S. D. Flynn, T. Liang, G. E. Douberly, J. Phys. Chem. 2010, 114, 8090

[6] J. M. Heuft, E. J. Meijer, J. Chem. Phys. 2003, 119, 11788

[7] A. Bankura, B. Santra, R. A. DiStasio Jr., C. W. Swartz, M. L. Klein, X. Wu, Mol. Phys. 2015, 113, 2842

[8] J. Henzl, K. Boom, K. Morgenstern, J. Am. Chem. Soc. 2014, 136, 13341

Molecular machines driven with electrons on surfaces: walkers and nanocars

G. Srivastava,[1] M. Parschau,[1] L. Zoppi,[1] P. Stacko,[2] B. Feringa,[2] K.-H. Ernst

[1] *Empa, Swiss Federal Laboratories for Materials Science and Technology, Dübendorf, Switzerland*

[2] *Zernike Institute, University of Groningen, 9700 AB Groningen, The Netherlands*

Artificial robots and machines at the nanoscale are one of the great challenges and goals of nanotechnology. Nature has mastered to use of molecular machines for directed transport of cargo or performing mechanical work needed in cellular processes. Motor proteins, for example, undergo conformational changes by using chemical fuel and perform work in the biological cell [1]. Today, chemists spend tremendous efforts to create artificial machines, but not many have been successful towards unidirectional movement [2].

Scanning tunneling microscopy (STM), the founding method of nanotechnology, has been successfully used to move atoms [3] and molecules [4] as well as inducing various molecular dynamical processes at surfaces, such as molecular desorption [5], dissociation [6], formation of chemical bonds [7], changes in conformation [8], and rotation or hopping of molecules [9]. However, all these manipulations did not involve any preferential movement of the species, unless dragged or pushed by the STM tip. Rotatory directional switching with electrons emanating from an STM tip has successfully been performed recently [10].

Here we briefly review our work of unidirectional translational motion of a 'four-wheeled' molecule, induced by electronic and vibronic excitation of four rotor units [11], and present a new molecular design for further studies.

Creating a molecular machine that performs the task of unidirectional movement is very difficult, but was mastered by the Feringa group at the end of the last millennium [12]. A unidirectional rotor of a helically overcrowded system was synthesized and brought into action by light excitation. Over time, Feringa's group improved the concept towards higher rotation speed, but also addressed the issue of surface-mounting of rotors [13]. The ultimate design included a large chassis and four rotors, whose stereochemical centers were carefully tuned in order to perform identical sense of rotation upon excitation.

In order to activate propulsion, electronic excitations that causes a cis-trans isomerization of the C=C bonds is required. This is achieved only at higher voltages when tunneling from the tip into the substrate. The molecule shows an almost linear movement and a different STM contrast appearance along the path. We attribute this to the motor action of the molecule that, as expected, led to linear unidirectional translation on the surface.

After demonstrating the first proof of concept of unidirectional propulsion of a molecule after clever chemical design more insight into the molecular motor dynamics is required. Currently we perform experiments with two-motor unit walkers (or 'waddling ducks'; Fig. 1), which, besides unidirectionality, show identical behavior upon excitation by inelastic electron tunneling.

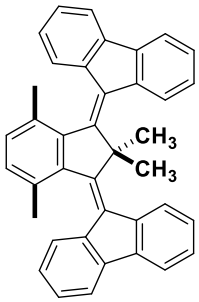

Fig. 1. Molecule with two motor units

[1] Schliwa, M. & Woehlke, G. Molecular motors. *Nature* **2003**, *422*, 759–765; van den Heuvel, M. G. L. & Dekker, C. *Science* **2007,** *317*, 333–336.

[2] M. Peplow, *Nature*, **2015**, *525*, 18.

[3] Eigler, D. M.; Schweizer, E. K. *Nature* **1990**, *344*, 524–526.

[4] Komeda, T. Prog. *Surf. Sci*. **2005**, *78*, 41–85.

[5] J. I. Pascual, N. Lorente, Z. Song, H. Conrad, H.-P. Rust, *Nature* **2003**, *423*, 525 – 528.

[6] P. A. Sloan, R. E. Palmer, *Nature* **2005**, *434*, 367–371; b] B. C. Stipe, M. A. Rezaei, W. Ho, S. Gao, M. Persson, B. I. Lundqvist, *Phys. Rev. Lett*. **1997**, *78*, 4410 – 4413.

[7] S. W. Hla, L. Bartels, G. Meyer, K.-H. Rieder, *Phys. Rev. Lett*. **2000**, *85*, 2777–2780; b] S. W. Hla, K.-H. Rieder, *Annu. Rev. Phys. Chem*. **2003**, *54*, 307–330.

[8] J. Gaudioso, L. J. Lauhon, W. Ho, *Phys. Rev. Lett*. **2000**, *85*, 1918–1921; F. Moresco, G. Meyer, K.-H. Rieder, H. Tang, A. Gourdon, C. Joachim, *Phys. Rev. Lett*. **2001**, *86*, 672 – 675.

[9] B. C. Stipe, M. A. Rezaei, W. Ho, *Phys. Rev. Lett*. **1998**, *81*, 1263 – 1266; T. Komeda, Y. Kim, M. Kawai, B. N. J. Persson, H. Ueba, *Science* **2002**, *295*, 2055 – 2058; c] B. C. Stipe, M. A. Rezaei, W. Ho, *Science* **1998**, *280*, 1732 – 1735.

[10] Perera, U. G. E. et al. *Nature Nanotech*. **2013** *8*, 46–51; Tierney et al. *Nature Nanotech*. **2011**, *6*, 625–629.

[11] Kudernac, T. et al. *Nature* **2011**, *479*, 208–211.

[12] Koumura, N., Zijlstra, R. W. J., van Delden, R. A., Harada, N. & Feringa, B. L. Light- driven molecular rotor. *Nature* **1999**, *401*, 152–155.

[13] van Delden, R. A. et al. *Nature* **2005**, *437*, 1337–1340.

Author Index

KREIOS 150

NEXT GENERATION ELECTRON ANALYZER
FOR SMALL SPOT ARPES AND MOMENTUM MICROSCOPY

KEY FEATURES

- Full 180° angle ARPES
- µARPES (< 2 µm field of view)
- Extractor zoom lens design
- Kinetic energy range 0-1500 eV
- Energy resolution < 15 meV
- Angle resolution < 0.1°

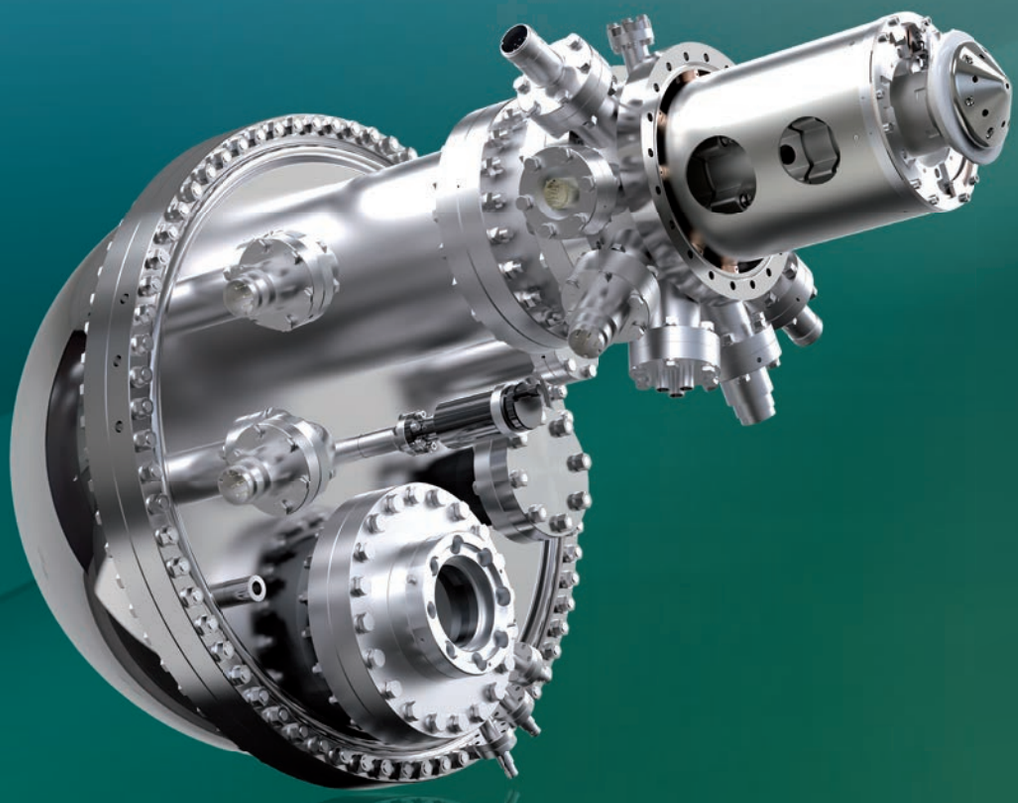

SPECS Surface Nano Analysis GmbH

T +49 30 46 78 24-0
E info@specs.com
H www.specs.com

SPECS™

SYMPOSIUM ON SURFACE SCIENCE 2018
St. Christoph am Arlberg, Austria
Feb. 25 - March 3, 2018

Friedrich Aumayr, Ulrike Diebold and Peter Varga, organizers
Institute of Applied Physics, TU Wien (Vienna University of Technology)

Sunday, 25 Feb. 2018

16:00 - 18:30	REGISTRATION
18:30 - 19:30	DINNER
20:00 - 20:20	OPENING

chair: VARGA

20:25 - 20:45	LIBUDA
20:45 - 21:05	REUTER
21:05 - 21:25	FASEL

Monday, 26 Feb. 2018

07:15 - 08:00	BREAKFAST

chair: TAGLAUER

08:00 - 08:20	PASCUAL
08:20 - 08:40	SETVIN
09:15 - 12:00	SKIING INSTRUCTIONS
12:00 - 13:00	LUNCH
13:30 - 15:30	SKIING INSTRUCTIONS

chair: DIEBOLD

16:40 - 17:00	WÖLL
17:00 - 17:20	ALTMAN
17:20 - 17:40	SCHNEIDER M A
17:40 - 18:00	SCHNEIDER W D
18:00 - 18:20	NETZER
18:30 - 19:30	DINNER

chair: ENDERS

19:30 - 19:50	STARKE
19:50 - 20:10	CURCELLA
20:10 - 20:30	SCHULER
20:30 - 20:50	ELTSOV

Tuesday, 27 Feb. 2018

07:15 - 08:00	BREAKFAST

chair: KOSHIKAWA

08:00 - 08:20	GÖLZHÄUSER
08:20 - 08:40	GUSTAFSON
09:15 - 12:00	SKIING INSTRUCTIONS
12:00 - 13:00	LUNCH
13:30 - 15:30	SKIING INSTRUCTIONS

chair: RENAUD

16:40 - 17:00	RUPPRECHTER
17:00 - 17:20	THORNTON
17:20 - 17:40	FELDBAUER
17:40 - 18:00	SANCHEZ-PORTAL
18:00 - 18:20	BRUNE
18:30 - 19:30	DINNER

chair: AUMAYR

19:30 - 19:50	BUCK
19:50 - 20:10	BARTH
20:10 - 20:30	MARBACH
20:30 - 20:50	KOCÁN

Wednesday, 28 Feb. 2018

07:15 - 08:00	BREAKFAST

chair: LEMELL

08:00 - 08:20	ECHENIQUE
08:20 - 08:40	EBERHARDT
09:15 - 12:00	SKIING INSTRUCTIONS
12:00 - 13:00	LUNCH
13:30 - 15:30	SKIING INSTRUCTIONS

chair: KALOUSEK

16:40 - 17:00	STEMPEL
17:00 - 17:20	MAIER

chair: HUG

17:25 - 18:20	POSTER INTRODUCTION
18:30 - 19:30	DINNER
19:30 - 21:30	POSTERSESSION

Thursday, 1 March 2018

07:15 - 08:00	BREAKFAST

chair: BETTAC

08:00 - 08:20	JELINEK
08:20 - 08:40	MICHELITSCH
09:15 - 12:00	SKIING INSTRUCTIONS
12:00 - 13:00	LUNCH
13:30 - 15:30	SKIING INSTRUCTIONS

chair: LINSMEIER

16:40 - 17:00	LUNDGREN
17:00 - 17:20	ORTEGA
17:20 - 17:40	HAMMER
17:40 - 18:00	SIKOLA
18:00 - 18:20	SUCHORSKI
18:30 - 19:30	DINNER

chair: MULLER

19:30 - 19:50	DE OTEYZA
19:50 - 20:10	GODLEWSKI
20:10 - 20:30	DIL
20:30 - 20:50	ESPINOZA

Friday, 2 March 2018

07:15 - 08:00	BREAKFAST

chair: BERGHAUS

08:00 - 08:20	KOLMER
08:20 - 08:40	GIESSIBL
09:15 - 12:00	GIANT SLALOM RACE
12:00 - 13:00	LUNCH
13:30 - 15:30	SKIING INSTRUCTIONS

chair: RIVA

16:30 - 16:50	KUNZE-LIEBHÄUSER
16:50 - 17:10	LINPE
17:10 - 17:30	VONK
17:30 - 17:50	CURIOTTO
17:50 - 18:10	MESSING

chair: ARNAU

18:30 - 18:50	MORGENSTERN
18:50 - 19:10	ERNST
19:10 - 19:40	GIANT SLALOM RACE AWARD CEREMONY
20:00	CONFERENCE DINNER